MASTER'S THESIS

Steady-State Hematopoiesis in the Spleen

Kaden, Jacqualine

Award date:
2020

Steady-State Hematopoiesis in the Spleen

Jacqualine Kaden

February 2020

Submitted in total fulfilment of the requirements of the degree of Master of Science by Research

Faculty of Health Sciences & Medicine

Assistant Professor Jonathan Tan and Professor Helen O'Neill

Stem Cells & Immunology Laboratory

Clem Jones Centre for Regenerative Medicine

This research was supported by an Australian Government Research Training Program Scholarship.

ABSTRACT

Mammalian blood cell production is maintained by a heterogenous hematopoietic stem cell (HSC) population with remarkable capacity for self-renewal and pluripotency. While bone marrow is the major site for HSC residence, the red pulp region of the spleen can also act as a niche for HSC, despite the lack of osteoblasts. HSC differentiation in bone marrow is influenced by signals imposed by the stromal niche. It is therefore important to consider how the splenic niche might signal hematopoiesis and how spleen-resident HSC might contribute to hematopoiesis in the steady-state and also across the life span of the animal. Hematopoiesis in spleen is commonly linked to stress and disease, a phenomenon termed extramedullary hematopoiesis. However, no studies have yet addressed lineage output in steady-state spleen. Evidence from *in vitro* studies and *in vivo* models of extramedullary hematopoiesis suggest that spleen-resident HSC might be primed for myeloid cell production.

Transplantation studies performed to address the precise hematopoietic potential of spleen HSC under physiological conditions have been hampered by the limitation of using traditional conditioning methods to ablate HSC niches. Clearance of HSC niches is required for donor engraftment to occur. With success with dietary-based HSC niche clearance techniques which are non-inflammatory, the study of steady-state hematopoiesis specific to the spleen is now possible. Here we attempt to address spleen-specific steady-state hematopoiesis using valine-restricted dietary conditioning, so removing the need for irradiation therapy prior to HSC transplantation. Following optimization of a dietary-based conditioning regime to clear HSC niches, donor chimerism was achieved within both the spleen and bone marrow, so demonstrating the potential value of this model particularly in regard to steady-state hematopoiesis involving the spleen.

Published lineage commitment models describing hematopoiesis are controversial and still incomplete in predicting how fate-decision occurs. Current models fall short of describing the symmetry by which HSC progress through lineage commitment, and whether there are defining genes or imprinted epigenetic programs driving the various differentiation pathways at particular periods during life. For example, myeloid-biased CD150^{hi} HSC appear increasingly with age, evident by an imbalance in myeloid and lymphoid cell development. Given that HSC localized in spleen reflect cells with myeloid-restricted potential, this study considers how the spleen contributes to the age-associated decline in balanced lineage output potential.

The overall hypothesis of this thesis is that HSC differentiation in spleen under steady-state conditions is biased towards myelopoiesis, and that throughout adult aging, the spleen microenvironment continually imprints myeloid bias into HSC programming, therefore contributing to a rise in myeloid-biased HSC numbers. The first aim of this study is to address these unknown gaps in research by optimizing a new transplant pre-conditioning method that maintains the host steady-state condition in order to study the spleen-specific contribution to hematopoiesis. These results then complement the second aim which is to investigate the role of spleen in the age-associated dominance of myeloid-biased HSC.

Optimization of valine-restriction preconditioning found that mice fed a valine-deficient diet for three weeks tolerated immediate complete diet reintroduction. By allowing 2-days of valine reintroduction prior to transplantation it was found that donor cell engraftment could be achieved. We suggest that cell-dose titration is necessary to enhance donor engraftment since valine-restriction preconditioning does not clear hematopoietic niches entirely. Results of investigation of the second aim indicate that spleen does not play a significant role in the progressive myeloid-biased HSC shift over an animal's lifetime. However, no firm conclusion can be drawn due to data variability found in aged mice. Overall, the work presented in this

thesis does not show conclusively that spleen contributes to the accumulation of myeloid-biased HSC over age. Optimization of a dietary-based preconditioning method will assist future investigation into the hematopoietic contribution of spleen in the steady-state condition.

Declaration

This thesis is submitted to Bond University in fulfilment of the requirements of the degree of Master of Science by Research.

This thesis represents my own original work towards this research degree and contains no material which has been previously submitted for a degree or diploma at this University or any other institution, except where due acknowledgement is made.

…….

Jacqualine Kaden

20th August 2019

Acknowledgements

Firstly, I would like to thank my supervisors Jonathan Tan and Helen O'Neill for all your support and guidance over these few years. Thank you for giving me the time of day to talk through all my ideas, theories and concerns and in return offering me encouragement and valuable lessons. This experience has been one I will never forget.

To my parents, Andries and Vauneen, thank you for your endless love and support throughout the poorest and most stressful years of my life to date. Especially to my mom for listening to me explain my thesis topic even while you have no idea what I'm talking about. I could always count on you both for a loving shoulder to cry on. My happiest moments have been with you and I can't thank you both enough.

To my lab group, thank you for listening to my run through my project and offering outside perspectives on things I never would have seen on my own. I especially would like to thank Christie for being my rock throughout this entire experience. All the late nights in the office together, midnight MacDonald's trips, little gifts of support and encouragement, and surprise ice cream visits when the FACS machine was giving me grief made everything so much more bearable. I am eternally grateful to have had you as my lab buddy and close friend.

To my friends, thank you for endlessly listening to me complain about literally everything over and over again without ever telling me to shut up. You all have the patience of saints.

And finally, I'd like to thank Vittorio. For the last year and 4 months of my degree you have been on the phone with me everyday making sure I have eaten enough, had enough sleep and make time for myself to avoid burn out. You have been an amazing rock in my life.

Abbreviations

APC	Allophycocyanine
Bala	Balanced
BM	Bone marrow
BV	Brilliant violet
CD	Cluster of differentiation
CD	Complete diet
CLP	Common lymphoid progenitor
CMP	Common myeloid progenitor
DC	Dendritic cell
DiR	1,1'-dioctadecyl-3,3,3',3'-tetramethylindotricarbocyanine
DMEM	Dulbecco's modified eagle's medium
DNA	Deoxyribonucleic acid
EMH	Extramedullary hematopoiesis
EPCR	Endothelial protein C receptor
FACS	Fluorescence activated cell sorting
FcBl	Fc block
FITC	Fluorescein isothiocyanate
FMOC	Fluorescence minus one control
FMOC	Forward minus one control
FSC	Forward scatter
GMP	Granulocyte-monocyte progenitor
HPC	Hematopoietic progenitor cell
HSC	Hematopoietic stem cell
Lin	Lineage
LMPP	Lymphoid primed multipotent progenitor
LSK	$Lineage^{-}Sca\text{-}1^{+}cKit^{+}$
LT-HSC	Long term-hematopoietic stem cell
Ly-Bi	Lymphoid-biased

MEP	Megakaryocyte-erythroid progenitor
MFI	Median fluorescence intensity
MI	Myocardial infarction
MPP	Multipotent progenitor
My-Bi	Myeloid-biased
MyRP	Myeloid repopulating progenitor
PBS	Phosphate buffered saline
PE	Phycoerythrin
PE-Cy7	Phycoerythrin-Cy7
PI	Propidium iodide
RBC	Red blood cell
RFU	Relative fluorescence units
ROS	Reactive oxygen species
SEM	Standard error of the mean
SLAM	Signaling lymphocyte activation molecule
SPL	Spleen
SSC	Side scatter
ST-HSC	Short term-hematopoietic stem cell
TB	Trypan blue
WBC	White blood cell

Table of Contents

List of Tables & Figures

CHAPTER 1

Introduction

1.1 Hematopoietic Stem Cells

1.2.1 Heterogeneity

In mammals, HSC are responsible for complete blood cell production during embryonic development which continues throughout adulthood. The ability of HSC to propagate production of all blood cell types can now be defined by key characteristics that distinguish those stem cells (Ng & Alexander, 2017). HSC have functional capacity for hematopoiesis, producing a complex hematopoietic hierarchy of quiescent, repopulating and self-renewing stem cells, multi-potential progenitor cells, lineage committed progenitors, and mature erythroid, myeloid and lymphoid blood cells (Ito & Frenette, 2016). Phenotyping and *in vivo* repopulation assays have been used effectively to divide the HSC compartment into long term (LT) and short term (ST) repopulating HSC (Osawa, Hanada, Hamada, & Nakauchi, 1996). LT-HSC are found in the bone marrow environment in niches existing under relatively hypoxic conditions (Nombela-Arrieta et al., 2013). LT-HSC give rise to lifelong production of lymphoid and myeloerythroid lineages after transplantation into lethally irradiated recipients (Christensen & Weissman, 2001). Their direct progeny are phenotypically and transcriptionally distinct ST-HSC (Dykstra et al., 2007), which have more limited self-renewing capacity than LT-HSC, but can still produce a transient wave of hematopoietic reconstitution giving rise to all blood lineages for ~8-12 weeks in murine hosts (Christensen & Weissman, 2001; Sawai et al., 2016). Multipotent progenitors (MPP) are functionally similar to ST-HSC, although they are known to have less proliferative potential (Dykstra et al., 2007).

1.2.2 LT-HSC Subsets and Differentiation

Historically, LT-HSC were considered to be a biologically homogenous population of stem cells (Dykstra et al., 2007). However, it is now accepted that they are a heterogeneous population (Christensen & Weissman, 2001; Kiel et al., 2005; Seita & Weissman, 2010). Heterogeneity within the HSC pool has been defined in terms

of multiple functional and behavioural properties, including size, self-renewal capacity, cell cycle status, differentiation capacity, surface molecule expression and lifespan (Christensen & Weissman, 2001; Ema, Morita, & Suda, 2014). The differentiative potential of cells within the HSC compartment is now a topic of rigorous investigation. In particular, the analysis of serially transplanted adult HSC have been reported to propagate distinct patterns of differentiation (Benz et al., 2012; Dykstra et al., 2007; Kent et al., 2009; Morita, Ema, & Nakauchi, 2010).

Recent lineage reconstitution assays in mice transplanted with cultured or freshly purified adult bone marrow cells now confirm that individual HSC have distinct differentiation capacities. The results of these studies have led to newly coined terms describing HSC with a bias towards either myeloid lineage, lymphoid lineage, or a balance of both lineages (Muller-Sieburg, Cho, Karlsson, Huang, & Sieburg, 2004). Durable self-renewal activity, but variable lymphopoietic activity in HSC, was first described as “myeloid-biased” and “balanced” in a study by Muller-Sieburg et al. (2004). Analysis was based on the measurement of the clonally-derived myeloid to lymphoid cell ratio in the peripheral blood of transplant recipients (Muller-Sieburg et al., 2004). Within the context of defining HSC as myeloid-biased and balanced, alternative terms are now used to describe slightly different HSC subtypes, which reflect a more precise classification (Benz et al., 2012). This classification compares clonal contribution of isolated stem cells to the total peripheral blood lymphoid and myeloid compartment. This circumvents the impact of host-specific variation on those values, as well as adjusts the calculation for defining lymphoid and myeloid ratios. These alternative terms are α-HSC (also known as My-bi HSC), β-HSC (balanced) and γ- and δ-HSC (Lymphoid-biased) (**Figure 1.2.1**) (Beerman et al., 2010; Benz et al., 2012; Ema et al., 2014; Morita et al., 2010).

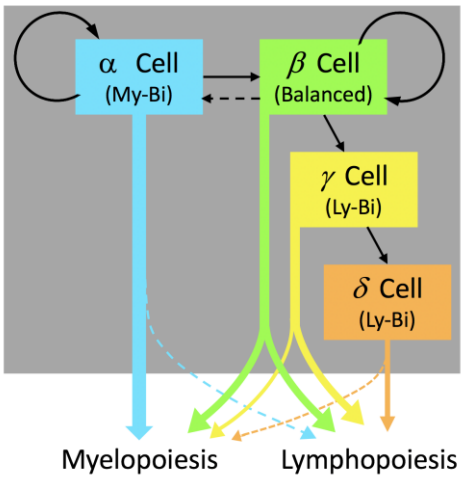

Figure 1.2.1 Differentiation classification of repopulating HSC from single-cell transplantation studies in mice.

Individual HSC have distinct differentiation capacities leading to new terms which describe repopulation potential and differentiation hierarchy. Within the grey box is the four cell types with long-term (>16 weeks) repopulating activity. α cells represent the LT-HSC with a strong propensity for myelopoiesis which can be independently and exclusively sustained as well as contribute to lymphoid repopulating potential. β cells are self-renewing LT-HSC with balanced lymphopoiesis and myelopoiesis output potential while γ- and δ-HSC are derived from α and β HSC and contribute mostly toward lymphopoiesis. Dotted lines suggest lineage contribution is minimal and thick lines suggest main pathway of contribution (Dykstra et al., 2007).

In a long term (≥16weeks) analysis of clonal progeny generated in irradiated mice transplanted with 352 single cells, or their immediate 4-day progeny, four distinct repopulation patterns arising from transplanted single cells were detected in the host (Dykstra et al., 2007). These included the previously introduced α and β HSC, as well as γ and δ type HSC (**Figure 1.2.1**) (Dykstra et al., 2007). The α and β patterns were distinct by having sturdy self-renewal activity and stable self-perpetuation of

the original α and β repopulation pattern amongst their progeny (Benz et al., 2012; Dykstra et al., 2007). The γ and δ patterns appeared to be closely related to ST repopulating cells (ST-HSC and MPP), but display multipotency and contribute to the circulating WBC pool for up to 16 weeks, distinguishing γ and δ from ST-HSC. The decline in their repopulating activity suggests exhaustion of self-renewal capacity within 6-7 months, identifying an intermediate stage of repopulating cells arising from β cells (Dykstra et al., 2007; Ema et al., 2014; Morita et al., 2010). In light of these recent findings on heterogeneity within murine HSC in terms of behavioural and differentiative capacity, the hierarchical model of the mouse hematopoietic system is now in dispute.

The classical differentiation model describes the stepwise, symmetrical and linear branching of cells that make up the hematopoietic system, initiated by HSC (LT then ST) within the top tier of the model (Akashi, Traver, Miyamoto, & Weissman, 2000; Kondo, Weissman, & Akashi, 1997; Reya, Morrison, Clarke, & Weissman, 2001). Phenotypically, HSC are contained within the cell fraction devoid of mature cell lineage markers, otherwise known as lineage negative (Lin^-) hematopoietic cell population. These are marked by expression of two common markers, Sca-1 and the cKit tyrosine kinase receptor. All three phenotypes are typically combined and referred as LSK (Spangrude, Heimfeld, & Weissman, 1988). The classical model defines three hematopoietic cell types that align with the LSK phenotype: LT-HSC, ST-HSC and MPP. To distinguish between LT-HSC and ST-HSC, one can use the CD34 marker of ST-HSC and other downstream progenitors (**Figure 1.2.2.A**). CD34 is a transmembrane phosphoglycoprotein that was first identified on HSC, but is not a specific marker and is also expressed by many other cells unrelated to the hematopoietic system (Sidney, Branch, Dunphy, Dua, & Hopkinson, 2014).

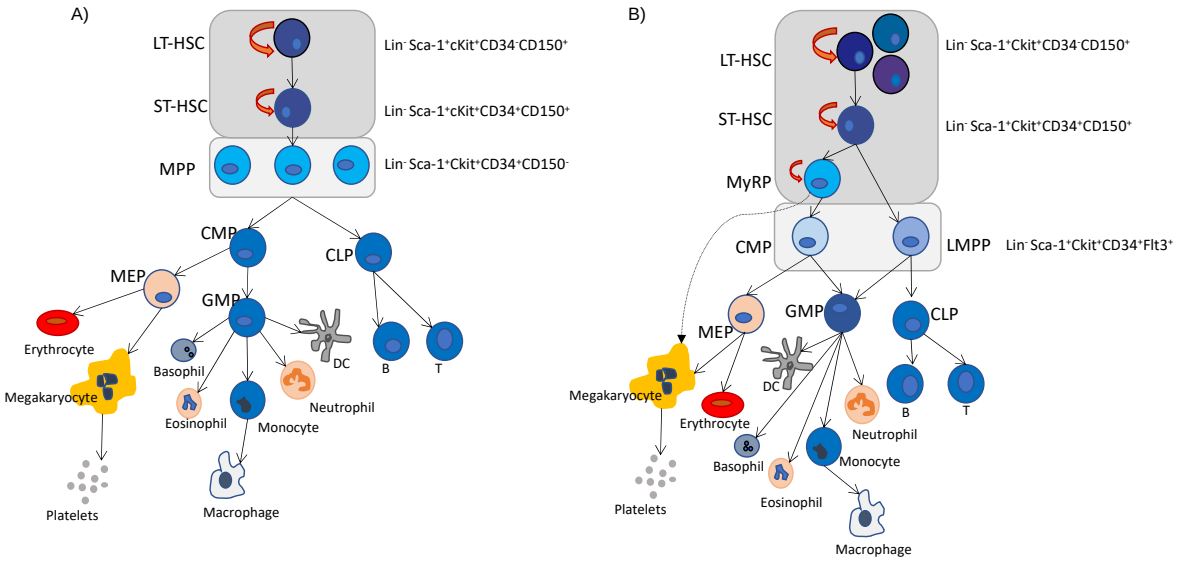

Figure 1.2.2 Classical differentiation and myeloid-bypass differentiation hierarchy.

Two varying models of HSC differentiation in the murine hematopoietic system. The dark grey box defines the HSC compartment and light grey defines MPP compartment in both models. A) Classical differentiation hierarchy is adapted from Shao et al. (2013) showing symmetrical differentiation. B) the myeloid-bypass model is adapted from Yamamoto et al. (2013) and Nimmo, May, and Enver (2015) showing myeloid restricted progenitors (MyRP) within the HSC compartment containing some potential for self-renewal. The lymphoid-primed multipotent progenitor (LMPP) lacks repopulating ability and stems from ST-HSC rather than MPP. The dotted line indicates a bypass pathway for megakaryocyte differentiation. Wide heterogeneity is known within the HSC compartment and is depicted with distinct LT-HSC clones at the hierarchy's apex.

The signaling lymphocyte activation molecule (SLAM) family markers can be used to definitively separate HSC subsets in mice. SLAM molecules comprise the family of CD150, CD48, CD229 and CD224 that regulate proliferation and activation of lymphocytes (Kiel et al., 2005). These are type I transmembrane receptors broadly expressed on immune cells and are typically self-ligands (Veillette, 2010). One

marker of HSC that has gained wide adoption is CD150, a member of the SLAM family (Oguro, Ding, & Morrison, 2013; Wilson et al., 2015). Expression of CD150 and CD48 can be used in conjunction with the LSK phenotype to distinguish LT-HSC, ST-HSC and MPP. It is known that the LSK/CD34^{-}CD150^{+}CD48^{-} subset is enriched for LT-HSC, the LSK/CD34^{+}CD150^{+}CD48^{-} subset is enriched for ST-HSC, and the LSK/CD34^{+}CD150$^{+/lo/-}$CD48^{+} subset is enriched for MPP (Kiel et al., 2005; Oguro et al., 2013). The classical hierarchical model for hematopoiesis also describes differentiation of MPP giving rise to oligopotent lineage-committed progenitors with both lymphoid and myeloid committed progenitors (Akashi et al., 2000). However, with MPP now known to be heterogeneous (Yamamoto et al., 2013), such a direct differentiation model towards committed progenitor production is now thought to be a simplification of many more comprehensive and complex pathways (Ema et al., 2014; Woolthuis & Park, 2016).

1.2.3 Evolving Models for HSC Differentiation

As more information on HSC heterogeneity is uncovered, the more complex the differentiation of HSC to blood cells appears to become (Adolfsson et al., 2005; Morita et al., 2010). For perspective, over the past 3 decades several hierarchy models have been proposed, including the stochastic model (Ogawa, Porter, & Nakahata, 1983), a model based on transcription factors (Singh, 1996), alternative and composite model (Adolfsson et al., 2005), the myeloid-bypass model (**Figure 1.2.2B**) (Yamamoto et al., 2013) and the newly suggested platelet-biased model (Kovtonyuk, Fritsch, Feng, Manz, & Takizawa, 2016). Similarities between the composite, alternative and myeloid-bypass model involve the deviation from ST-HSC towards a lymphoid-primed multipotent progenitor (LMPP) and a myeloid progenitor that may have distinct megakaryocyte/erythroid potential. The myeloid-bypass model suggests that a myeloid-restricted progenitor (MyRP) exists within the CD34^{-} HSC compartment which can self-renew and supply the majority of the of myeloid cells (eg. platelet, erythroid, neutrophil/monocyte) (Yamamoto et al., 2013).

Long-term multilineage reconstitution of lethally irradiated murine bone marrow from individual purified HSC or limiting doses of whole bone marrow transplants reveal this functional heterogeneity within HSC.

HSC heterogeneity, LT-repopulating capacity and HSC age can all be examined through measurement of CD150 expression (Beerman et al., 2010; Kiel et al., 2005; Morita et al., 2010). A study by Morita et al. (2010) transplanted single $CD150^{high}$, $CD150^{medium}$ and $CD150^{negative}$ $CD34^{-}$LSK cells into primary recipients and found repopulating activity was detected in all fractions, suggesting repopulating potential in the primary recipient is relatively equal amongst $CD150^{+/-}CD34^{-}$LSK cells. However, secondary transplantation of only $CD150^{high}CD34^{-}$LSK cells exhibited LT-repopulating potential. Consistent with other studies, $CD150^{high}CD34^{-}$LSK cells predominantly reconstituted myeloid lineages, whereas $CD150^{negative}CD34^{-}$LSK cells reconstituted lymphoid lineages and $CD150^{medium}CD34^{-}$LSK cells intermediately reconstituted both myeloid and lymphoid lineages in a pattern in between $CD150^{high}$ and $CD150^{negative}$ activity (Morita et al., 2010). Furthermore, Beerman et al. (2010) competitively transplanted 10 or 50 purified aged (24-month-old) murine HSC and reported predominantly myeloid-biased reconstitution, in contrast to recipients transplanted with young (4-month-old) HSC. Beerman et al. (2010) further reported that the majority of aged HSC with increased myeloid-biased potential also expressed CD150 in high amounts, which is consistent with the results of Morita et al. (2010).

One limitation of the Beerman et al. (2010) study is the transplantations of multiple HSC as opposed to single cell transplants. Single cell transplants identify the rare HSC that may be $CD150^{high}$ but produce a low level of primary myeloid-reconstitution and sustain multilineage secondary reconstitution (Morita et al., 2010). In contrast, bulk HSC transplantation can mask and neglect the contribution of heterogeneous cells within a theoretically pure and highly enriched HSC population. Surprising and recent findings exploiting single-cell transplantation and lineage tracing technologies

now suggest that a platelet-biased HSC sit at the apical of the hematopoietic hierarchy (Sanjuan-Pla et al., 2013). Platelet-biased HSC express the blood plasma glycoprotein, von Willebrand factor, and can give rise to platelets and erythroid lineages earlier than other lineages and so generate both myeloid- and lymphoid-biased HSC (Grover et al., 2016; Kovtonyuk et al., 2016; Sanjuan-Pla et al., 2013). This heterogeneity within highly conserved classical progenitors suggests that an alternative lineage commitment pathway is at work. Advances in single-cell analysis provide a pathway to study heterogeneity and fate-mapping processes within a cell population.

1.2.4 Lineage Commitment

Commitment is the irreversible point at which the cell becomes restricted in its potential to differentiate into any other cell type. HSC are multipotent, and able to form many cell types, while myeloid and lymphoid progenitors are historically considered restricted to producing myeloid or lymphoid lineage cells. An understanding of how HSC differentiate into different cell types and how they attain their various functions has clinical significance. It was previously thought that lineage commitment occurred at the lineage-restricted progenitor level, rather than at the level of the HSC (Cavazzana-Calvo et al., 2011). However, extensive self-renewal capacity and the ability to reconstitute all mature cells, albeit at different lengths of time, are characteristics that set lineage-biased HSC apart from lineage restricted progenitors (Muller-Sieburg, Sieburg, Bernitz, & Cattarossi, 2012).

HSC have long been assumed to be epigenetically primed to give equal probability in differentiation. However, variation in mature blood cell populations produced from individual HSC has now been characterized (Beerman et al., 2010; Challen, Boles, Lin, & Goodell, 2009; Copley & Eaves, 2013; Morita et al., 2010). Single-cell imaging and tracking methods are firmly established for observing cell differentiation, lineage determination and homing patterns. Several studies have used single-cell tracking

technology to study continuous long-term single-cell blood generation (Cao et al., 2004; Eilken, Nishikawa, & Schroeder, 2009), co-regulation of transcription factors in differentiation dynamics of single-HSC (Hoppe et al., 2016), and real-time early dynamics of hematopoietic reconstitution in live animals (Cao et al., 2004). Each of these studies cannot conclude definitively whether intrinsic or extrinsic mechanisms are responsible for lineage-commitment but rather a multitude of extracellular signals activating upstream regulators of lineage-specific transcription factors (Eilken et al., 2009; Hoppe et al., 2016; Krause et al., 2001). It is clear that mechanisms that drive cell fate decision for lineage commitment are crucial to understanding the development of blood malignancies and the age-associated decline of a balanced hematopoietic output.

1.3 The Aging HSC

Hematopoietic aging is driven by intrinsic and extrinsic factors that leads to a decrease in immune response (Linton & Dorshkind, 2004) and regenerative capacity (Ergen & Goodell, 2010; Florian et al., 2012), and an increase in myeloid cell proliferative diseases (Kiss, Sabry, Lazarus, & Lipton, 2007). Multiple studies analysing the murine hematopoietic system over age have reported a progressive increase in myeloid cells and a decrease in erythropoiesis and T and B cell production (Beerman et al., 2010; Florian et al., 2012). Functional changes within the HSC compartment have been reported as contributors to the decline of balanced HSC differentiation (Beerman & Rossi, 2014). Studies using limiting dilution transplant HSC assays confirmed a functional heterogeneity amongst the conserved HSC subtypes found in the bone marrow of young mice (Beerman et al., 2010; Dykstra et al., 2007). HSC which exhibit preference toward myeloid lineage differentiation represented <25% of LT-HSC in young mice, but gradually increased following normal physiological aging (Beerman et al., 2010). Lineage-biased HSC subsets could also be isolated from both young and old mice based on differential CD150 expression, and HSC sorted as side population^{low} (with ~80% of the lower

side population CD150^{hi}) cells presented a functional capacity for myeloid-bias upon transplantation. This suggested that differential CD150 expression was a defining and reliable marker for HSC heterogeneity (Challen et al., 2009). Major alterations in functionality and molecular regulatory pathways commonly identified across HSC aging studies include lineage-biased clonal composition (Beerman et al., 2010), cell polarity changes (Florian et al., 2012), epigenetic dysregulation induced by increased inflammation (Chambers et al., 2007), increased levels of radical oxygen species (ROS) (Ito et al., 2006), and accumulation of DNA damage (Rossi et al., 2007; Wang et al., 2012). The factors contributing to intrinsic and extrinsic mechanisms of HSC aging, age-associated progression of lineage-bias, and the functional changes of HSC with age, are considered further below.

1.3.1 Intrinsic Mechanisms

It is understood that HSC aging could be driven by both cell-intrinsic mechanisms (eg. epigenetic preprograming) and cell-extrinsic (eg. environmental-, cytokine- and stress- mediated) mechanisms. A key hallmark of HSC aging is the gradual predominance of myeloid differentiation, although the mechanism behind this progressive lineage-biased skewing is unknown, whether spleen contributes to this age-related change is addressed in this study. Hematopoietic stem cells are capable of sustaining lifelong blood cell production, and repeated serial transplantation shows that HSC can outlive their original donor. Other studies however report evidence of HSC exhaustion (Harrison, 1979) perhaps due to telomere loss during cell division (Kamminga et al., 2005; Van Zant, de Haan, & Rich, 1997). Heterogeneity within the HSC compartment is well known, and lifespan of HSC is also a heterogeneous characteristic detected in all clonal analyses (Muller-Sieburg et al., 2004; C. Muller-Sieburg & Sieburg, 2008; Sieburg et al., 2006). More recent analysis of the intrinsic nature of changes in LT-HSC during age includes altered lineage potential, whereby genes responsible for function and specification were down-regulated (CD150^{lo}) within the lymphoid compartment and up-regulated

(CD150^{hi}) within the myeloid compartment (Beerman et al., 2010; Morita et al., 2010; Rossi et al., 2005).

1.3.2 Extrinsic Mechanisms

Aging is a risk factor for myeloproliferative diseases such as leukaemia, and studies have suggested that the niche environment that HSC interact with, and not only cell-intrinsic mechanisms, have the capacity to shift lineage output as we age under a dominant CD150^{hi} HSC clone (Vas, Senger, Dorr, Niebel, & Geiger, 2012). Serial HSC transplant assays have been used as a model to study stem cell aging, shedding light on the reconstitution kinetics and lineage-commitment preference of aging HSC. The Beerman et al. (2010) study showed that CD150^{lo} balanced HSC became progressively more myeloid-biased with each successive round of transplantation so that by the third transplant 88% of recipients displayed myeloid-biased reconstitution patterns similar to reconstituted old transplanted HSC. This suggests that the spleen niche impacted the behaviour of the HSC long after they had left the niche. Furthermore, the study detailed that there were no differences observed between CD150^{hi} and CD150^{lo} HSC in cell cycle activity. These data together suggest that CD150^{hi} HSC do not progressively dominate the HSC compartment over time due to and increased rate of cycling but through another mechanism in the spleen.

Bone marrow HSC which enter the spleen adopt a pre-activated cell cycle status allowing HSC in the spleen to quickly enter the cell cycle for fast hematopoietic response (Coppin et al., 2018). This suggests that the spleen microenvironment, not only varies to that of the bone marrow microenvironment, but does indeed instruct HSC to behave differently. One major stromal cell that bone marrow has and spleen lacks is osteoblasts. A study showed that loss of osteoblasts induced dramatic hematopoietic alterations, including decreased bone marrow hematopoiesis and distinctly increased spleen hematopoiesis which showed a relative increase in the

myeloid compartment (Visnjic et al., 2004). Alterations in signaling can be linked with decreased bone formation and osteopontin secretion, increased adipogenesis, changes in extracellular matrix, tissue structure damage and receptor insensitivity, all of which contribute to an aging-associated decline in HSC (Guidi et al., 2017). How the spleen contributes to hematopoiesis has only been studied in diseased conditions, but in each of these studies the spleen is found to be a niche with the capacity to prime HSC for myeloid response (Bronte & Pittet, 2013; Robbins et al., 2012; Wu et al., 2018).

1.4 Hematopoiesis in the Spleen

HSC in the spleen are rare, however transplanted HSC isolated from the spleen display long term reconstitution potential (Wolber et al., 2002). Since HSC are known to enter blood circulation in steady-state (Wright, Wagers, Gulati, Johnson, & Weissman, 2001), it is no surprise that the spleen hosts a small population of HSC which contribute to erythropoiesis, alongside bone marrow HSC (Dzierzak & Philipsen, 2013; Yanai, Satoh, & Obinata, 1991). However, the splenic niche and bone marrow niche are quite different, and therefore spleen-specific hematopoiesis is presumably distinct. For example, spleen lacks the presence of osteoblastic cells, which play a key role in maintaining non-dividing HSC, or quiescence, in the bone marrow (Calvi et al., 2003). Likewise, HSC in the spleen are reported to be phenotypically distinct and exist in a pre-activated state, allowing spleen-derived HSC to respond to emergency signals quicker by entering cell cycle, compared to the more quiescent HSC counterpart in bone marrow (Coppin et al., 2018). However, hematopoiesis in spleen remains difficult to analyse.

1.4.1 Pre-conditioning for HSC Transplant

Current methods for transplantation of HSC requires niche clearance to provide the best chance of donor engraftment. HSC transplant pre-conditioning irradiation

permanently damages bone marrow microenvironment (Abbuehl, Tatarova, Held, & Huelsken, 2017) which is also required for cell signaling and engraftment for HSC reconstitution. Irradiation damage subsequently initiates systemic inflammatory responses and perhaps augments the true behavioral profile of HSC reconstitution. Moreover, hematopoiesis in bone marrow has been more widely studied than in the spleen, and hematopoiesis in the spleen during steady-state is even more enigmatic.

Transplantation studies addressing the precise function of spleen during steady-state hematopoiesis have been hampered by limitations in traditional HSC conditioning. A recent study proposed novel niche clearance methods that allow a promising future for steady-state hematopoiesis studies. Taya et al. (2016) suggested that selectively restricting the essential amino acid, valine, from the diet for a small period of time significantly decreased the number of host HSC. Complete blood counts from mice fed valine restricted diets for 4 weeks showed marked reduction in WBC, and RBC, whereas platelet counts, bone marrow T cells and megakaryocyte-erythroid progenitor cells were unaffected. Depletion of valine from the diet appears to reduce the number of lifelong side effects typically experienced from chemotherapy and irradiation as myeloablative treatments. Such side effects include growth retardation, infertility, and significantly shorter lifespan (<1-year post-transplant). The integrity of the splenic niche structure during valine restriction to achieve HSC depletion is yet to be studied. One systemic effect of the valine restriction was splenic atrophy. However, spleen rapidly reverted to normal size, evident by a gain of splenic red and white pulp, once a complete diet was resumed (Taya et al., 2016). The Taya et al. study reported good engraftment (>1% donor chimerism) from 5 $x10^3$ transplanted donor LSK cells and $1x10^7$ transplanted donor bone marrow cells (2016). Valine restriction may offer a promising look into spleen hematopoiesis during the steady-state as concurrent comparative studies.

1.4.2 Extramedullary Hematopoiesis

Extramedullary hematopoiesis (EMH) is the production of blood cells outside of the medullar of the bone marrow cavity, where hematopoiesis typically occurs. It is trilineage, meaning it gives rise to each of the myeloid, lymphoid and erythroid lineages. However, it has been reported that a particular lineage or cell type may dominate, depending on the underlying pathogenesis (Johns & Christopher, 2012). Studies on prevalence and cell production during extramedullary hematopoiesis are limited, partly due to the perception that it is an epiphenomenon or state which is secondary to a primary condition of inflammation, infection, myeloproliferative disease, or physiological stress (Johns & Christopher, 2012). This leads to the migration of HSC into the spleen where they undergo hematopoiesis in sinusoidal niches (Inra et al., 2015) and contribute to blood cell production (Bronte & Pittet, 2013; Wright et al., 2001). Nevertheless, EMH in the spleen contributes to disease pathogenesis for conditions like atherosclerosis (Robbins et al., 2012; Tall & Yvan-Charvet, 2015), acute myocardial infarction (Kim, Kim, Kang, & Seo, 2014; Thackeray et al., 2015) and myeloproliferative diseases (Prakash et al., 2012; Song, Park, & Uhm, 2018).The conditions are not yet understood (Johns & Christopher, 2012).

Extramedullary hematopoiesis develops in spleen during pregnancy, induced by an increase in estrogen levels in females (Nakada et al., 2014). Pregnant mice display significantly increased cellularity, erythropoiesis and myelopoiesis in spleen, as well as increased numbers of HSC (Nakada et al., 2014). Following deletion of the *Esr1* gene responsible for estrogen production, pregnant mice showed a reduction in pregnancy-associated hematopoiesis and HSC numbers, but no change in HSC frequency in bone marrow. *Esr1* deletion was also associated with reduced cellularity and erythropoiesis in spleen (Nakada et al., 2014). This finding indicated mobilization of proliferating HSC to the spleen was critical to sustain erythropoiesis during

pregnancy (Nakada et al., 2014). Alternatively, *Esr1* could control HSC proliferation, rather than mobilization of HSC from bone marrow towards the spleen. A recent study demonstrated that expression of transcription factor *Tlx1* on splenic stromal cells are required for mobilizing HSC into the spleen during extramedullary hematopoiesis (Oda et al., 2018). Interestingly, Oda et al. reported that the overexpression of *Tlx1* was sufficient to induce extramedullary hematopoiesis, without any additional stimulating factors (2018). The human spleen in pregnancy is less studied. However, an increase in spleen cellularity, erythropoiesis and overall size during human pregnancy is consistent with murine studies (Maymon et al., 2006). Here, pregnancy is used as an inducible model for studying extramedullary hematopoiesis in spleen.

Evidence from *in vitro* studies (O'Neill et al., 2004) and *in vivo* models of extramedullary hematopoiesis (Coppin et al., 2018; Nakada et al., 2014; Swirski & Robbins, 2013) suggests that spleen-resident HSC are primed for myeloid cell production. This is shown by atherosclerosis studies which report that approximately 50% of myeloid cells are produced by spleen (Swirski & Robbins, 2013). In myocardial infarction (MI) increased total myeloid cells have been reported in spleens of mice (Coppin et al., 2018). Moreover, splenic HSC exhibit a pre-activated, with splenic HSC readily in G1 cell cycle phase in the steady-state condition, as opposed to bone marrow HSC which are robustly retained in a quiescent G0 phase (Coppin et al., 2018). More interestingly, when pre-activated HSC in spleen mobilize back to bone marrow, the HSC are able to resume the quiescent G0 state (Coppin et al., 2018). Taken together, the spleen is known to, 1) favor myelo- and erythro-poiesis in stressed or inflammatory conditions, 2) maintain HSC in a pre-activated state, and pregnancy can increase HSC mobilization into the spleen which in turn increases hematopoiesis. Therefore, the spleens role in age-related myeloid-biased HSC differentiation can be assessed by inducing multiple cycles of pregnancy as a model for aging, driven by the repeated bone marrow to spleen mobilizing events.

1.4.3 Spleen in Mice and Humans

The spleen acts as an accessory organ in both humans and mice during stress-induced or diseased states (Dor et al., 2006; Nakada et al., 2014). In contrast, hematopoiesis under physiological steady-state conditions remains poorly understood. In rodents, the spleen acts largely as a site for erythropoiesis (Yanai et al., 1991) and megakaryocytopoiesis (Slayton et al., 2002), and an important filter for turnover of red blood cells. Most studies on spleen as a hematopoietic organ involve the murine model, which has similarities with human spleen in terms of immune cell development and function, although structural differences involving the marginal zone, the ratio of white and red pulp, and the vasculature are apparent (Mebius & Kraal, 2005; O'Neill, 2012; Steiniger, 2015). As a site for steady-state extramedullary hematopoiesis, both murine and human spleen remain poorly investigated in terms of HSC development during adult ontogeny. Splenectomy in murine models was once thought to have no impact on hematopoietic development. However, recent *in vitro* studies may indicate an important function for spleen in myelopoiesis, with evidence of spleen endothelial cells supporting the presence of a specific dendritic-like cell progenitor endogenous to the spleen (Bronte & Pittet, 2013; Tan & O'Neill, 2012). The spleen is a secondary lymphatic organ, that lacks afferent lymphatics, facilitating leukocyte collection directly from the blood and is thus important in immunity to bacterial infections (Steiniger, 2015). A consequence of splenectomy in human patients is increased susceptibility to infection with encapsulated bacteria like *Streptococcus pneumoniae, Neisseria meningitidis* and *Hemophilus influenza* type B, thus demonstrating how the spleen serves to protect the human body (Brendolan, Rosado, Carsetti, Selleri, & Dear, 2007; Bronte & Pittet, 2013).

Murine spleen offers a unique perspective into the mechanisms that govern HSC development, however reports replicating and translating murine research into human studies to validate human HSC in spleen have been few. A notable study

comparing human and porcine spleen reported human spleen cells giving rise to multiple hematopoietic colonies, but only when EMH was evident (Dor et al., 2006). The pig spleen, although it is larger than human spleen (by an average of 4g/kg body weight), appears to hold HPC in similar number to primate spleen, which is similar to human spleen. Although the primate spleen results were described as preliminary, they suggested human adult spleens may be equally a source of early HPC, or even HSC, that may prove of clinical use (Dor et al., 2006). Some similarities with age-associated changes found in both mice and humans exist, including increased incidence of myeloproliferative disorders, progressive decline in lymphopoiesis and rise in dominance toward myeloid-biased HSC differentiation, suggesting hematopoietic aging is an evolutionary conserved process (Muller-Sieburg et al., 2012; Pang et al., 2011). Humans also present with splenomegaly during pregnancy, suggesting increased cellularity in the spleen, as does in murine spleen during pregnancy (Nakada et al., 2014). Thus, murine studies have been an essential means for understanding and predicting human biology.

1.5 Rationale

Hematopoietic stem cells (HSC) are responsible for mammalian blood cell production. As adult stem cells, they are equipped with the remarkable capacity for self-renewal and multi-potency. While most of the adult HSC population resides and develops within the bone marrow niche, a smaller population of HSC has been identified within the spleen of several animal models (Dor et al., 2006; Wolber et al., 2002). Hematopoiesis within the spleen is commonly associated with stress or disease and is referred to as extramedullary hematopoiesis (Johns & Christopher, 2012). This can occur when bone marrow is compromised due to an inflammatory response or disease and cannot meet increased hematopoietic demand. One example is leukaemia, where the medullary cavity of bone marrow becomes overcrowded with immature white blood cells and reduces the capacity for normal hematopoiesis (Johns & Christopher, 2012).

Little is known about HSC differentiation in spleen, the precise function of spleen in steady-state hematopoiesis, or how hematopoiesis in spleen contributes to changes in cell differentiation associated with age and disease. Spleen-specific hematopoiesis varies from that of bone marrow in terms of the HSC activation state (Coppin et al., 2018), and hematopoietic output under *in vitro* conditions (O'Neill, 2012). However, it has been difficult to determine the precise lineage output of differentiating HSC in the spleen *in situ*, especially under physiological conditions. HSC transplantation studies require conditioning methods to clear stem cell niches in order for transplanted HSC to engraft. More specifically, these conditioning regimes typically involve full-body lethal irradiation which generates systemic inflammation. Recently, a dietary-based method of HSC niche clearance that does not stimulate an inflammatory response was described (Taya et al., 2016). This method now permits the study of steady-state hematopoiesis in spleen following adoptive HSC transfer.

An understanding of hematopoiesis due to splenic HSC has further implications in terms of whether spleen specifically contributes to myeloid-bias amongst HSC and hence the aging HSC phenotype. Evidence from *in vitro* studies (O'Neill et al., 2004) and *in vivo* models of extramedullary hematopoiesis (Nakada et al., 2014) suggests that spleen-resident HSC are 'primed' for myeloid cell production. Furthermore, the shift towards myeloid-biased differentiation has already been shown to increase with age (Balazs, Fabian, Esmon, & Mulligan, 2006; Beerman et al., 2010; Morita et al., 2010). Investigations into the cause of this shift focused on HSC intrinsic or extrinsic factors, with a clear knowledge gap surrounding the influence of the spleen microenvironment on HSC differentiation. Recent studies report that the expression of cell surface marker CD150 is higher on aged myeloid-biased HSC (Beerman et al., 2010; Morita et al., 2010). In addition, an imbalance in myeloid-biased $CD150^{hi}$ HSC is evident with age. By comparing the expression level of the CD150 marker on the surface of HSC in normal aged mice and normally aged splenectomised mice, one can assess the contribution of spleen to the accumulation of $CD150^{hi}$ myeloid-biased HSC. Furthermore, exbreeder mice that have gone through multiple cycles of pregnancy-induced extramedullary hematopoiesis can be used as a model for the contribution of extramedullary hematopoiesis in spleen towards increasing myeloid-biased HSC with aging.

1.6 Aims

The specific aims of this study are:

1. To determine the steady-state lineage output of HSC which differentiate in spleen.
2. To assess the role of spleen in age-related myeloid-biased HSC differentiation.

1.7 Significance

A knowledge of how the splenic niche signals HSC will provide insight into extramedullary hematopoiesis and its relationship with disease. The prevalence, distribution and molecular basis of extramedullary hematopoiesis in spleen is important for a complete understanding of hematopoiesis during aging and disease. In this study, we firstly hypothesize that lineage output in spleen under steady-state conditions predominantly involves myeloid and erythroid lineages. The contribution of spleen under steady-state condition towards the development of myeloid and erythroid lineages will impact our understanding of HSC fate mapping, and could direct understanding away from the classic symmetrical differentiation model (Akashi et al., 2000; Kondo et al., 1997), towards models based on single cell studies, such as the myeloid-bypass model (Nimmo et al., 2015; Yamamoto et al., 2013). Our second hypothesis predicts that the absence of a spleen in both aging and pregnant animal models will lead to a decrease in myeloid-bias amongst LT-HSC. The significance of such a finding is that the splenic niche would contribute to the progressive age-associated myeloid-biased differentiation and would drive the aging myeloid-biased phenomenon.

CHAPTER 2

Methodology & Materials

Mice

Adult male and female C57BL/6JArc (C57BL/6J), adult female B6.SJL-*Ptprc*^{a}*Pepc*^{b}/BoyJArc (B6.SJL) and adult female BALB/cARC (BALB/c) mice were purchased from the Animal Resource Centre (ARC; Perth, Western Australia, Australia) and held at the Bond University animal holding facility for experimentation. Mice were sacrificed via cervical dislocation. All mice were handled and housed according to protocols approved by the University of Queensland Animal Ethics Committee (Approval number: BOND/453/15/ARC/NHMRC).

Cell preparation

Cells were isolated from the spleen, bone marrow or peripheral blood. Bone marrow was collected from the femur and tibia of each leg by flushing into ice-cold phosphate buffer solution (PBS) (Thermo Fisher, Waltham, MA, USA) using a 26G hypodermic needle (Terumo, NSW Australia). Spleen was harvested and placed in ice-cold PBS. Approximately 1mL of peripheral blood was collected via retro-orbital bleeding using a 1.1mm x 75mm capillary micro-haematocrit tube (heparinized) (Thomas Scientific, New Jersey, USA), and collecting flow-through in 1mL Titertube micro test tubes (Biorad, CA, USA). Solid tissues were coarsely crushed through a wire sieve using a 5mL syringe plunger (Livingstone International, NSW, Australia) and transferred into a 14mL Falcon tube (BD, San Jose, USA) for centrifugation (200xg for 5 minutes, 4°C) (Heraus Megafuge 40R Centrifuge series; Thermo Fisher, Waltham, MA, USA). After discarding the supernatant (SN), cells were resuspended in red blood cell (RBC) lysis buffer (NH_4Cl, 0.017M Tris-base [pH7.5]) (eBioscience, San Diego, CA, USA) at 1mL buffer/organ, or 5mL lysis buffer/1mL whole blood. Cells were incubated for 10 minutes at room temperature (RT) and then washed with 10mL ice-cold PBS and centrifuged. The supernatant was discarded, and the cell pellet resuspended in 1ml FACS buffer (PBS/2%BSA/0.01%NaN_3). The cells were then filtered through a 70µm single cell strainer (Greiner Bio-One, Kremsmunster, Austria) into a new 14mL Falcon tube and kept on ice.

Magnetic cell separation

To enrich cell preparations for HSC isolation, mature lineage-positive cells were first magnetically depleted. A cocktail of lineage-specific biotinylated antibodies was used for depletion of mature cells (refer to **Table 2.1** for antibody list). Antibodies were specific for the mature cell markers: CD3 (T cells), CD11c (dendritic cells), CD19 (B cells), Gr-1 (monocytes and neutrophils), CD48 (T/B/myeloid cells) and NK1.1 (natural killers and T cell subsets). Anti-lineage antibody cocktails that label up to 10^7 cells were prepared by adding 1 µL of each antibody and 1µL of Fc Block (FcBl) to cells in a total volume of 100 µL FACS buffer. Cells were mixed and incubated with antibodies on ice for 10 minutes before washing with 5ml FACS buffer. After centrifugation and discard of SN, the cells were resuspended and incubated with anti-biotin MACS® Ultra-pure Microbeads (Miltenyi Biotec, Bergisch Gladbach, Germany) at 20µL/10^7 cells for 10 minutes on ice. Cells were resuspended in 2mL FACS buffer and transferred to a 5mL Falcon round bottom tube (StemCell Technologies, Vancouver, Canada). Tubes were placed into an EasySep Magnet (single 5mL tube holding capacity; StemCell Technologies, Vancouver, Canada) for 10 minutes at RT. To deplete lineage-positive cells, the supernatant containing unbound lineage-negative cells was poured into a fresh tube. The depletion step was repeated twice to increase lineage negative cell purity.

Cryosectioning tissues

Whole C57BL/6JARC adult spleen (7-months old) was immersed in a 10x10x5mm biopsy style Tissue-Tek Cryomold (Sakura Finetek, Tokyo, Japan) containing Tissue-Tek O.C.T (Sakura Finetek, Tokyo, Japan). Spleen tissue was placed into a foil vessel and frozen above liquid nitrogen. A CM1900 Leica cryostat (Leica Microsystems, Wetzlar, Germany) was set at approximately -14°C and sections were cut to 7µm thickness before applied to Sodalime white glass (UberFrost) Printer Slides (75.4 x 25.4 x 1 mm) (InstrumeC, Victoria, Australia).

Tissue section fixation and staining

Spleen sections were fixed in acetone (Sigma-Aldrich, St. Louis, MO, USA) for 5 minutes at RT. The section slides were then washed three times in PBS for 3 minutes at RT. The underside of the slide was completely dried using a Kimwipe (Kimberly-Clark, Irving, TX, USA). Each tissue section was first blocked with 25µL of Fc block (CD16/32) solution (see **Table 2.4** for section staining concentrations) and incubated at room temperature for 30-minutes inside an incubation chamber (Cosmo Bio, Tokyo, Japan) to protect from light and moisture loss. Slides were drained of excess FcBl before 25µL of primary antibody solution was applied and incubated for 1-hour at RT. **Table 2.4** lists staining concentrations used for primary antibodies. All tissue section slides were then washed three times in PBS for 3-minutes at RT. The underside of the slides was dried and a coverslip mounted using Mowiol 4-88 mounting medium (Sigma-Aldrich, St. Louis, MO, USA). Sections were visualized after 1-hour using a Nikon Live Cell Ti2 Microscope (details). All captured images were processed using ImageJ; FIJI v2.0.0 open source software (Laboratory for Optical and Computational Instrumentation; Maddison, MI, USA).

Flow cytometry

To analyse or isolate cells, flow cytometry was used in conjunction with a combination of primary antibodies and secondary reagents. **Table 2.2** lists HSC staining antibodies, **Table 2.3** lists antibodies used for homing and lineage characterization and **Table 2.4** lists antibodies used for lineage reconstitution studies. Antibody cocktails were prepared by diluting primary antibodies 1:100 into FACS buffer, and secondary reagents prepared as a 1:400 dilution. Cell staining was performed in a 96-well tissue culture U-bottom plate (Sigma Aldrich, St. Louis, MO, USA) aliquoting a maximum of 2 x 10^6 cells per well. OneComp eBeads (eBioscience, San Diego, CA, USA) were added for all single colour controls except propidium iodide (PI). For antibody staining, 10µL of primary antibody cocktail was added to wells, mixed, then incubated for 10 minutes on ice protected from light.

Cells were washed once with 150µL of FACS buffer and centrifuged again (5 minutes, 200g at 4°C). The supernatant was discarded and the secondary reagent was added to wells for a further 10-minute incubation on ice, protected from light. Cells were washed again (150µL of FACS buffer), centrifuged and resuspended in 150µL of FACS buffer. Cells were then transferred into a 5mL Falcon round bottom tube (StemCell Technologies, Vancouver, Canada) containing 2µl (10µg/mL) PI to discriminate cells as live (PI^-) or dead (PI^+). Cells were analysed or sorted using a FACSAria Fusion (Becton Dickinson Biosciences, San Jose, CA, USA). FlowJo v10.4.2 software (FlowJo, Ashland, OR, USA) was used for all post-acquisition analysis of FACS recorded experiments.

Adoptive cell transfer via tail vein injection

For intravenous injection via the tail vein, mice were gently placed underneath a heat lamp before placement in a cylindrical restraint device. The tail was swabbed with 80% ethanol and 100µl cell solution injected into the tail vein using a 26G insulin syringe (BD, San Jose, CA, USA). The needle was removed and pressure applied at the insertion site to stem bleeding. Once the bleeding ceased, the animal was returned back to its cage.

Intrasplenic injection

Mice were sacrificed via cervical dislocation. An incision was introduced approximately 1.5cm in length above the spleen along the transverse plane on the left oblique abdomen. The skin was separated from the peritoneal wall using blunt scissors and the peritoneal wall above the spleen was incised. The spleen was either exteriorized with gentle pressure or excised completely from the body prior to injection. A 1:8 dilution of trypan blue (Sigma-Aldrich, St. Louis, MO, USA) in phosphate buffer solution (PBS) (Thermo Fisher, Waltham, MA, USA) was used at volumes of either 50µL, 25µL or 20µL in an Ultra-Fine 0.3mL 30G insulin syringe (BD Bioscience, San Jose, CA, USA).

Injections administered to an excised spleen were held steady with Fine Point High Precision Forceps (Fisher Scientific, Hampton, NH, USA) while the needle was introduced along the coronal plane from the posterior extremity of the spleen. After slow fluid release, the needle was held *in* situ for approximately 30 seconds before the needle was slowly removed. The spleen was then observed by eye for 2 minutes after administration to assess progressive leakage with each volume.

Injections into an exteriorized spleen, 10µL of standard formulation Corning® Matrigel® Matrix (Corning Inc., Corning, NY, USA) was first gently aspirated into an Ultra-Fine 0.3mL 30G insulin syringe (BD Bioscience, San Jose, CA, USA). Then in the same syringe, 20µL of trypan blue was carefully aspirated, avoiding bubbles and mixing of trypan blue/Matrigel layers. The exteriorized spleens were steadied using a Fine Point High Precision Forceps (Fisher Scientific, Hampton, NH, USA) as the needle was introduced along the coronal plane from the posterior extremity of the spleen. Once the volume had been slowly introduced, the needle was held *in* situ for approximately 30 seconds before slow needle removal. The spleen was then observed by eye for 2 minutes after administration to assess progressive leakage. Temperature of the spleen was not measured during the procedure.

Dietary valine restriction

Mice receiving cell transplantations were “pre-conditioned” using a dietary-based method for depleting HSC from bone marrow (Taya et al., 2016). Dietary-based preconditioning first involved a short fasting phase, followed by valine-restricted feeding, and finally valine reintroduction into the diet (**Figure 2.1**). During fasting, mice were restricted from feed for two days but given unrestricted access to water. During valine-restricted feeding, ‘L-amino acid rodent diet without L-valine’ (Research Diets Inc., New Brunswick, NJ, USA) was introduced for three weeks. Reintroduction of valine into the diet then commenced, coinciding with cell transplantation. Over this period, L-valine (Sigma Aldrich, St. Louis, MO, USA) was returned to the diet, either through supplementation in the drinking water over two

weeks at various concentrations (see **Table 2.5**) or through immediate introduction of a complete diet.

Splenectomy

Splenectomies were performed by anaesthetizing mice using a Darvall Stinger Streamline Isoflurane vaporizer (Darvall Vet; Gladesville, NSW, Australia) set at 5% for induction, and 3% for abdominal surgery. Analgesic (Buprenorphine, Temgesic, NSW, Australia) was administered via subcutaneous injection at 0.02mg/kg. To access the spleen, the abdomen was shaved and swabbed with 80% ethanol. An incision was made approximately 1.5cm in length above the spleen along the transverse plane on the left oblique abdomen. The skin was separated from the peritoneal wall using blunt scissors and the peritoneal wall above the spleen was incised. Using gentle application of pressure to exteriorize the spleen, the major arteries located under the spleen were ligated with a 26mm 1/2c taper suture needle and Ethicon Vicryl 5/0 suture thread (Ethicon Inc., Somerville, NJ, USA) before spleen was removed. To close the surgical site, the peritoneal cavity was sutured using 26mm 1/2c taper suture needle and Ethicon Vicryl 5/0 suture thread (Ethicon Inc., Somerville, NJ, USA) and the skin closed using an Autoclip device (BD, San Jose, CA, USA), affixing two wound clips (BD, San Jose, CA, USA) to close the incision site. Mice were monitored daily for signs of distress or discomfort. Non-surgery control mice were housed in the same holding conditions over the same period. Splenectomised C57BL/6J mice used for aged analysis were maintained for 9 - 18 months.

Preparation of ex-breeder mice

Female C57BL/6J mice splenectomised at the age of 4 weeks were bred for six cycles of litter production and held until nine months of age. Normal female C57BL/6J mice (aged 4 weeks) were simultaneously bred for six cycles as age-matched exbreeders.

Statistics

This study ensures biological triplicates were performed as a minimum for each experiment, aiming for reproducibility of all data collected. Statistical analysis and graphics were conducted using GraphPad Prism version 7 (GraphPad Software, San Diego, CA, USA). For statistical analysis, a ***student's t-test*** was used to compare 2 normally distributed data sets. For non-parametric data analysis, a Wilcoxon test was used. A One-way ANOVA was used when 3 or more groups of parametric data were compared, with Tukey multiple-comparison post-hoc test or Dunnett's multiple comparison test to compare multiple data groups against a control group. Non-parametric data was analysed using the Kruskal-Wallis multiple comparison test with Dunn's correction test. P values were considered statistically significant when $p \leq 0.05$.

Table 2.1 Reagents used for lineage staining and magnetic separation

Specificity	Clone	Isotype	Conjugate	[Stock] (mg/mL)	Source¤
NK1.1	PK136	Mouse IgG2a, k	Biotin	0.5	1
Ly-6G/Ly-6C (Gr-1)	RB6-8C5	Rat IgG2a, k	Biotin	0.5	1
CD48	HM48-1	Armenian Hamster IgG	Biotin	0.5	1
CD11c	N418	Armenian Hamster IgG	Biotin	0.5	1
CD16/CD32 (FcBl)	93	Rat IgG2a, l	Purified	0.5	1
Biotin	-	Mouse IgG1	Microbead	-	2

¤ Source:

1. Biolegend (San Diego, CA, USA)
2. Miltenyi Biotec (Bergisch Gladbach, Germany)

Table 2.2 Primary and secondary reagents used for HSC staining

Specificity	Clone	Isotype	Conjugate[a]	[Stock] (mg/mL)	Source[¤]
CD117 (cKit)	2B8	Rat IgG2b, k	FITC	0.5	3
Ly-6A/E (Sca-1)	D7	Rat IgG2a, k	BV421	0.2	1
CD150	mSHAD150	Rat IgG2b	PE-Cy7	0.2	3
CD34	RAM34	Rat IgG2a, k	eFluor 660	0.2	3
CD201 (EPCR)	eBio1560	Rat IgG2b, k	PE	0.2	3
Secondary reagent					
Streptavidin	-	-	APC-eFluor 780	0.2	3

¤ Source:

1. Biolegend (San Diego, CA, USA)
2. eBioscience (San Diego, CA, USA)

[a] eFluor660 (APC), allophycocyanin; APC-eFluor780 (APC-Cy7), allophycocyanin-Cy7; BV421, Brilliant Violet 421; FITC, fluorescein isothiocyanate; PE, phycoerythrin; PE-Cy7, phycoerythrin-Cy7

Table 2.3 Primary and secondary reagents used for lineage reconstitution analysis

Specificity	Clone	Isotype	Conjugate[a]	[Stock] (mg/mL)	Source[¤]
CD19	eBio1D3	Rat IgG2a, k	PE-Cy7	0.2	2
CD45R/ B220	RA3-6B2	Rat, IgG2a, k	PE	0.2	2
CD5	53-7.3	Rat IgG2a, k	BV510	0.2	1
CD11c	N418	Armenian Hamster IgG	APC	0.2	2
CD11b	M1/70	Rat IgG2b, k	PE-Cy7	0.2	1
CD45.1	A20	Mouse IgG2a, k	Pacific Blue	0.5	1
CD45.2	104	Mouse IgG2a, k	Biotin	0.5	1
Secondary reagent					
Streptavidin	-	-	APC-eFluor 780	0.2	2

¤ Source:

1. Biolegend (San Diego, CA, USA)

2. eBioscience (San Diego, CA, USA)

[a] APC, allophycocyanin; BV510, Brilliant Violet 510; PE, phycoerythrin; PE-Cy7, phycoerythrin-Cy7

Table 2.4 Primary and blocking reagents used for spleen section staining

Specificity	Clone	Isotype	Conjugate[a]	[Stock] (mg/mL)	Source[¤]
CD16/CD32 (FcBl)	93	Rat IgG2a, l	Purified	0.5	2
CD105	MJ7/18	Rat IgG2a, k	PE	0.2	1
ER-TR7	SC-73355	Rat IgG2a, k	AF488	0.05	3

¤ Source:

1. eBioscience (San Diego, CA, USA)
2. Biolegend (San Diego, CA, USA)
3. Santa Cruz Biotechnology (Dallas, TX, USA)

[a] AF488, Alex Fluor 488; PE, phycoerythrin

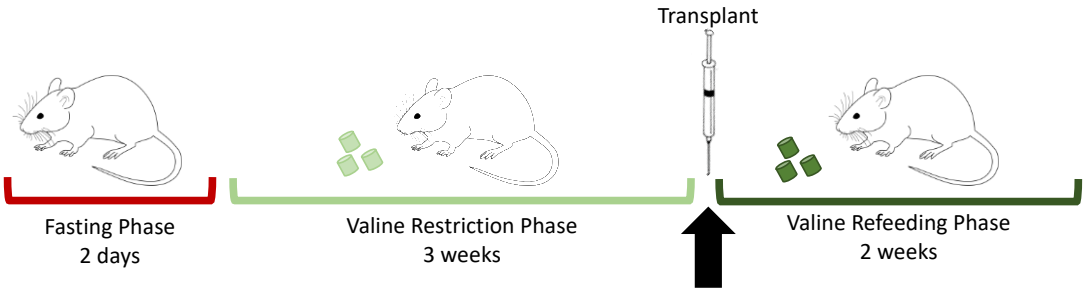

Figure 2.1 Timeline for dietary valine restriction and donor cell transplantation

Phase 1: The red zone indicates the 2 days during which mice are fasted before a 3-week valine-deficient diet (Phase 2; light green zone). The dark green zone indicates the time of reintroduction of valine coincident with donor cell transplantation (Phase 3; black arrow and dark green zone).

Table 2.5 Valine concentration in water during reintroduction diet

Treatment group	Week 1 (g/L)	Week 2 (g/L)
1	0	0
2	0.1	1
3	1	Complete diet
4	Complete diet	Complete diet

Valine concentration in drinking water for various treatment groups.

Table 2.6 Timepoints and conditions used for transplantation studies

Analysis Timepoint	Analysis	Adoptive transfer: Cell type and number	Double-staining
18 hours	Homing	$2x10^6$ whole spleen WBC	$DiR^+CD45.2^+$
48 hours	Homing	$2x10^6$ whole spleen WBC	$DiR^+CD45.2^+$
1 month	Short-term reconstitution	$1x10^6$cells lineage depleted BM	$CD45.1^-CD45.2^+$
8 months	Long-term reconstitution	$1x10^6$cells lineage depleted BM	$CD45.1^-CD45.2^+$

Timeframes for homing and lineage reconstitution studies in valine-restriction preconditioned mice are shown.

CHAPTER 3

Transplantation conditions for analysis of steady-state spleen

3.1 Introduction

The spleen is an organ that filters blood. It also supports hematopoiesis and contributes to blood cell production. While spleen has been extensively investigated during stress or inflammatory events that trigger extramedullary hematopoiesis (McKim et al., 2018; Robbins et al., 2012; Tian et al., 2016; Wu et al., 2018), the contribution of spleen to hematopoiesis under steady-state conditions remains poorly understood. This is largely due to a lack of experimental methodologies that facilitate maintenance of steady-state conditions, and can discriminate between bone marrow and spleen-derived hematopoiesis.

Irradiation and cytotoxic chemotherapy have been standard clinical practices for patient conditioning prior to HSC transplantation (Schofield, 1978). Niche preconditioning and HSC transplantation is also considered the gold standard method for studying hematopoiesis in animal models. However, such treatments severely damage the HSC microenvironment, potentially distorting the typical process of homing and differentiation (Chatterjee, Mills, Katz, McGarrigle, & Goldstone, 1994; Lapidot, Dar, & Kollet, 2005; Mohty & Apperley, 2010; Socie et al., 2003; Tichelli et al., 2009). This includes changes in the level of secreted chemokines which can impact stem cell migration and repopulation potential (Lapidot et al., 2005). Therefore, alternate conditioning approaches are required to study hematopoiesis in the spleen under steady-state conditions.

Many studies have focused on developing alternate approaches to HSC ablation in order to avoid the need for irradiation (Bueno, Montes, de la Cueva, Gutierrez-Aranda, & Menendez, 2010; Czechowicz, Kraft, Weissman, & Bhattacharya, 2007; Palchaudhuri et al., 2016; Taya et al., 2016). Antibody-mediated methods involve the administration of ACK2, an antibody which is a cKit antagonist antibody. It depletes HSC through inhibition of cKit signaling rather than by bone marrow mobilization of cells out of bone marrow (Czechowicz et al., 2007). However,

successful HSC engraftment in mice has not been achieved through antibody-mediated approaches without combined low-dose irradiation (Xue et al., 2010). More recently, coupling ACK2 with CD47 antagonists was found to reduce the need for irradiation by initiating a macrophage-mediated phagocytic response (Chhabra et al., 2016). It is not yet known whether this method will contraindicate patient infection risk (Chhabra et al., 2016). Hematopoietic preconditioning through internalization of immunotoxins, produces excellent niche clearance and efficient chimerism in normal mice (Palchaudhuri et al., 2016). The immunotoxin used is specific for hematopoietic cells and utilizes the cell surface CD45 molecule on all blood forming progenitor and stem cells (Palchaudhuri et al., 2016). It is conjugated with saporin (SAP) (Palchaudhuri et al., 2016), a catalytic *N*-glycosidase ribosome-inactivating protein that inhibits protein synthesis (Bergamaschi et al., 1996). Exposure to SAP induces cell apoptosis and when coupled to a cell-specific antibody, such as CD45, allows highly targeted cell killing. This targeted killing occurs independently of cell cycle status and gives prompt immunological recovery unlike total body irradiation (Rodriguez, Lim, Bartkowski, & Simons, 1998; Weidle et al., 2014). However, immunotoxin-mediated therapies are still in under development. Further investigation will be required to evaluate the risks associated with immunogenicity and the toxicity of immunotoxins, induced by either adaptive resistance mechanisms (Axelrod et al., 2013) or extensive cytokine-release (Jeyarajah & Thistlethwaite, 1993).

The extent to which hematopoiesis following preconditioning and transplantation is reflective of true physiological proliferation and differentiation remains unclear. Novel technical approaches to HSC tracking allow clonal dynamics to be monitored over time using transposon-based genetic tags (Gerrits et al., 2010) (Lu, Czechowicz, Seita, Jiang, & Weissman, 2019). The development of genetically modified immunodeficient mice engrafted with functional human immune systems now enables the human immune system to be studied on a small scale without putting patients at risk (King et al., 2009). However, humanized mouse models do have

shortcomings. For example, the development of graft-versus-host disease is inescapable in any transplantation model (King et al., 2009; Laing, Griffey, Moreno, & Stoddart, 2015), and the murine cytokine system is not competent at initiating human cell signaling cascades (Shultz, Brehm, Garcia-Martinez, & Greiner, 2012). The development of humanized mice deficient in murine MHC and/or CD47 may protect against graft-versus-host disease making them a unique and valuable model for long-term transplantation analysis (Lavender et al., 2013).

Nutrition-based methods to condition mice have been assessed in order to circumvent the need for irradiation. One preconditioning approach previously reported by Taya et al. (2016) involves restricting the dietary intake of the essential amino acid valine to deplete HSC and progenitors from the bone marrow niche. The mechanism of action behind HSC-dependent valine sensitivity is not yet understood, although a recent report suggests that a valine deficient diet restricts HSC maintenance within the niche (Wilkinson, Morita, Nakauchi, & Yamazaki, 2018). One limitation of this method for HSC depletion is neurotoxicity in rats fed a diet deficient in valine, although symptoms can be quickly reversed upon reintroduction of valine into the diet (Cusick, Koehler, Ferrier, & Haskell, 1978; Taya et al., 2016). Since this study was initiated, a new dietary-based conditioning method has been published which shows that a lack of valine in the diet is not the primary cause of neurotoxicity in rats (Cusick et al., 1978) or of diminished HSC expansion in mice (Wilkinson et al., 2018). Instead it was found that an imbalance in the presence of the branched chain amino acids leucine and isoleucine was to blame (Wilkinson et al., 2018). This study suggested that depletion of all three branched chain amino acids may be a safer alternative for bone marrow conditioning (Wilkinson et al., 2018).

A dietary-based pre-conditioning approach was investigated here as a cost-effective method to study steady-state hematopoiesis in preference to other procedures using antibody-mediated or hematopoietic-cell-specific immunotoxin-based approaches, or of less accessible techniques like HSC barcoding. In comparison with specialized

humanized mouse models, dietary-based pre-conditioning allowed the use of mice on a common C57BL/6 background, and congenic variants for distinguishing donor cells from host. This study uses the dietary-depletion of valine in order to investigate steady-state spleen HSC lineage reconstitution.

Migration of HSC through blood to various organs, and vice versa, requires active navigation mediated by functional cell adhesion molecules and chemokine stimulatory signals, a process called homing (Lapidot et al., 2005). Homing is a crucial process intrinsic to HSC. It is apparent from the first moments of ontogeny, seeding fetal bone marrow hematopoiesis, physiological roles in adult bone marrow homeostasis, through to the first essential step of therapeutic stem cell transplantation engraftment. Until recently, bone marrow was thought to be the primary site of HSC engraftment following HSC transplantation. It is now understood that spleen plays a crucial role in hematopoiesis and is one of the first sites visited by migrating transplanted HSC (Cao et al., 2004; Szilvassy, Bass, Van Zant, & Grimes, 1999).

Spleen-specific hematopoiesis in the steady-state is challenging to study and therefore is fairly unexplored. One limitation of early reconstitution studies is the analysis of transplanted HSC weeks or even months after transplantation, while critical homing events occur within the first hours to days posttransplant (Cao et al., 2004). Studies using bioluminescence imaging to track transplanted cell migration and homing report that approximately 37% of transferred HSC migrate to spleen, confirming spleen as the most frequent initial site of stem cell engraftment (Cao et al., 2004). Stem cells possess intrinsic programming that determines differentiation fate (Dykstra et al., 2007), however HSC within the spleen reportedly contribute to myelopoiesis, predominantly observed during stress-induced extramedullary hematopoiesis (Nakada et al., 2014), but also in the steady-state (Tan & O'Neill, 2010). The power of the splenic niche to persuade stem cell fate decision may be underestimated. A study which transplanted $CD34^-$ LSK from either bone marrow or

spleen into primary recipients identified that HSC derived from spleen produced a larger proportion of myeloid than lymphoid cells than bone marrow derived HSC (Morita et al., 2011). Taken together with the understanding that HSC become progressively more myeloid-biased with age, it is important to consider whether frequent migration through the splenic niche is linked with myeloid-biased HSC accumulation. However, no previous studies have focused on this connection.

Cellular expansion following transplant engraftment can be visualized in real time using live-cell imaging of fluorescence or bioluminescence. Furthermore, these technological applications have the potential to demonstrate homing and migratory patterns for individual cells in specific microenvironments. The study by Cao et al. (2004) reported that bioluminescence intensity gradually increased in HSC transplanted animals, which likely represented local proliferation and differentiation of donor-derived HSC and progeny. They also reported that bioluminescence foci could shift from the initial site of engraftment to other sites as bioluminescence intensity grew, indicating migration to other organs as proliferation occurred. Interestingly, Cao et al. (2004) identified a period of time when transplanted cells engraft and remain within the initial site of engraftment before foci begin to shift throughout the mouse, thus determining the time point after transplantation in which cells migrate. Provided lineage output analyses are conducted within the small window of time from initial engraftment, spleen-specific contribution to HSC lineage differentiation following transplantation can now be studied without the interference of bone marrow derived contributions.

An important consideration for investigating spleen-specific hematopoiesis is separation of the confounding effects of hematopoiesis occurring in the bone marrow from hematopoiesis occurring in the spleen. Following transplantation, HSC migrate to multiple tissue niches in the body (Massberg et al., 2007). Intrasplenic injection has therefore been explored as a means of directly delivering HSC to the spleen, so allowing HSCs a greater chance of retention in the spleen environment for analysis

of splenic hematopoietic output. However, even following intrasplenic injection, steady-state migration of HSC across various niches in the body (Cao et al., 2004) mitigates the initial localization of HSC to the spleen. This would compromise downstream hematopoietic reconstitution analysis typically performed 8-16 weeks after HSC transplantation. Therefore, to investigate tissue-specific hematopoiesis, we have analysed HSC differentiation in the spleen at early timepoints following either intravenous or intrasplenic transplantation. This is based on live cell tracing evidence of HSC homing, proliferation and migratory patterns specific to the spleen and bone marrow from a live cell tracing study (Cao et al., 2004). In mice transplanted with luciferase^{+} HSC intravenously, foci of engrafted HSC were found to remain localized in the spleen and bone marrow for 12 days after transplantation (Cao et al., 2004). This finding suggests that there is a specific 12-day window after HSC lodge in a hematopoietic niche while subsequent HSC proliferate and remain localized in the niche before migration occurs. Thus, in order to characterize spleen-specific hematopoiesis, analysis must take place no more than 12 days after transplantation.

Research surrounding proliferation and cell migratory patterns from newly engrafted HSC therefore offers a potential window to study HSC differentiation specific to the spleen microenvironment (Cao et al., 2004). In combination with a dietary-based method for conditioning HSC recipients, we have attempted to identify spleen-endogenous HSC lineage differentiation and output under non-inflammatory conditions. This study is expected to bridge the gap between our understanding of extramedullary and steady-state spleen hematopoiesis in the spleen, and to elucidate the specific immune cell lineages which develop locally within spleen tissue.

3.2 Results

3.2.1 Optimizing HSC clearance

In order to investigate spleen-specific HSC differentiation under non-inflammatory conditions, we first attempted to 1) confirm the depletion of LT-HSC from niches including bone marrow following dietary valine restriction, and 2) identify the minimum amount of dietary valine needed to support HSC viability. These aims were concurrently assessed by varying concentrations of valine in the drinking water, while providing a valine-restricted diet over the entire depletion phase (**Figure 3.1A**). Analysis of percent LT-HSC in the bone marrow (**Appendix A.1**) following valine depletion revealed no significant difference between control animals given a complete diet, and animals given a valine-restricted diet (**Figure 3.1B**). Similarly, there was no significant difference found between either of the valine-restricted treatment groups compared with the complete diet positive control group, suggesting that valine-restriction did not deplete HSC. However, our finding of ~0.001% HSC remaining after 3-week valine restriction is consistent with previous depletion reports (Taya et al., 2016), and would suggest that this HSC frequency in bone marrow would be sufficient to permit donor cell engraftment. Instead, we consider that the HSC count for control mice given a complete diet was unexpectedly low. This was consistent with LT-HSC frequency reported for control mice given a complete diet in the study by Taya et al. (2016), and also complete diet control mice in the refeeding analysis of this study (**Figure 3.1C**).

It should be noted that previous data published in relation to valine-mediated HSC depletion pays particular attention only to HSC within the bone marrow niche. This study is therefore the first to analyse spleen tissue to assess whether HSC within the spleen niche were also simultaneously depleted as in the bone marrow (**Figure 3.1D**). Initial results showed that HSC frequency amongst Lin^- splenocytes was lower in the spleens of valine-restricted mice compared with mice fed on a complete diet.

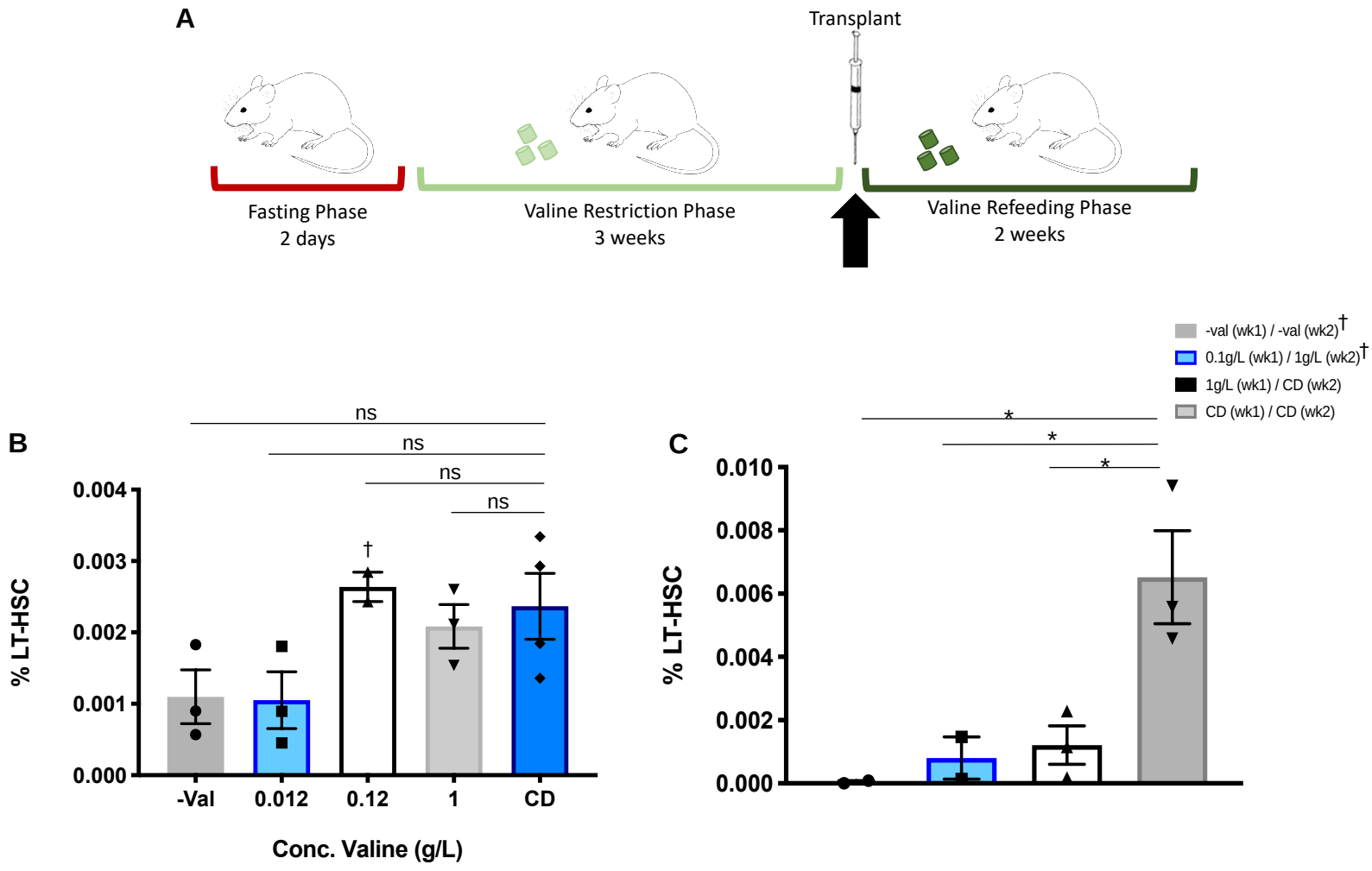
A
Transplant
Fasting Phase
2 days
Valine Restriction Phase
3 weeks
Valine Refeeding Phase
2 weeks
B
ns
ns
ns
ns
†
% LT-HSC
0.004
0.003
0.002
0.001
0.000
-Val
0.012
0.12
1
CD
Conc. Valine (g/L)
C
-val (wk1) / -val (wk2)†
0.1g/L (wk1) / 1g/L (wk2)†
1g/L (wk1) / CD (wk2)
CD (wk1) / CD (wk2)
*
*
*
% LT-HSC
0.010
0.008
0.006
0.004
0.002
0.000

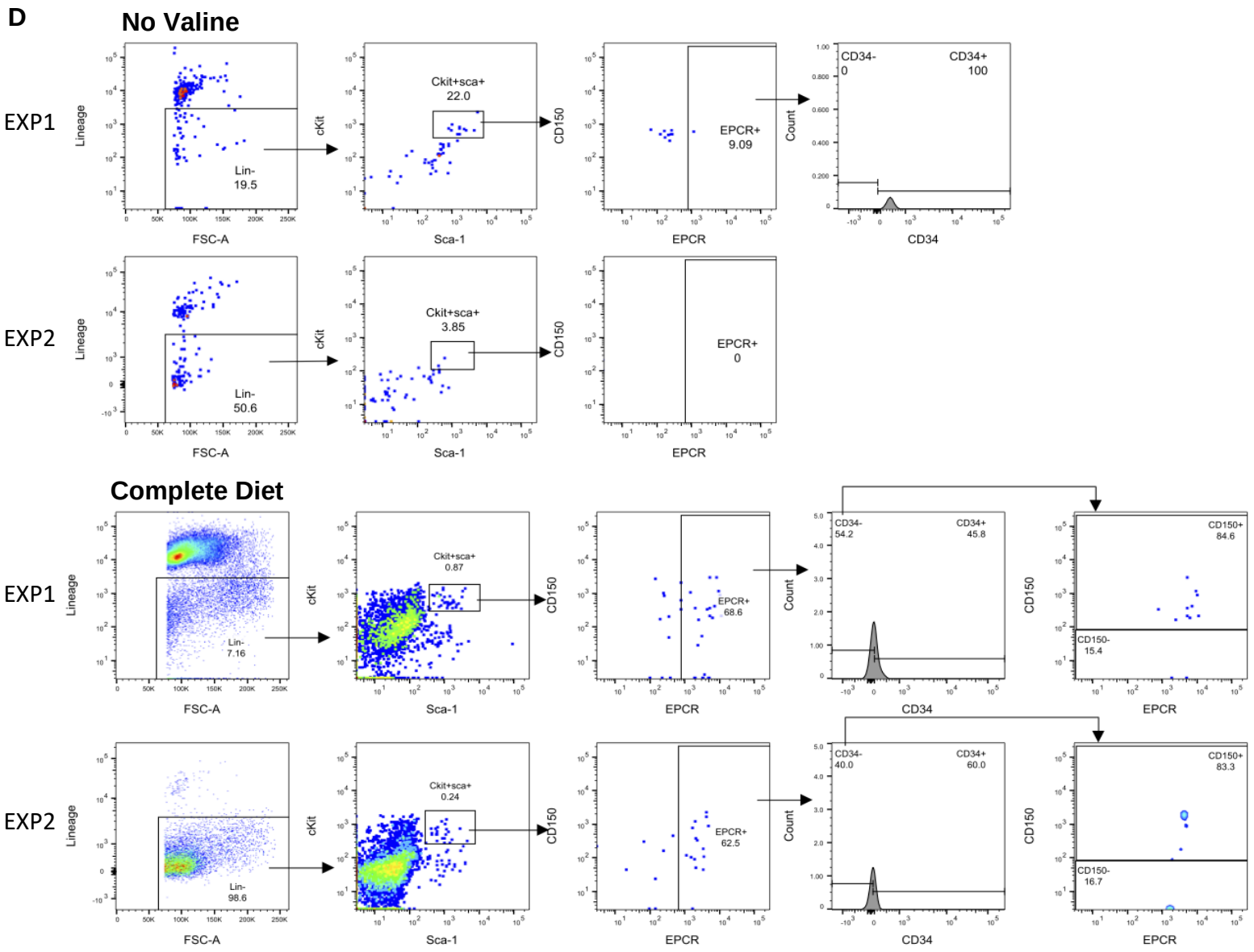
D
No Valine
EXP1
Lineage
Lin-
19.5
FSC-A
cKit
Ckit+sca+
22.0
Sca-1
CD150
EPCR+
9.09
EPCR
Count
CD34-
0
CD34+
100
CD34
EXP2
Lineage
Lin-
50.6
FSC-A
cKit
Ckit+sca+
3.85
Sca-1
CD150
EPCR+
0
EPCR
Complete Diet
EXP1
Lineage
Lin-
7.16
FSC-A
cKit
Ckit+sca+
0.87
Sca-1
CD150
EPCR+
68.6
EPCR
Count
CD34-
54.2
CD34+
45.8
CD34
CD150
CD150+
84.6
CD150-
15.4
EPCR
EXP2
Lineage
Lin-
98.6
FSC-A
cKit
Ckit+sca+
0.24
Sca-1
CD150
EPCR+
62.5
EPCR
Count
CD34-
40.0
CD34+
60.0
CD34
CD150
CD150+
83.3
CD150-
16.7
EPCR

Figure 3.1 The effects of valine depletion and reintroduction on bone marrow and spleen LT-HSC

Optimization of valine-restriction to achieve hematopoietic stem cell (HSC) depletion. A) A schematic protocol for the depletion and reintroduction of valine into the diet. The fasting phase was initiated by a 2-day fast (red zone). Valine restriction was then commenced by introduction of a valine-deficient diet (light green pellet) for 3 weeks (light green zone). Cell transplantation occurs following valine-restriction (black arrow), after which complete diet was returned (dark green pellets) as the valine refeeding phase (2 weeks; dark green zone). B) To determine the minimum valine concentration required to support HSC in the bone marrow niche, varying concentrations of valine were supplemented in the drinking water during the valine restriction phase. Lineage depleted (Lin^-) bone marrow of 11-week-old C57BL/6J mice was analysed by flow cytometry to calculate LT-HSC frequency (frequency data not shown). LT-HSC have a $L^-S^+K^+CD150^+CD48^-CD34^-EPCR^+$ phenotype. Data represent the mean±SEM of 3 independent experiments (1 mouse/experiment), except for CD (complete diet; *n=4*). C) Varying concentrations of valine were reintroduced in weekly steps during the refeeding phase followed by analysis of bone marrow in 9-week-old mice. Data represent the mean±SEM of 3 independent experiments (1 mouse/experiment): -Val (wk1)/-Val (wk2),0.1g/L (wk1)/ 1g/L (wk2), 1g/L (wk1)/ CD (wk2) and CD (wk1)/ CD (wk2) (frequency data not shown). Statistical analysis was performed using a one-way ANOVA with Dunnett's multiple comparisons test. *P<0.05. † Indicates that an animal died. D) Two independent experiments were carried out to analyse LT-HSC in the spleen of 8-week-old C57BL/6J mice given no valine compared with a complete diet (EXP1, EXP2) (frequency data not shown).

Based on these observations, we were satisfied that valine restriction led to depletion of HSC from the body.

Next, we optimized the valine reintroduction protocol to determine the safest method to support hematopoietic engraftment. To avoid metabolic shock, valine was previously added to the drinking water incrementally at 0.12g/L of valine in the first week, and 1.2g/L in the second week (Taya et al., 2016). This method reduces mortality normally associated with immediate resumption of a complete diet. To determine the minimum dose of valine which supports HSC during the refeeding phase, we analysed bone marrow HSC frequency following the reintroduction of four varying concentrations of valine (**Figure 3.1C**). We confirmed a significant increase in HSC in mice fed a complete diet immediately after the valine depletion phase (0.00652±0.00147%SEM) compared with mice that were maintained on a valine restricted diet during the entire reintroduction phase (0.00004±0.00004%SEM).

The percentage of LT-HSC in bone marrow gradually increased as the concentration of valine increased during refeeding. The 0.1g/L (wk1) group increased 20 times that of the 'no valine' refed group, while the least affected group was 1g/L (wk1) which increased 1.25 times the 0.1g/L (wk1) group, and lastly, the complete diet refed group increased by 6 times that of 1g/L (wk1) group. Amongst these groups, we determined that the minimum supporting dose of valine was 0.1g/L in the first week and 1g/L in the second week. Interestingly, we demonstrated the safety of valine reintroduction for 7 out of 7 mice surviving after immediate complete diet reintroduction. Therefore, based on HSC capacity for valine tolerance and demonstration of safety, we elected to reintroduce valine via resumption of a complete diet to support HSC transplantation.

3.2.2 Investigating intrasplenic injections as an alternative route for transplants

To confirm that valine restriction sufficiently preconditions the host HSC microenvironment while allowing donor cell homing, we tested the homing capacity of adoptively transferred hematopoietic cells using different transplant delivery routes. Homing is the first step following cell transplantation, with homing events measured in hours and typically lasting no longer than 1-2 days (Cao et al., 2004; Lapidot et al., 2005). We specifically wanted to confirm that any transplanted cells could home to the spleen, as the hematopoietic site of interest. We explored methods of improving the spleen-homing frequency by directly transferring donor cells into the spleen, instead of through intravenous administration. Considering that approximately 37% of intravenously transplanted cells lodge in spleen (Cao et al., 2004), we hypothesized that transplanting cells directly into spleen would increase localization efficiency, and therefore increase the ability to detect HSC differentiation endogenous to spleen.

In preparation for intrasplenic injection, we measured the maximum volume of fluid that could be injected into spleen (**Figure 3.2A & B**). Spleens excised from animals were imaged before intrasplenic injection of 50µL or 20µL volumes, and after delivery while the needle was still *in situ*, and then immediately after the needle was removed. We identified progressive leakage of trypan blue over 3-minutes using either 50µL or 20µL volumes, prompting further investigation into blocking the site of injection following fluid delivery.

To reduce fluid escape from the injection site, we tested the introduction of a small Matrigel aliquot following adoptive cell transfer. Matrigel is an extracellular matrix-based hydrogel that is liquid at cold temperatures and solid at body temperature. To achieve a plug following intrasplenic injection, ice-cold Matrigel was first aspirated into a syringe followed by trypan blue dye to create a layered effect (**Figure 3.2C**). Injection of trypan blue only and trypan blue/Matrigel was directly compared showing a reduction in leakage when Matrigel was co-administered (**Figure 3.2D**). However, a small amount of leakage was still observed.

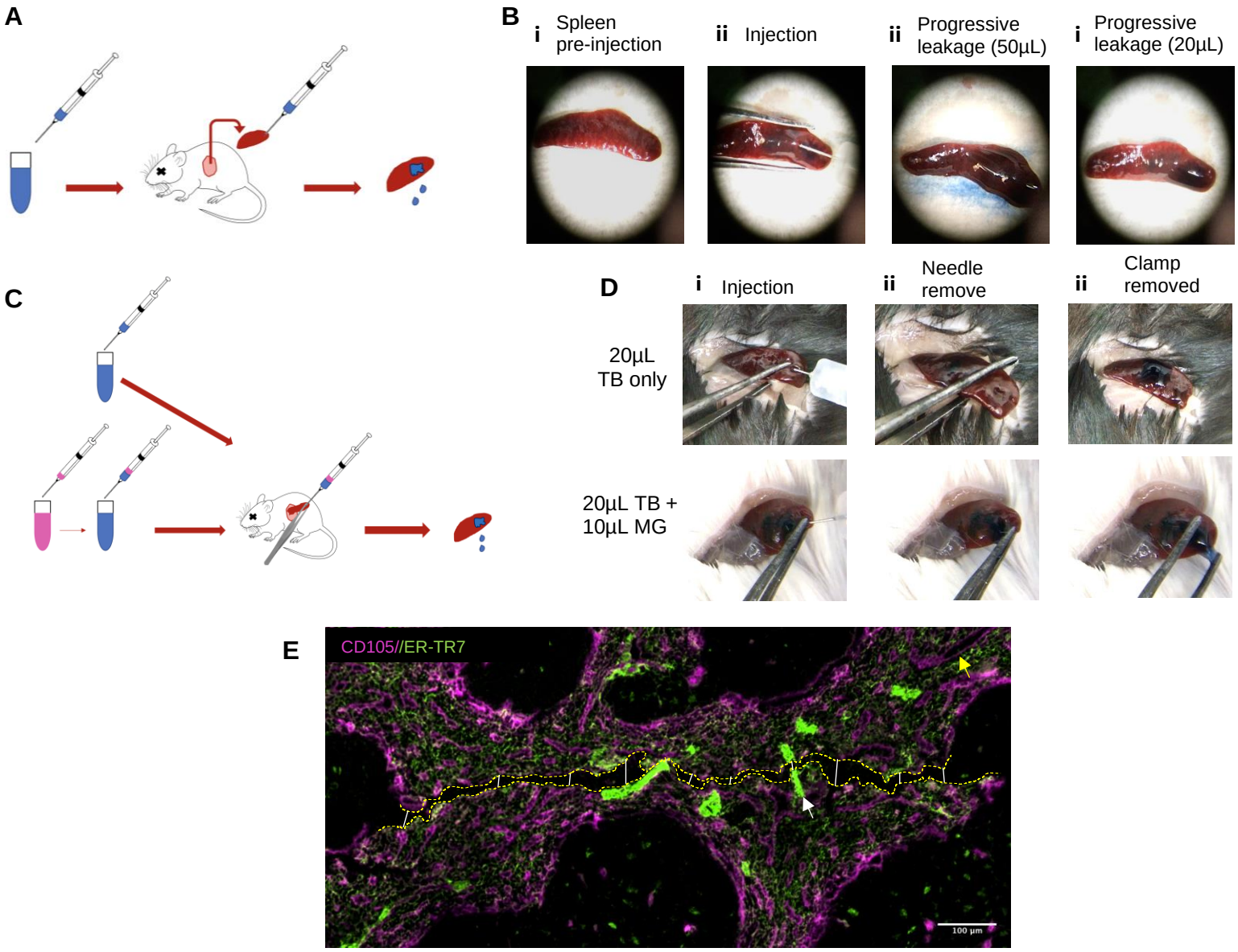
A
B
i Spleen pre-injection
ii Injection
ii Progressive leakage (50µL)
i Progressive leakage (20µL)
C
D
i Injection
ii Needle remove
ii Clamp removed
20µL TB only
20µL TB + 10µL MG
E
CD105//ER-TR7
100 µm

Figure 3.2 Investigating the viability of intrasplenic adoptive cell transfer

Freshly harvested spleens from C57BL/6J or BALB/c mice were used to test the volumetric capacity of fluid injected directly into spleen, and to assess tissue damage associated with the injection. A) Schematic protocol for testing various injected volumes of trypan blue (TB) into a spleen to identify fluid retention and leakage. TB was drawn (20µL or 50µL) into an 30G ultrafine syringe and inserted into an excised spleen. B) Images of spleen (i) prior to injection, (ii) with needle *in situ*, then progressive leakage (imaged 3-minutes post-needle removal) from (iii) 50µL and (iv) 20µL trials. C) Schematic protocol for testing whether progressive leakage could be reduced by using Matrigel (MG; indicated in pink) in layered effect, alongside normal TB control (indicated in blue), delivering MG into the spleen last. The site of injection was clamped with forceps. Intrasplenic injections were conducted in the exteriorized, but still attached spleen from the sacrificed host. D) Images of injections (i) using 20µL TB only and 20µL TB and 10µL Matrigel. Images also show the needle removed while clamping is maintained (ii), and progressive leakage once the clamp is removed (3-minutes post-clamp removal) (iii). E) Spleen tissue following intrasplenic injection was frozen and cryo-sectioned for analysis by immunofluorescence staining. Sections (7µm) were stained with CD105 (MJ7/18; PE) (magenta) and ER-TR7 (SC-73355; AF488) (green). Yellow dotted line indicates path of injection. White arrow indicates trabecular damage, yellow arrow indicates endothelial cell lining of sinusoidal vasculature and white lines indicates points where diameter was measured. Original magnification X10. Scale bar, 100µm.

To determine whether any tissue damage occurred following intrasplenic injection, spleen was sectioned and stained for expression of an endothelial marker (CD105) and fibroblastic marker (ER-TR7) (**Figure 3.2E**). A needle insertion path measuring 26µm (±15.5µm SD) in diameter was identified over two 7µm slides (**Appendix A.2**). In summary, due to technical difficulties and local tissue damage associated with intrasplenic injections, we used intravenous tail vein injections in order to examine spleen-specific hematopoiesis and to maximize steady-state conditions.

3.2.3 Homing of transplanted cells following valine depletion as a pre-conditioning treatment

To confirm that intravenously administered cells were capable of homing to the spleen, we transferred $2x10^6$ C57BL/6 (CD45.2) spleen leukocytes into valine-restricted B6.SJL (CD45.1) congenic hosts. To increase the specificity of donor (CD45.2) cell detection, a near-infrared lipophilic carbocyanine dye 1,1'-dioctadecyl-3,3,3',3'-tetramethylindotricarbocyanine iodide (DIR) was used to stain donor cell membranes prior to transplantation (Carlson et al., 2013). $CD45.2^+DIR^+$ cells were observed in all tissue samples analysed at 48-hours but not at 18-hours post-transplantation (**Figure 3.3**). Amongst the tissues analysed, the majority of transplanted cells were found in spleen and peripheral blood (0.13%). Percent donor cells in the bone marrow (0.020%) was below the detection threshold of 0.1%. However, DIR cell membrane dye offered a robust double-positive stain that certified that any cell detection above 0% was donor-derived. This was confirmed using B6.SJL controls on which $CD45.2^+$ DIR^+ gates were set (**Appendix A.3**). Additional myeloid and lymphoid antibody staining found that most donor cells were $B220^+$ B cells. Spleen and peripheral blood harbored a small percentage of $F4/80^-$ $CD11b^+CD11c^+$ myeloid cells, with 4.6% myeloid cells detected in spleen and 11.1% detected in peripheral blood. Furthermore, 37.5% of donor cells detected in peripheral blood and 10.2% in spleen could not be classified as either myeloid, lymphoid or macrophage according to the staining panel used.

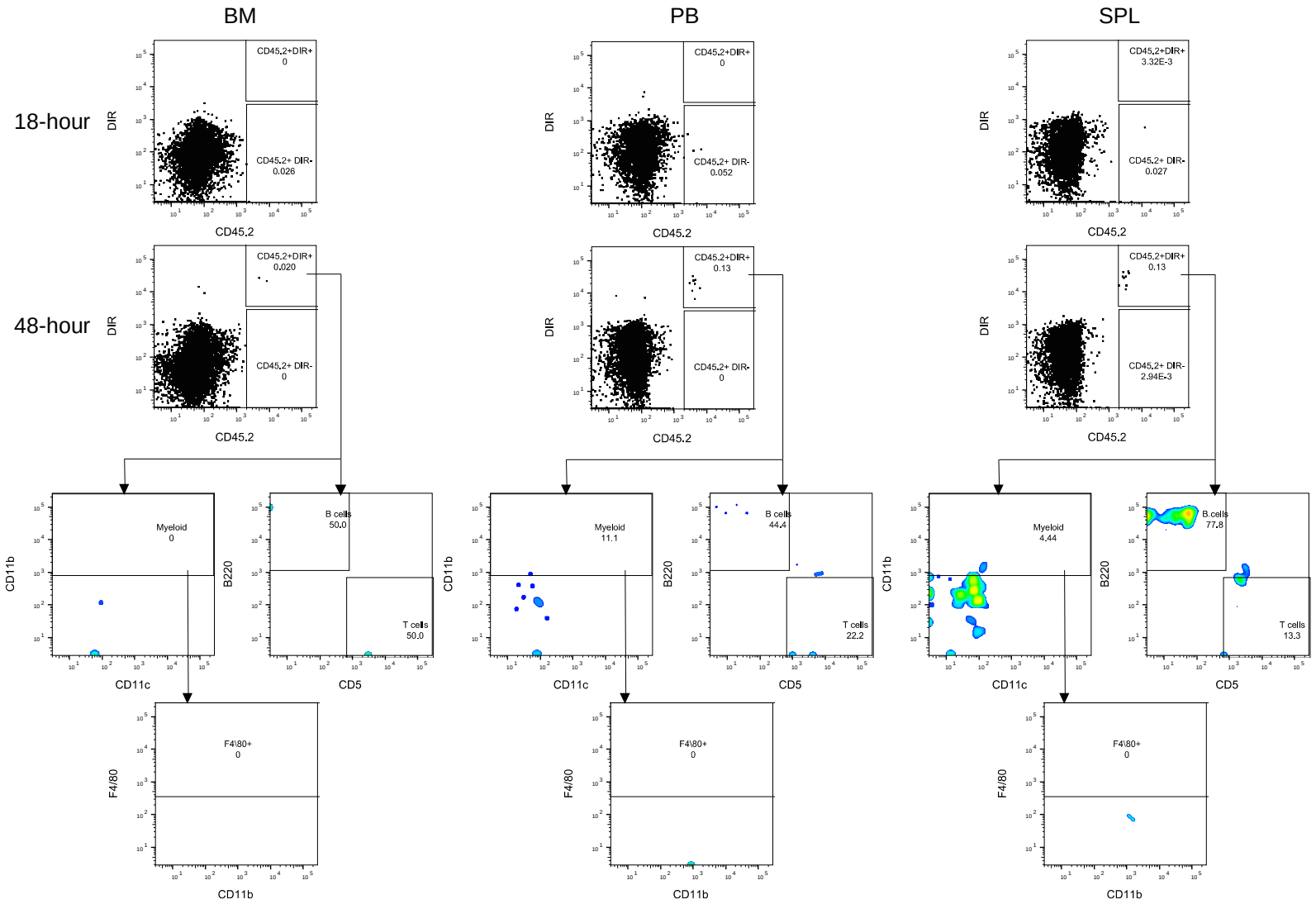
BM
PB
SPL
18-hour
48-hour
DIR
CD45.2
CD45.2+DIR+
0
CD45.2+ DIR-
0.026
CD45.2+DIR+
0
CD45.2+ DIR-
0.052
CD45.2+DIR+
3.32E-3
CD45.2+ DIR-
0.027
CD45.2+DIR+
0.020
CD45.2+ DIR-
0
CD45.2+DIR+
0.13
CD45.2+ DIR-
0
CD45.2+DIR+
0.13
CD45.2+ DIR-
2.94E-3
CD11b
B220
CD11c
CD5
F4\80
F4\80+
Myeloid
0
B cells
50.0
T cells
50.0
Myeloid
11.1
B cells
44.4
T cells
22.2
Myeloid
4.44
B cells
77.8
T cells
13.3
F4\80+
0
F4\80+
0
F4\80+
0

Figure 3.3 General homing capacity of cells transplanted into valine-depleted recipients

Donor spleen leukocytes ($2x10^6$) were isolated from C57BL/6 ($CD45.2^+$) mice, stained with the lipophilic carbocyanine dye 1,1'-dioctadecyl-3,3,3',3'-tetramethylindotricarbocyanine iodide (DIR), and transplanted into valine-depleted B6.SJL ($CD45.1^+$) host mice. At 18- and 48-hours post-transplantation, bone marrow (BM), spleen (SPL) and peripheral blood (PB) were collected and prepared for staining with antibodies to CD45.2 (104; Pacific Blue), B220 (RA3-6B2; AF647), CD5 (53-7.3; BV510), F4/80 (BM8; PE), CD11b (M1/70; PE-Cy7), CD11c (N418; biotin) and streptavidin (BB515). Multi-colour FACS analysis was used to detect donor-derived $DIR^+CD45.2^+$ cells. Dot plots showing DIR and CD45.2 expression display a standardized number of events (5578). $DIR^+CD45.2^+$ cells were further assessed for myeloid cells based on CD11c (N418; biotin & streptavidin; BB515), CD11b (M1/70; PE-Cy7) and F4/80 (Bm8; PE) expression. B and T cells were assessed through B220 (RA3-6B2; AF647) and CD5 (53-7.3; BV510) expression, respectively. Control B6.SJL ($CD45.2^-DIR^-$) mice were used to set (A) CD45.2 and DIR gates, and F4/80 fluorescence minus one controls (FMOC) were used to set (B) F4/80 (BM8; PE) gates (data shown in **Appendix A.3**). Numbers in gates represent percent cells amongst the parent population. The subset of interest is identified as $DIR^+CD45.2^+$ for each tissue sample. Data were obtained from a single independent experiment.

3.2.4 Lineage reconstitution potential from a valine depleted niche

To initially determine the hematopoietic reconstitution potential of mice conditioned through valine restriction, $1x10^6$ lineage-depleted $CD45.2^+$ bone marrow cells from C57BL/6 mice were transplanted into valine depleted B6.SJL (CD45.1) recipients to perform a long-term reconstitution analysis. After 8 months, mice were considered positive for engraftment when hematopoietic ($CD45.1^+$) chimerism was greater than 0.1% (Camargo, Chambers, Drew, McNagny, & Goodell, 2006). This represents a threshold which accounts for background staining (<0.0072%) observed in CD45.2 negative control mice (**Appendix A.5**). Here, we observed no donor engraftment in either bone marrow or spleen following long-term reconstitution. Despite transplanting a calculated 2-fold higher number of LSK cells (see **Appendix A.6** for LSK frequency of $lineage^-$ bone marrow) than comparable studies (Taya et al. (2016), bone marrow donor chimerism for our study was 0.024%, lower than an expected ~15% chimerism. This finding suggests that pre-conditioning hosts using valine restriction requires further investigation to determine whether the lack of valine restricts engraftment efficacy of the host niche, and whether engraftment can be improved if valine is returned to the diet prior to HSC transplantation.

To address whether host valine-deficiency at the time of transplantation was the cause of poor lineage reconstitution, we returned valine to the diet one or two days prior to transplantation of $1x10^6$ lineage-depleted bone marrow cells (**Figure 3.4B**). After 4 weeks for analysis of short-term lineage reconstitution, 1-day of valine prefeeding prior to transplant resulted in 1 out of 2 mice being positive for donor cell engraftment, with 0.56% donor chimerism in the single successfully engrafted mouse (**Figure 3.4C**).

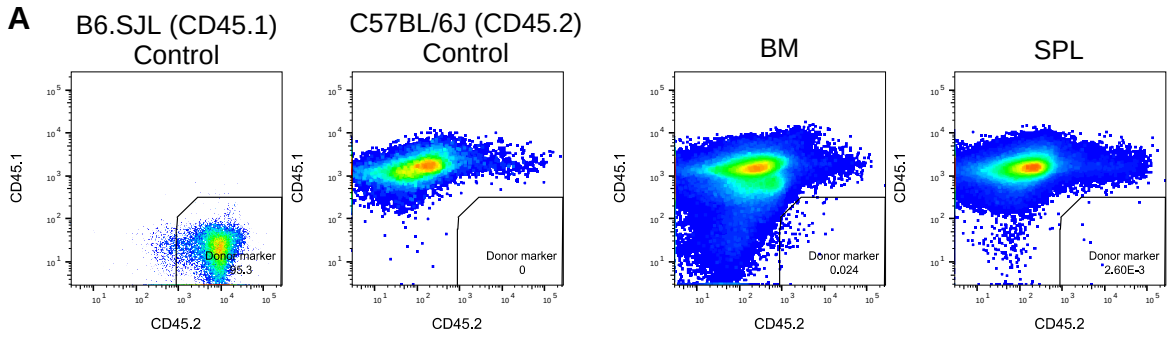
A
B6.SJL (CD45.1)
Control
C57BL/6J (CD45.2)
Control
BM
SPL
CD45.1
CD45.2
Donor marker
95.3
Donor marker
0
Donor marker
0.024
Donor marker
2.60E-3

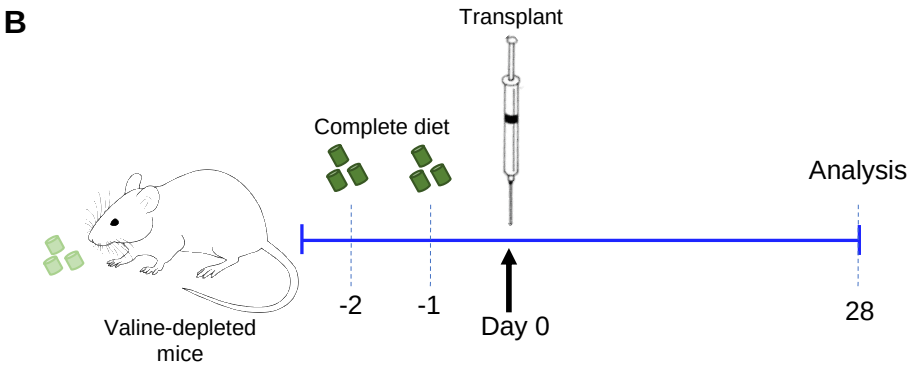
B
Transplant
Complete diet
Analysis
Valine-depleted
mice
-2
-1
Day 0
28

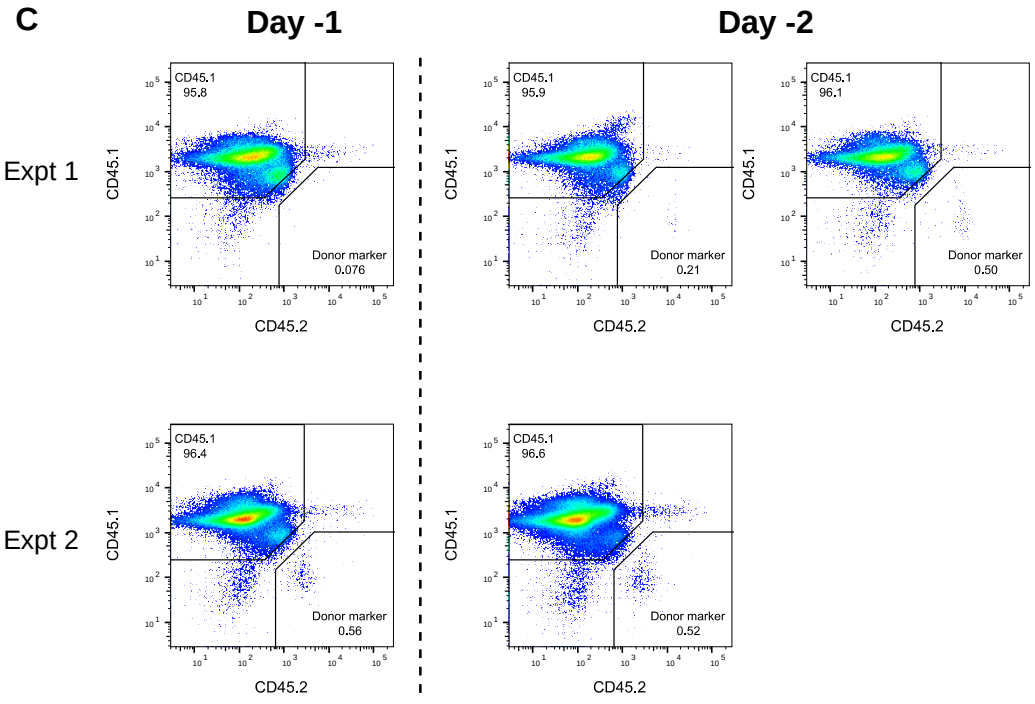
C
Day -1
Day -2
Expt 1
Expt 2
CD45.1
CD45.2
95.8
Donor marker
0.076
95.9
Donor marker
0.21
96.1
Donor marker
0.50
96.4
Donor marker
0.56
96.6
Donor marker
0.52

Figure 3.4 Optimizing donor hematopoietic reconstitution in valine-depleted hosts

$1x10^6$ lineage-depleted BM cells were prepared and transplanted into valine-depleted hosts as described in **Figure 3.1A**. A) At 8 months following transplantation, bone marrow (BM) and spleen (SPL) tissue was harvested and analysed by flow cytometry for long-term donor chimerism. Antibodies specific for CD45.1 (A20; Pacific Blue) and CD45.2 (104; biotin & streptavidin; APC-eFluor 780) were used to delineate donor cell populations ($CD45.2^+CD45.1^-$). Recipients were considered positive for engraftment when donor chimerism was >0.1%. C57BL/6ARC (CD45.2) and B6.SJL (CD45.1) mice were prepared separately as gating controls. B) Schematic protocol for re-introducing dietary valine (complete diet) -1 and -2 days prior to cell transplantation (Day 0). C) Valine-depleted mice were refed with complete diet at either 1 day (*n=2*) or 2 days (*n=3*) prior to transplantation with $1x10^6$ CD45.2 lineage depleted bone marrow cells. Donor chimerism in the bone marrow was assessed at 4-weeks post transplantation. Donor chimerism is positive when engraftment was >0.1%.

The group given two-day valine pre-feeding displayed positive engraftment with an average donor chimerism level of 0.41% (±0.1% SEM) from 3 mice. Lineage differentiation analysis revealed that the majority of donor-derived cells expressed B220 (B cell marker) for both day -1 (88.1%±5.8%SEM) and -2 groups (55.7%±19%SEM), but no $CD5^+$ T cells were identified (**Appendix A.5**). Myeloid expression was only successful in one technical experiment reporting 12.7% on day -1 and 50.9% (±12%SEM) on day -2 (**Appendix A.5**). Controlled lineage analysis, using C57BL/6 mice, found 67.5% (±2.8%SEM) of cells were B cells, 25.8% (±1.8%SEM) were T cells and 13.3% were myeloid cells (**Appendix A.5**). The distinction evident between the experimental and control findings is the absence of T cell expression in all mice transplanted for short-term reconstitution. This finding confirms greater lineage chimerism and engraftment results than this study has seen before, suggesting that valine pre-feeding is required for transplant engraftment. Pre-feeding valine 2 days before transplant administration yielded the greatest B cell and myeloid cell reconstitution.

3.3 Discussion

In this study, we adapted a novel preconditioning method, first reported by Taya et al. (2016), to investigate steady-state lineage differentiation of HSC in spleen. As this was a recently published model, we first attempted to optimize the technique for our purpose, with the end goal of transplanting HSC for analysis of spleen-specific differentiation. Overall, we achieved an optimized method for valine depletion, assessed transplantation delivery options, and optimized an adoptive cell transfer protocol for maximum engraftment. These findings now set a foundation for future HSC studies.

We designed the first trials for valine-restricted preconditioning using the protocol from Taya et al. (2016). In this report, mice were fasted prior to diet introduction and maintained on a valine-deficient diet or complete diet for a maximum of 4 weeks, followed by valine reintroduction. No change was observed in the reduction of HSC frequency between week 3 and 4 of valine restriction (Taya et al., 2016). We therefore began our initial experiments with a 3-week depletion phase (**Figure 3.1A**).

We did not detect a significant difference in LT-HSC number between the valine depleted negative control and the control group fed a complete diet. Since LT-HSC percentages in the bone marrow of valine depleted mice were within the range of previously published data (Taya et al., 2016), this indicated that control mice had a lower than expected LT-HSC frequency. This was further supported by LT-HSC frequency in valine-restricted mice fed a complete diet (**Figure 3.1C**) which was higher and within the range of normal mice (Chen et al., 2008; Kiel et al., 2005; Oguro et al., 2013; Taya et al., 2016). We also analysed the spleen in addition to bone marrow since no previous study has investigated whether valine-restriction depletes LT-HSC from spleen (**Figure 3.1D**). We report that HSC in spleen appear to be virtually depleted in comparison with HSC in spleens from mice fed a complete diet. However, since these results are based on two independent experiments, the data can only be considered preliminary.

The valine refeeding phase was initially approached with caution due to reports of metabolic shock in mice immediately refed valine after a period of depletion (Taya et al., 2016). We tested different valine refeeding concentrations over the course of 2 weeks, increasing the valine concentration weekly. Contrary to the report by Taya et al. (2016), we found that no mice died after immediate reintroduction of a complete diet (**Figure 3.1C**). It is not clear as to why our mice did not die from immediate reintroduction of complete diet since both studies used 8-12 week-old C57BL/6 mice and were fed a valine depleted diet purchased from the same company (Research Diet; New Brunswick, NJ, USA).

Next, we compared intrasplenic adoptive cell delivery with traditional intravenous delivery method for cell homing towards the spleen. The aim was to characterize the small LT-HSC population localized in the spleen for their hematopoietic output. Since the LT-HSC population is much smaller than that in the bone marrow, we hypothesized that direct introduction of donor cells into the spleen would offer a greater chance for cells to engraft and proliferate in the spleen environment, creating a larger and more easily detectable output for characterization. Since intrasplenic injection is no longer a recommended route of administration as detailed by the most current global authority on the care of mice in laboratory research (Hirota & Shimizu, 2012), the technique was investigated before use in a transplantation experiment. We first tested intrasplenic injections on excised spleens of sacrificed mice (**Figure 3.2A**). Aliquots of 50µL and 20µL trypan blue were given to visualise the fluid retention and spillage from spleen (**Figure 3.2B**). Progressive leakage was noted for both volumes. This finding was at odds with other published protocols that use this method with much higher volumes (up to 200µL) and no apparent leakage (Miki, Takano, Garcia, & Grubbs, 2019).

We questioned whether leakage was due to the lack of blood circulation in the sacrificed mouse, and whether fluid retention increased when the spleen remained attached to the host. We hypothesized that spleen attachment via its vasculature may support fluid displacement upon injection. We also tested whether layering a small aliquot of Matrigel in the syringe after cell aspiration would create a seal around the site of injection to

prevent spillage (**Figure 3.2C**). Matrigel changes from a liquid to solid state at body temperature, and so a clamp was used at the site of injection to give time for the Matrigel to solidify once introduced into the spleen. From trials with Matrigel, we noticed that the layering effect (Matrigel aspirated first, then cells) was not achievable without having some of the cells mixing with the Matrigel during the liquid state in the syringe. Even with the addition of a Matrigel 'plug', progressive leakage was still evident (**Figure 3.2D**).

Finally, to confirm that intrasplenic injections were an effective method for cell transfer, we analysed spleen sections stained for fibroblastic and endothelial markers to identify architectural damage in the spleen microenvironment (**Figure 3.2E**). A clear path of destruction was evident in the injected spleen consistent with development of an inflammatory response (Chen et al., 2018), so compromising the steady-state condition (**Appendix A.2**). In conclusion, intrasplenic injection was not viable due to technical difficulties. Thus, only intravenous adoptive cell transfer was used for further transplantation experiments.

Next, the homing capacity of intravenously delivered cells was analysed. We failed to see any homing to spleen, bone marrow and peripheral blood by 18-hours after delivery (**Figure 3.3**). This was surprising as previous reports showed that approximately 4% and 5% of transplanted murine bone marrow cells could be found in the spleen and bone marrow at 18 hours after transplantation, respectively (Szilvassy et al., 1999). It is likely that donor cells home to non-hematopoietic organs like the lungs, rather than the bone marrow or spleen (Cui et al., 1999; Massberg et al., 2007; Szilvassy et al., 1999). We then identified donor cells at 48 hours after transplantation in the peripheral blood and spleen (Lanzkron, Collector, & Sharkis, 1999), but not in bone marrow. One hypothesis is that the lack of donor cell detection in bone marrow is due to the homing selectivity of cells (Plett, Frankovitz, & Orschell, 2003; Szilvassy et al., 1999). Transplanted HSC or bone marrow-derived leukocytes migrate to the spleen for the first 3 hours posttransplantation and then preferentially home towards the bone marrow (Szilvassy et al., 1999). However whole spleen leukocytes were transplanted and B cells were identified as the major cell type detected (**Figure 3.3**). Evidence points to organ-selective

homing (Szilvassy et al., 1999) as an explanation for the lack of donor cell detection in the bone marrow. For example, B cells are reported to selectively home towards spleen (Wols et al., 2010). Our findings were confirmed since HSC in spleen are rare (Tan & O'Neill, 2010), and approximately 50% of spleen leukocytes comprise B cells (**Appendix A.4**). Overall, donor spleen leukocytes are detectable at low levels in peripheral blood and spleen of valine depleted hosts at 48 hours posttransplantation, but bone marrow homing was not apparent.

Long-term lineage reconstitution assays were also performed (**Figure 3.4A**) using lineage$^-$ bone marrow, however no donor chimerism was detected after 8 months. Explanations for the lack of donor chimerism are that, firstly, the cell dose given was too low, consistent with evidence that transplantations achieve different donor chimerism levels for different cell doses transplanted (Rao et al., 1997; Westerhuis, van Pel, Toes, Staal, & Fibbe, 2011). On the premise that LSK constitutes 0.5% of lineage depleted bone marrow (Challen et al., 2009), we injected 1x10^6 lineage$^-$ bone marrow cells, comprising ~5000 LSK. From our own data we identified that the frequency of LSK cells within lineage$^-$ bone marrow is ~ 0.01% (**Appendix A.6**). This suggests that our transplants contained only 100 LSK as opposed to the predicted 5000 LSK. However, engraftment and long-term lineage reconstitution has been previously reported in mice transplanted with as few as 10 LSK (Camargo et al., 2006), suggesting that cell dose was not a limiting factor. The second potential reason could be the lack of valine at the time of transplantation, since valine is a vital amino acid necessary for proliferation and maintenance of HSC (Taya et al., 2016). A previous study reported donor chimerism of ~15% (±~10%SD), although this result was low and variable. We therefore reasoned that it would be necessary to address niche conditions and valine availability at the time of transplantation with a view of increasing the likelihood of engraftment.

By transplanting 1x10^6 lineage depleted CD45.2$^+$ bone marrow either 1- or 2-days following valine reintroduction into the diet (**Figure 3.4C**), donor chimerism was achieved at levels higher than previously observed (**Figure 3.4A**). The same number of lineage$^-$ bone marrow cells (1x10^6) was transplanted in both the long- and short-term lineage

reconstitution experiments, although only successful engraftment was achieved in short-term analyses (>0.1%). We attribute this success to either increased valine availability or to the fact that the donor cells comprise short-term progenitors (Camargo et al., 2006). Low numbers of LT-HSC in the transplant (Benveniste, Cantin, Hyam, & Iscove, 2003), and low survival rate of transplanted cells on engraftment in hematopoietic organs versus non-hematopoietic organs (eg. lungs, etc.) (Cui et al., 1999), are also confounding factors that could reduce engraftment. This is especially prominent in unirradiated hosts. A limitation of our short-term refeeding analysis was the absence of a day-0 valine refed control. Donor cells should have been transplanted on the day that valine refeeding was commenced, alongside the 1- and 2-day refed groups in order to directly compare differential valine availability. We recommend that refeeding should recommence 2-days prior to transplant since only one out of two 1-day refed transplantations worked, and all 2-day refed replicates were successful. Inefficient transplant delivery, and the likelihood that cells delivered failed to home to a hematopoietic organ, could account for the unsuccessful 1-day transplant (Benveniste et al., 2003; Cui et al., 1999).

Based on results presented here, we conclude that spleen-specific lineage output characterization studies in the steady-state condition can be best achieved using the optimized valine-restriction preconditioning method and by allowing 2-days of valine reintroduction prior to transplantation. Cell-dose titration is necessary to enhance donor engraftment since valine-restriction preconditioning does not clear hematopoietic niches entirely. Further research is required to identify the appropriate cell dose prior to performing optimal transplantation assays. LT-HSC must be sorted and intravenously transplanted, such that cell differentiation in this period must originate from LT-HSC. One third of intravenously transplanted HSC engraft in the spleen, and based on single HSC transplantation studies, do not migrate from the initial site of engraftment for up to 12 days (Cao et al., 2004). Bulk as opposed to single cell LT-HSC transplantation and engraftment will increase the sensitivity of detecting small numbers of progeny cells at early timepoints. Spleen-specific analysis must take place between 12-17 days post-transplantation, before proliferation and migration of engrafted cells occurs (Cao et al., 2004). LT-HSC require analysis at >16-weeks post-transplantation to assess complete

differentiation of all mature hematopoietic cell types (Yamamoto et al., 2013), otherwise expansion within the first 12 days will not distinguish between short term or long term reconstitution without progenitor analysis. Further analysis could investigate whether a ST-HSC or an MPP subtype would best suit the short-term reconstitution analysis, or whether progenitor characterization versus mature lineage characterization would best describe the spleen-specific contribution to lineage output in the steady-state condition.

CHAPTER 4

The role of spleen in age-related changes to myeloid-biased HSC

4.1 Introduction

Little is known about hematopoiesis in spleen under physiological conditions and whether this has any impact on overall changes in hematopoietic cell output associated with aging. Long-term (LT)-HSC are defined by a lineage$^-$cKit$^+$Sca-1$^+$(LSK)CD48$^-$CD150$^+$CD34$^-$ phenotype, and the addition of EPCR (CD201) as a marker further delineates tissue-resident stem cells (Balazs et al., 2006; Gur-Cohen et al., 2015). LT-HSC can also be functionally distinguished as balanced or myeloid-biased based on differential CD150 expression. This classification of HSC is important because hematopoiesis from HSC over age is characterized by a gradual skewing of lineage output shifting from a balanced (1:4 to 1:2) myeloid and lymphoid output in young animals towards a myeloid-dominant (>1:2) output with aging (Beerman et al., 2010; Benz et al., 2012). This change over time is indicated by a change in relative proportion of CD150^{lo} versus CD150^{hi} HSC populations, representing balanced (CD150^{lo}) and myeloid-biased (CD150^{hi}) HSC respectively. Within the LSKCD34$^-$Flt3$^-$ compartment, the proportion of the different subsets have been defined:17% CD150^{hi}, 56% CD150^{lo} and 26% CD150$^-$ HSC in young animals corresponding with balanced hematopoietic cell output (Beerman et al., 2010). In the same study, myeloid-biased hematopoiesis in old (24-month) mice was associated with 58% CD150^{hi}, 34% CD150^{lo} and 8% CD150$^-$ HSC distribution (Beerman et al., 2010). Thus, younger animals display a higher proportion of CD150^{lo} balanced HSC, compared with older animals which express a higher proportion of CD150^{hi}, or myeloid-biased LT-HSC (Beerman et al., 2010).

The question of whether intrinsic or extrinsic factors control HSC fate is an area of debate and investigation. One hypothesis is that age-associated myeloid-biased lineage skewing could be due to HSC mobilization into niche spaces outside of the bone marrow, for example spleen. Extramedullary hematopoiesis occurs mostly under stress conditions and leads to the migration of HSC from bone marrow towards spleen, where they contribute to hematopoiesis within sinusoidal niches (Inra et al., 2015; Wright et al., 2001). While hematopoiesis within spleen predominantly supports myelopoiesis (Inra et al., 2015; Nakada et al., 2014; Tan & O'Neill, 2012), HSC isolated from the spleen and

adoptively transferred into irradiated hosts can demonstrate multi-lineage potential (Tan & O'Neill, 2010). Therefore, microenvironmental cues delivered specifically by the spleen could exert myelopoietic programming on otherwise multipotent HSC.

One important issue, therefore, is the extent to which HSC might become “programmed” during mobilization into the spleen and then maintain a myeloid-biased differentiation pattern following migration back into the bone marrow. In one study (Morita et al., 2011), LSKCD34$^-$ HSC from either the bone marrow or spleen were transplanted into irradiated mice (**Figure 4.1.1A**). Bone marrow from primary recipients containing either donor BM-derived or donor spleen-derived HSC was then transplanted into secondary recipients (**Figure 4.1.1B**). This study reported increased myeloid cell production in secondary recipients originally given spleen-derived donor HSC as a primary transplant (**Figure 4.1.1C**). Spleen-derived HSC originally transplanted into the primary recipient must have first migrated into bone marrow, and then retained myeloid-biased programming upon secondary bone marrow transplantation (**Figure 4.1.1**). This finding offers evidence that the spleen microenvironment not only enforces local myelopoiesis, but may imprint this behavior even after HSCs have left the spleen.

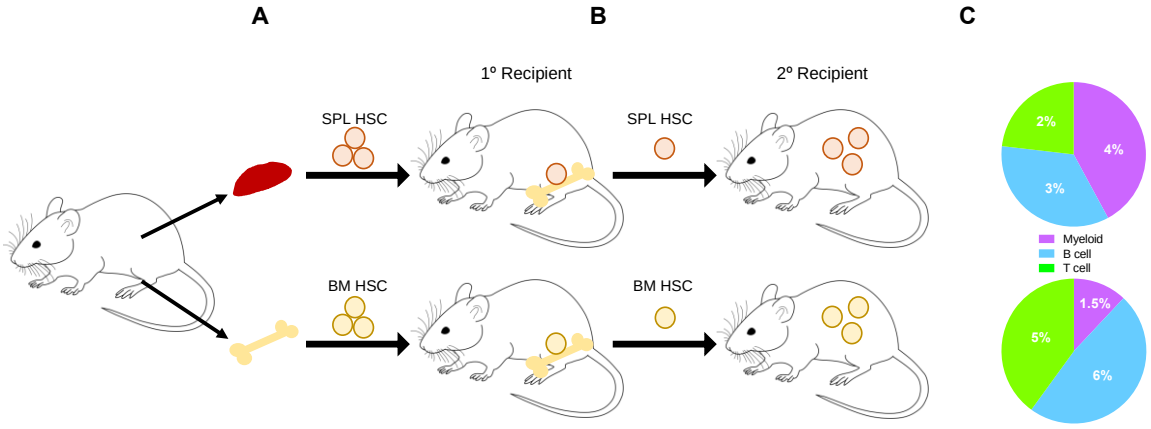

Figure 4.1.1 *Long-term reconstitution by bone marrow or spleen LSKCD34$^-$ cells. Figure adapted from (Morita et al., 2011). A) Primary recipient transplant. B) Secondary recipient transplant. C) Average % chimerism and lineage analysis from secondary transplant recipients represented.*

It is therefore our hypothesis that through this mechanism, the spleen microenvironment contributes to the skewing HSC to give a myeloid-bias in the bone marrow with age. Under steady-state conditions, HSC are constantly migrating between niches in the body, evidenced by HSC found in the peripheral blood outside of stem cell niches (Wright et al., 2001). If stem cells are constantly shuffling between hematopoietic niches in body, and if the spleen niche imprints migratory HSC with myeloid-biased programming, then over a lifetime, the movement of HSC between the spleen and bone marrow may result in the gradual accumulation of myeloid-biased HSC within the animal.

One potential method to test whether the spleen contributes to the build-up of myeloid-biased HSC over a lifetime is to push stem cell emigration towards the spleen at a higher rate, so replicating or exacerbating the characteristics of aging. Pregnancy, in particular, is known to induce extramedullary hematopoiesis in the spleen due to an increase in estrogen levels (Nakada et al., 2014). In this study, we propose a model for accelerating the effects of steady-state aging by increasing the rate of HSC mobilization and movement between bone marrow and spleen hematopoietic niches, through inducing pregnancy on multiple occasions. Here, large number of HSCs are expected to migrate into spleen and become imprinted with a myeloid bias before returning to bone marrow niches. Therefore, splenectomised exbreeder mice that have undergone multiple rounds of pregnancy would maintain a ‘younger’ HSC phenotype, in comparison with normal exbreeder mice which would exhibit a higher proportion of myeloid-biased HSC.

In the previous chapter, we began to address the contribution of spleen to steady-state myeloid cell production. In this chapter, we aim to determine whether spleen contributes to an accumulation of myeloid-biased LT-HSC over age by directly comparing the frequencies of $CD150^{hi}$ HSC in normal young, normally aged and aged asplenic mice. Here we use pregnancy as a model of HSC aging. Comparisons have been made between age-matched normal exbreeder and asplenic exbreeder mice that have undergone multiple cycles of pregnancy to induce extramedullary hematopoiesis. These mice were tested to determine whether increased exposure to splenic niches drives the age-associated myeloid-biased within the HSC population.

4.2 Results

4.2.1 Determining CD150$^{hi/lo/-}$ expression amongst LT-HSC

To assess whether the spleen plays a role in the rise of myeloid-biased CD150^{hi} HSC with old age, we first verified that a CD150$^{hi/lo/-}$ gating strategy could be applied to LT-HSC in order to distinguish myeloid-biased and balanced HSC, respectively. Myeloid-biased LT-HSC have previously been identified using a lineage^{-}cKit^{+}Sca-1^{+}CD150^{hi}CD48^{-}CD34^{-} phenotype. For this study, a gating strategy was adapted from both Beerman et al. (2010) and Benz et al. (2012) to distinguish tissue-endogenous EPCR^{+} HSC as CD150^{hi} myeloid-biased LT-HSC, balanced LT-HSC as CD150^{lo}, and lymphoid-biased ST-HSC as CD150^{-} (Challen, Boles, Chambers, & Goodell, 2010; Morita et al., 2010) (**Figure 4.2.1)**.

Following several different experimental trials, a strategy which delineated differential CD150 expression amongst LT-HSC was established. Gating for no expression of CD150 and CD34 was achieved using two separate fluorescence minus one controls (FMOC) for each antibody. To prepare LT-HSC for flow cytometric analysis, magnetic depletion of cells expressing mature lineage cell markers (CD11c, Gr-1, NK1.1, CD48) was performed with biotinylated antibodies. The remaining lineage^{+} cells were identified by flow cytometry using APC-eFluor 780-conjugated streptavidin for exclusion during the gating process. Following the lineage^{-} gate, cKit^{+} and Sca-1^{+} cells, otherwise known as the LSK subset, were subsequently selected to display CD150 and EPCR expression. Boundaries for EPCR^{+} gates as well as CD150^{lo} gates were applied using an internal control population (Lin^{-}cKit^{+}Sca-1^{-}). This control represents a myeloid progenitor (CMP or MEP) population (Beerman et al., 2010).

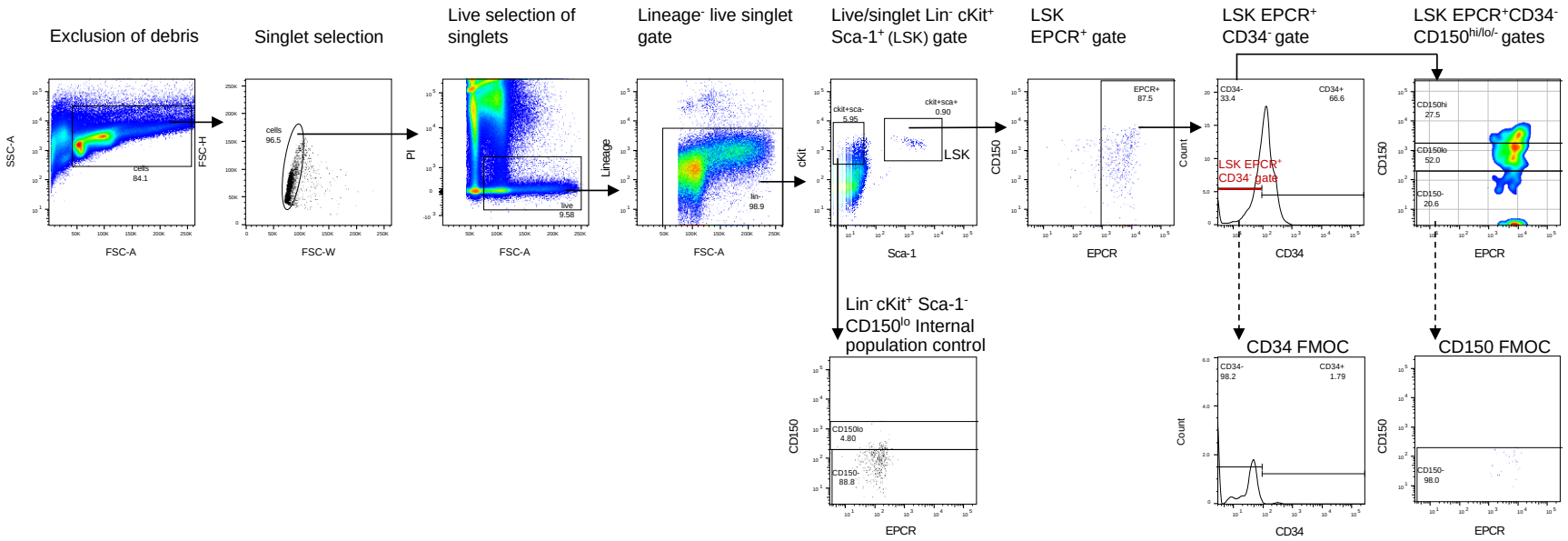
Exclusion of debris
Singlet selection
Live selection of singlets
Lineage- live singlet gate
Live/singlet Lin- cKit+ Sca-1+ (LSK) gate
LSK EPCR+ gate
LSK EPCR+ CD34- gate
LSK EPCR+CD34- CD150hi/lo/- gates
SSC-A
FSC-H
cells 84.1
FSC-A
cells 96.5
FSC-W
PI
live 9.58
Lineage
lin- 98.9
cKit
ckit+sca- 5.95
ckit+sca+ 0.90
LSK
Sca-1
CD150
EPCR+ 87.5
EPCR
Count
CD34- 33.4
CD34+ 66.6
LSK EPCR+ CD34- gate
CD34
CD150hi 27.5
CD150lo 52.0
CD150- 20.6
Lin- cKit+ Sca-1- CD150lo Internal population control
CD150lo 4.80
CD150- 88.8
CD34 FMOC
CD34- 98.2
CD34+ 1.79
CD150 FMOC
CD150- 98.0

Figure 4.2.1 Defining a gating strategy to consistently report differential CD150 expression on LT-HSC.

The gating strategy used to define LT-HSC and sub-populations of short-term ($CD150^{-}$), long-term balanced ($CD150^{lo}$) and myeloid-biased ($CD150^{hi}$) HSC is shown. Plots are representative of a 5-month-old C57BL/6J female mouse. Red blood cell lysed bone marrow cells were magnetically depleted of mature cells using biotinylated CD48 (HM48-1), NK1.1 (PK136), CD11c (N418), and Gr-1 (RB6-8C5) lineage marker antibodies. Cells were analysed by flow cytometry for the $Lineage^{-}cKit^{+}Sca\text{-}1^{+}$(LSK) $CD150^{+}CD34^{-}EPCR^{+}$ phenotype using antibodies specific for cKit (2B8; FITC), Sca-1 (D7; BV421), CD150 (mSHAD150; PE-Cy7), CD34 (RAM34; eFluor 660) and CD201 (eBio1560; PE). Streptavidin (SA)-APC-eFluor 780 was used as a secondary reagent to detect any remaining undepleted $lineage^{+}$ cells. Prior to flow cytometry, cells were stained with propidium iodine (PI^{-}) to include only PI^{-} viable cells in further analyses. The gating strategy identifies the criteria which define LT-HSC and $CD150^{hi/lo/-}$ subsets. Percent positive cells is indicated in each plot. Fluorescence minus one controls (FMOC) for CD34 and CD150 were used to set gates to exclude CD150 and CD34 expression. Final plots represent a 'smoothed' display with outlier's present.

In order to accurately set the $CD150^{lo}$ gate, all plots were standardized to display the same number of events for internal controls (592). With a constant event number displayed, the upper boundary of the $CD150^{lo}$ gate was placed at the level of the highest recorded event, or gating 98% of events in cases where outliers were evident (events registering at intensity levels of $\geq 10^4$). In this representative example, we show that the $CD150^{hi}$, $CD150^{lo}$ and $CD150^{-}$ populations make up 27.5%, 52% and 20.6% of HSC, respectively.

Aging studies that focus on myeloid-biased HSC proliferation typically rely on CD150 expression changes in variably aged animals. In an alternative approach, the median fluorescence intensity (MFI) of CD150 staining can be investigated as a potentially more sensitive method of detecting shifts in CD150 expression amongst variably aged LT-HSC populations. A 5-month-old C57BL/6J female mouse was analysed for the $CD150^{+}$ LT-HSC population to establish a baseline reading for young animals (**Figure 4.2.2**). Since $CD150^{-}$ expression phenotypically defines ST-HSC, this population was excluded in order to allow assessment of only $CD150^{+}$ LT-HSC. In the representative figure, the MFI for LT-HSC in a 5-month-old animal was 1276 relative fluorescence units.

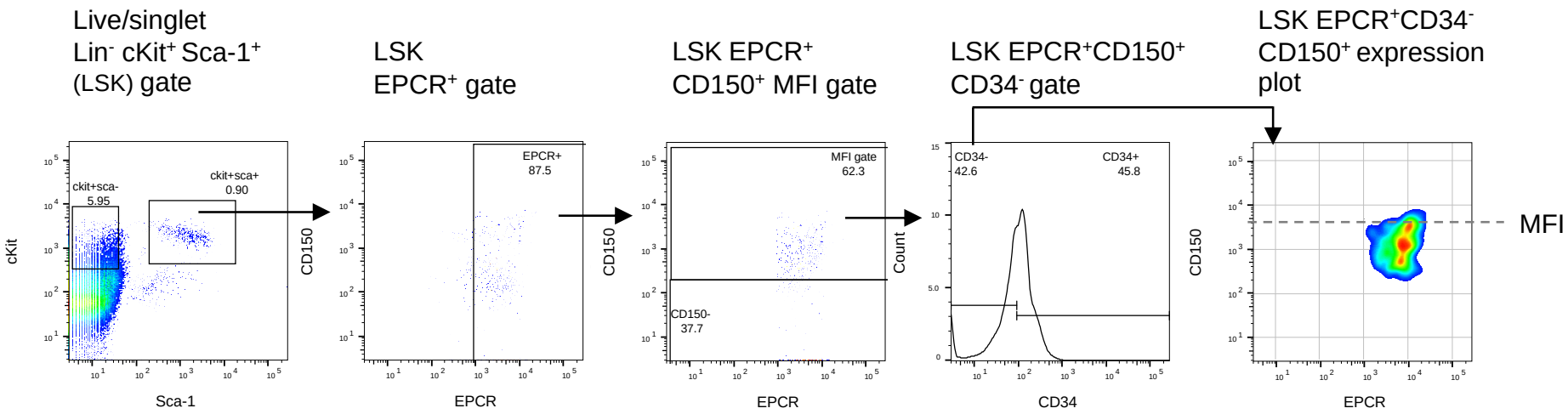
Live/singlet
Lin- cKit+ Sca-1+
(LSK) gate
LSK
EPCR+ gate
LSK EPCR+
CD150+ MFI gate
LSK EPCR+CD150+
CD34- gate
LSK EPCR+CD34-
CD150+ expression
plot
ckit+sca-
5.95
ckit+sca+
0.90
cKit
Sca-1
CD150
EPCR+
87.5
EPCR
MFI gate
62.3
CD150-
37.7
Count
CD34-
42.6
CD34+
45.8
CD34
MFI

Figure 4.2.2 Gating strategy to determine CD150 median fluorescence intensity on LT-HSC

The gating strategy used to define HSC and sub-populations of short-term ($CD150^{-}$), long-term balanced ($CD150^{lo}$) and myeloid-biased ($CD150^{hi}$) HSC in Figure 4.1 was modified to identify the median fluorescence intensity (MFI) of CD150 expression. Plots are representative of lineage-depleted bone marrow cells isolated from a 5-month-old C57BL/6J mouse. Bone marrow cells were prepared as outlined in Figure 4.1. Live, singlet, $lineage^{-}cKit^{+}Sca\text{-}1^{+}$ (LSK) $EPCR^{+}$ cells were initially selected before all $CD150^{+}$ cells were gated, indicated by the "LSK EPCR+ CD150+" MFI gate. Subsequently, $CD34^{-}$ gated cells were analysed for CD150 MFI. The MFI of the representative figure is identified as a grey dotted line on the final $LSKCD34^{-}EPCR^{+}CD150^{+}$ plot. Final plots are illustrated as a 'smoothed' display with outlier's present. Axis intensity values are arbitrary and can be classified as relative fluorescence units.

4.2.2 Assessing the spleen's influence on LT-HSC populations in young and old mice

Once $CD150^{hi/lo/-}$ expression levels could be established, the proportions of $CD150^{hi}$ to $CD150^{lo}$ to $CD150^{-}$ cells amongst ESLAM gated LT-HSC of young (2-5 months), old (18-22 months) and old asplenic (18-22 months) mice were compared (**Figure 4.2.3A**). A significant increase in frequency of $CD150^{hi}$ HSC was found in young over old control groups. This was expected as previously reported (Beerman et al., 2010). However, there was no significant difference in the frequency of $CD150^{lo}$ HSC between young and old mice. We observed no statistical difference in the frequency of $CD150^{hi}$, $CD150^{lo}$ or $CD150^{-}$ HSC populations between aged normal and aged asplenic mice. We also compared the $CD150^{+}$ LT-HSC compartment (**Figure 4.2.3B**), but found no significant difference in $CD150^{hi}$ HSC frequency amongst total $CD150^{+}$ cells between young, old or old asplenic groups.

The MFI of CD150 expression was then calculated for the $LSKCD34^{-}CD48^{-}EPCR^{+}$ LT-HSC population for each animal group (**Figure 4.2.3C**). Consistent with previous research, CD150 MFI was lowest in young mice (1632.2 ± 346.1). However, we did not detect any significant increase in CD150 MFI between young and old mice. Similarly, the CD150 MFI between old (3165.4 ± 305.4) and old asplenic (3658±777.8) mice was not significantly different. Taken together HSC frequency (**Figure 4.2.3A & B**), and MFI of CD150 (**Figure 4.2.3C**), all results confirm that between old and old asplenic animals, the absence of spleen does not appear to have an effect on the development of aged $CD150^{hi}$ HSC.

Lastly, we analysed the frequency of bone marrow $CD150^{+}$ LT-HSC (**Figure 4.2.3D**) and total bone marrow cellularity (**Figure 4.2.3E**) for each group. There was no statistical difference in $CD150^{+}$ LT-HSC number between young and old control mouse groups, or between old and old asplenic groups (**Figure 4.2.3D**). Similarly, no difference was observed in bone marrow cellularity between any group (**Figure 4.2.3E**). These data suggest that the absence of a spleen did not change the normal physiological aging characteristics of LT-HSC when compared to aged counterparts. This must however be

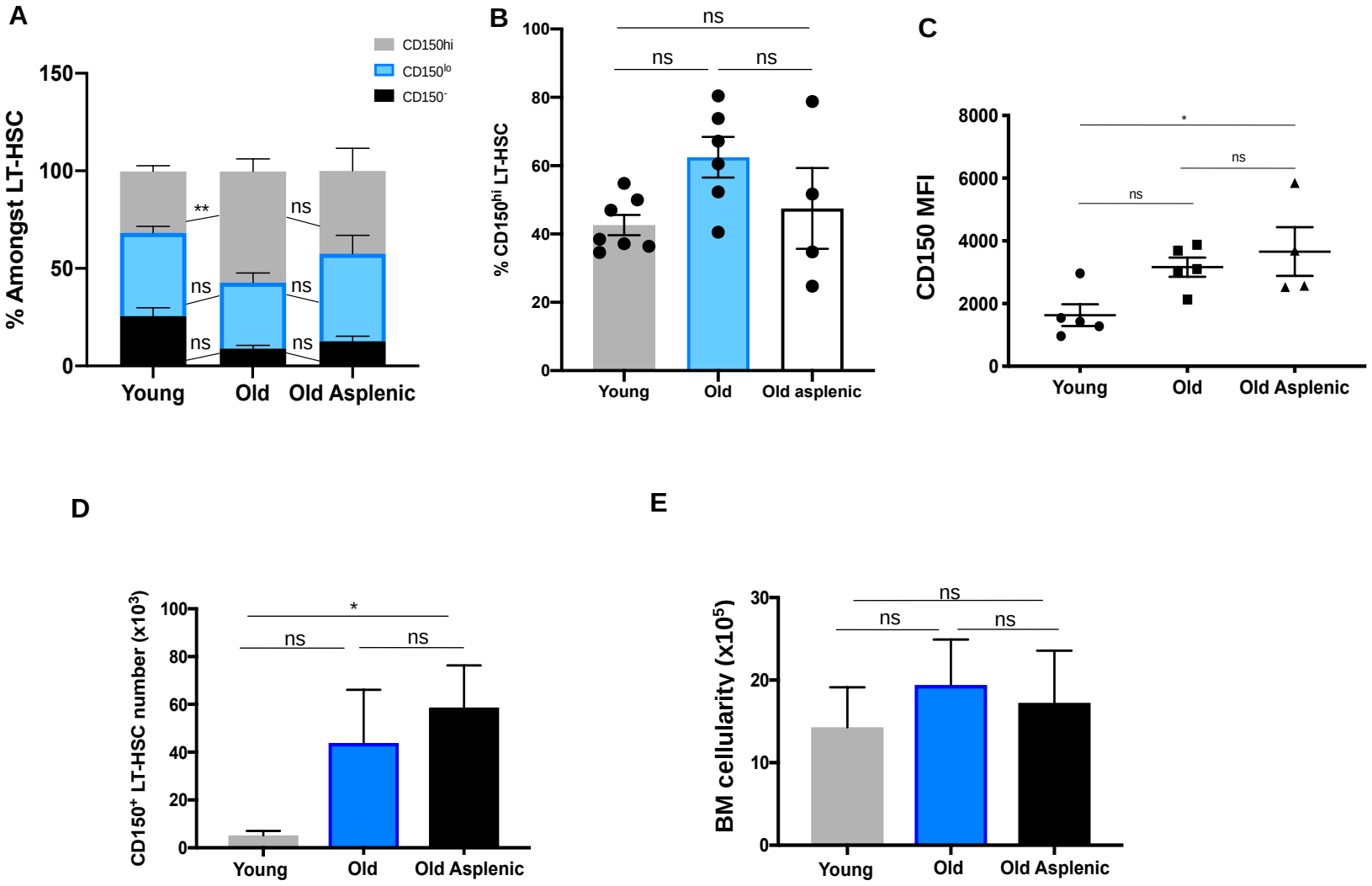
A
CD150hi
CD150lo
CD150-
% Amongst LT-HSC
150
100
50
0
**
ns
ns
ns
ns
Young
Old
Old Asplenic
B
% CD150hi LT-HSC
100
80
60
40
20
0
ns
ns
ns
Young
Old
Old asplenic
C
CD150 MFI
8000
6000
4000
2000
0
*
ns
ns
Young
Old
Old Asplenic
D
CD150+ LT-HSC number (x10^3)
100
80
60
40
20
0
*
ns
ns
Young
Old
Old Asplenic
E
BM cellularity (x10^5)
30
20
10
0
ns
ns
ns
Young
Old
Old Asplenic

Figure 4.2.3 Analysis of HSC populations amongst young, old and old asplenic mice.

Lineage depleted bone marrow cells were prepared as outlined in Figure 4.1 and stained with antibodies specific for cKit (2B8; FITC), Sca-1 (D7; BV421), CD150 (mSHAD150; PE-Cy7), CD34 (RAM34; eFluor 660) and CD201 (eBio1560; PE). Streptavidin (SA)-APC-eFluor 780 was used as a secondary reagent to stain any remaining undepleted lineage$^+$ cells. Prior to flow cytometry, cells were stained with propidium iodide (PI) to discern live viable cells (PI$^-$) from apoptotic cells. A) Graph shows percent CD150^{hi}, CD150^{lo} and CD150$^-$ cells amongst LSKCD34$^-$CD48$^-$EPCR$^+$ LT-HSC from young (2-5-months-old) (*n=7*), old (18-22-months-old) (*n=5*) and old asplenic (18-22-months-old) (*n=4*) mice over seven independent experiments. B) Percent CD150^{hi} LT-HSC amongst CD150$^+$ LT-HSC from (A). C) Median fluorescence intensity (MFI) of CD150 on LT-HSC from young (●; *n=5*), old (■; *n=5*), and old asplenic (▲; *n=4*) mice. Data show the mean±SEM of five independent experiments. D) CD150$^+$ LT-HSC number calculated from percent of total CD150$^+$, multiplied by total live lineage depleted bone marrow cells, collected from two femurs of the same mouse. E) Cellularity represents total live lineage-depleted bone marrow cells, collected from two femurs of the same mouse. All error bars represent SEM. Data was analysed using either a parametric one-way ANOVA with Tukey multiple comparisons test (B, C, D & E) or a two-way mixed effect ANOVA with Tukey's multiple comparisons test (A). Significant P values are indicated as (*) when $P<0.05$ and (**) when $P<0.005$ and non-significant (ns) P values are indicated when $P>0.05$.

interpreted with caution since differences between control young and old mice were also not detected (**Figure 4.2.3B, C, D & E**).

4.2.3 Assessing myeloid-biased CD150^{hi} LT-HSC in asplenic and normal exbreeder mice

Pregnancy is known to increase the migration of HSC from the bone marrow into spleen during extramedullary hematopoiesis (EMH) (Nakada et al., 2014). The exbreeder mice used in this experiment had undergone six cycles of pregnancy, and consequently repeated EMH events of BM HSC mobilization into the spleen. Therefore, we investigated whether the absence of a spleen would reduce the frequency of CD150^{hi} HSC present in the bone marrow compared to non-splenectomised exbreeder counterparts. Such an outcome may suggest that the increase in myeloid-biased HSC with age is linked to the spleen HSC microenvironment.

In order to test this, we analysed bone marrow HSC from normal exbreeder and asplenic exbreeder mice. The gating strategy from **Figure 4.2.1** was applied to identify differential CD150 expression on LT-HSC in all experiments. We found no significant difference in proportion of CD150^{hi} or CD150^{-} HSC between normal and asplenic exbreeder. However, we did observe a small but significant (P=0.034) increase in the size of the CD150^{lo} HSC population in asplenic exbreeder compared with normal exbreeder mice (49.5%±3.3 and 34.1%±4.7%, respectively) (**Figure 4.2.4A**). Interestingly, the size of the CD150^{hi} HSC population did not increase with the decrease in size of the CD150^{lo} HSC population in normal exbreeder mice as might be expected. This could be due to large variation in CD150^{hi} expression in normal exbreeder (53.9%±8.3%) over asplenic exbreeder (36.6%±2.8%) mice. Lastly, we compared the median fluorescence intensity of CD150 expression, analysed as described in **Figure 4.2.2**, between exbreeder (3587±618) and asplenic exbreeder mice (2764±496). We did not observe a statistical difference between these two groups (**Figure 4.2.4B**).

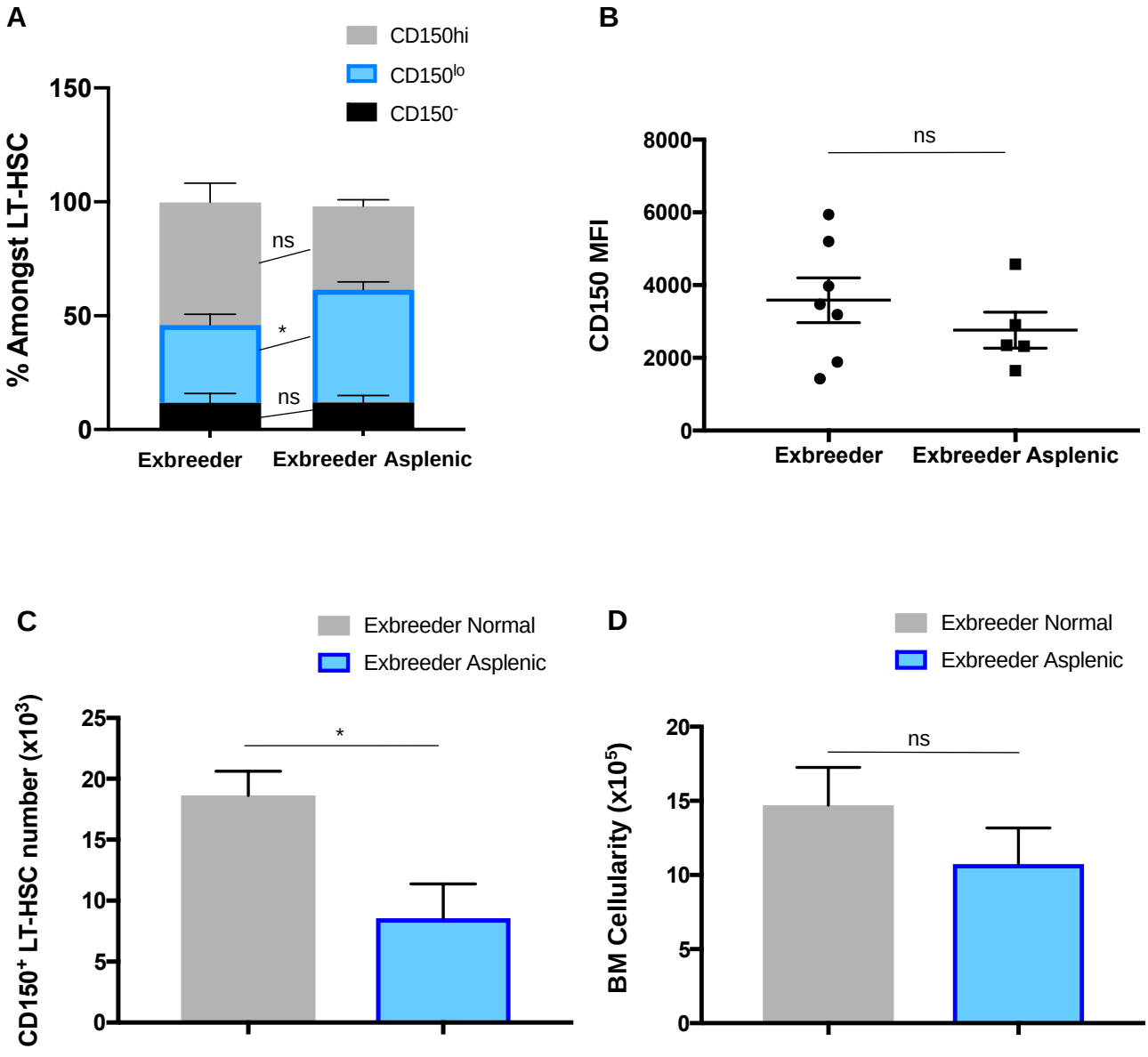
A
CD150hi
CD150lo
CD150-
% Amongst LT-HSC
150
100
50
0
ns
*
ns
Exbreeder
Exbreeder Asplenic
B
CD150 MFI
8000
6000
4000
2000
0
ns
Exbreeder
Exbreeder Asplenic
C
Exbreeder Normal
Exbreeder Asplenic
CD150+ LT-HSC number (x10^3)
25
20
15
10
5
0
*
D
Exbreeder Normal
Exbreeder Asplenic
BM Cellularity (x10^5)
20
15
10
5
0
ns

Figure 4.2.4 Bone marrow HSC analysis in normal and asplenic exbreeder mice.

Exbreeder C57BL/6J mice underwent at least six bouts of pregnancy and were approximately 9 months old. Asplenic exbreeder mice were splenectomised at 4-weeks, and allowed to age and breed under the same conditions as the normal exbreeder control group. A) Bone marrow derived LT-HSC were gated according to Figure 4.1 to define $CD150^{hi/lo/-}$ expression. B) Median fluorescence intensity (MFI) of CD150 on LT-HSC from normal exbreeder (●) and asplenic exbreeder (■) mice. C) $CD150^{+}$ LT-HSC number was calculated by multiplying the % LT-HSC by the number of live lineage-depleted bone marrow cells (exbreeder = grey; asplenic exbreeder = blue). D) The live lineage-depleted bone marrow count was used to estimate bone marrow (BM) cellularity for normal exbreeder (grey) and asplenic exbreeder (blue) mice. In this study, normal exbreeder (*n=7*) and asplenic exbreeder (*n=5*) mice were analysed in seven independent experiments. All error bars represent SEM. Data was first analysed for a Gaussian distribution using the Shapiro-Wilk normality test before either a one-way ANOVA with Sidak multiple comparisons test (A), or unpaired Student's t-test (B, C & D) (* = $P<0.05$; ns = $P>0.05$).

The total number of $CD150^+$ LT-HSC in bone marrow was calculated by multiplying the percentage of gated $CD150^+$ LT-HSC by the live lineage-depleted bone marrow white cell count. The total $CD150^+$ LT-HSC number in asplenic exbreeder mice showed a significant decrease of ~2.8 fold compared to normal exbreeders (**Figure 4.2.4C**). Cellularity between the two groups was not different (**Figure 4.2.4D**) suggesting that the presence of spleen during pregnancy is essential for the expansion of $CD150^+$LT-HSC and does not affect the overall bone marrow cellularity. Overall, these results do not support the hypothesis that splenic microenvironment contributes to age-associated myeloid-biased amongst HSC, assuming that HSC repeatedly migrate into spleen during EMH.

4.3 Discussion

The isolation of LT-HSC has been achieved using different combinations of cell surface markers. In this study, markers were chosen by combining and adapting two methods previously published (Balazs et al., 2006; Beerman et al., 2010). For this study, it was necessary to identify LT-HSC on the basis of age-associated myeloid-bias characterized by increased CD150 expression on LT-HSC (Beerman et al., 2010). As with the Beerman et al. (2010) study, our marker panel included CD34 and CD150 alongside the traditional LSK panel of markers used for enrichment. However, instead of FLT3, the marker panel included EPCR (CD201). EPCR has been described as a marker that identifies tissue endogenous HSC as well as a subset of LT-HSC (Balazs et al., 2006; Benz et al., 2012). Overall, this marker panel enabled investigation into whether HSC exposed to the splenic microenvironment contributed to overall age-associated increases in myeloid-biased $CD150^{hi}$ HSC.

Myeloid-biased HSC are characterized by high CD150 expression, while low CD150 expression is associated with a balanced differentiation potential (Beerman et al., 2010; Morita et al., 2010). In this chapter, the frequency of $CD150^{lo/hi}$ HSC was assessed for each experimental group as in existing HSC studies (Beerman et al., 2010; Dykstra, Olthof, Schreuder, Ritsema, & de Haan, 2011; Morita et al., 2010). Multiple limitations were identified with traditional $CD150^{lo/hi}$ population analysis, including inconsistency in gating between independent experiments which predisposes data to potential subjectivity during flow cytometry analyses (Lux et al., 2018). This was compounded by the inclusion of antibodies against CD48 in the lineage depletion panel. Initially we analysed CD48 co-expression with a variety of common hematopoietic lineage markers (CD3, CD19, CD11a, CD11c, CD34, Gr-1 and NK1.1) and found that CD48 was co-expressed with many lineage markers but not with Gr-1, NK1.1, CD11a and CD11c (**Appendix A.8**). For this reason, we included CD48 in the lineage depletion cocktail. We subsequently encountered limitations with this approach when establishing the $CD150^{lo}$ gate using an internal

Lineage$^-$cKit$^+$Sca-1$^-$ MEP control population. All MEP cells express CD48 (Draper et al., 2018). As a consequence, CD48 depletion impacted the number of these control cells and showed variability across preparations. We therefore standardized the event count for all internal control Lineage$^-$cKit$^+$Sca-1$^-$ populations and set the CD150^{lo} gate to include 98% of events (**Figure 4.2.1**). This last step removed variability in gating CD150^{hi} cells in the event of outliers. Given the difficulty associated with gating HSC populations, we also calculated the level of CD150 expression amongst LT-HSC through assessment of MFI as an alternative method to detect age-associated HSC population change (**Figure 4.2.2**). This method allowed us to circumvent CD150 gating altogether, and to represent data in a more objective manner.

Increased CD150 expression on LT-HSC is considered a defining characteristic of myeloid-biased HSC (Beerman et al., 2010). Old control animals in this study displayed a significantly larger proportion of CD150^{hi} HSC compared with young control animals (**Figure 4.2.3A**), verifying that the ageing model was viable despite increased %LSK variation in old mice (Dykstra et al., 2011). While a significant increase in CD150^{hi} HSC frequency was found between control young and control old animal groups (**Figure 4.2.3A**), no difference was found between young, old and old asplenic groups when CD150^{hi} LT-HSC populations were compared (**Figure 4.2.3B**). Furthermore, direct comparison of young versus old versus old asplenic mice against 12-month and 24-month data recalculated from Beerman et al. (2010) revealed striking similarities (**Appendix A.9**). However, it is important to note that neither the current nor previous study reported significant differences between any group.

In addition, our model did not reproduce the reduction in CD150^{lo} HSC number between young and old animals that was previously reported (Beerman et al., 2010; Morita et al., 2010). In our hands, this finding suggests that myeloid-biased CD150^{hi} LT-HSC do not increase at the same rate as CD150^{lo} HSC decrease. Importantly,

we did not detect a statistically significant decrease in CD150^{hi} HSC in old asplenic animals compared with old normal animals. While this finding may be impacted by naturally higher variation amongst %LSK cells in older animals (Dykstra et al., 2011), in combination with CD150 MFI data (**Figure 4.2.3C**), our results suggest that the spleen does not contribute to an increase in myeloid-biased CD150^{hi} HSC over a lifetime.

In terms of HSC numbers, previous research has reported an expansion of CD150^{+} LT-HSC in older mice (Dykstra et al., 2011; Sudo, Ema, Morita, & Nakauchi, 2000; Yamamoto et al., 2018). These reports suggest that young mice maintain strict control of the LSK CD34^{-}EPCR^{+}CD150^{+} pool size, whereas in old mice pool size varies (Dykstra et al., 2011). In this study, we observed no difference between normal young and old groups. This is also attributed to the reported high variability in HSC numbers observed in aged mice. This variability was seen here not only in the old group, but also in the old asplenic group, suggesting that a similar age-associated lack of control exists in the old asplenic group (**Figure 4.2.3D**). The absence of a spleen did not impact the development of an expanded and variable HSC pool.

Lastly, bone marrow cellularity did not differ significantly between young, old and old asplenic groups (**Figure 4.2.3E**). Although variability in bone marrow cell number was observed in all groups consistent with published data (Sudo et al., 2000), the cellularity of murine bone marrow does not vary with age (Sudo et al., 2000). Bone marrow cellularity was an important parameter in studying HSC numbers in normal and asplenic mice, to ensure that the absence of a spleen did not affect lineage^{-} cell numbers in bone marrow over age. Because bone marrow cellularity remained consistent across all three treatment groups, the expansion of CD150^{+} LT-HSC expansion is confirmed with confidence.

Pregnancy was used as a model to induce extramedullary hematopoiesis in order to study whether multiple mobilization events phenotypically aged HSC through repeated exposure to the spleen environment. In comparison with normal exbreeder mice, we hypothesized that asplenic exbreeder mice would display a lower number of $CD150^{hi}$ HSC, and therefore a "younger" HSC phenotype. We note that the number of $CD150^{lo}$ HSC in asplenic exbreeder mice significantly increased by ~15.4% above normal exbreeders (**Figure 4.2.4A**). While this was associated with a decrease in percentage of $CD150^{hi}$ HSC between asplenic and normal exbreeder mice, this was not significant (**Figure 4.2.4A**). In terms of MFI, CD150 expression on LT-HSC did decrease in aged exbreeder mice which had lost a spleen, but again this was not significantly different (**Figure 4.2.4B**), supporting findings from **Figure 4.2.3**. The data available to date do not support the hypothesis that absence of a spleen during pregnancy contributes to changes in the HSC population in terms of CD150 expression. A retrospective power analysis of this experiment predicts that a sample size of 108 mice would be needed to show significance.

In the absence of a spleen, and of pregnancy induced extramedullary hematopoiesis associated with spleen, a significant decrease in number of $CD150^{+}$ LT-HSC in bone marrow of asplenic versus normal exbreeder mice was identified (**Figure 4.2.4C**). One explanation is that in the absence of a spleen, HSC would migrate from bone marrow in search of extramedullary sites, perhaps homing into organs which do not support hematopoiesis (Bowling et al., 2008). HSC that remain in bone marrow may expand within the limited confines of the bone marrows niche (**Figure 4.2.4C**), resulting in changes in the HSC population. The contribution of spleen is well known particularly for support of stress-induced extramedullary hematopoiesis. Previous studies have demonstrated the ability of spleen to induce a pre-activated cell-cycle state amongst HSC (Coppin et al., 2018), allowing faster proliferation of HSC to meet the high demands that stress and pregnancy impose (Nakada et al., 2014; Oguro et al., 2017). A recent study suggested marker CD61 identified myeloid-biased LT-HSC that were primed to respond to inflammatory events (Mann et al., 2018).

Incorporating CD61 into future analyses of pregnancy-induced extramedullary hematopoiesis may allow better insight of the proportion of collected LT-HSC that were primed for, and contributed to, the cellular expansion within the spleen. Bone marrow cellularity was found to remain constant in normal and asplenic exbreeder mice (**Figure 4.2.4D**) consistent with results obtained through comparison of young, old and old asplenic mice (**Figure 4.2.3D**). This is consistent with the cellular space in bone marrow being finite, compared with spleen where capacity for expansion is not restricted (Nakada et al., 2014).

In our exbreeder study, an age-matched normal counterpart should ideally have been used as a control to determine whether LT-HSC number, bone marrow cellularity and CD150 expression differed between young and old, and between aged and exbreeder aged mice. At this point, we cannot determine the impact of pregnancy on the aging phenotype. We can only conclude that the presence of a spleen is associated with higher $CD150^{+}$ LT-HSC numbers in bone marrow, and may have slightly decreased the percentage of $CD150^{lo}$ or balanced LT-HSC in exbreeders.

In summary, we used two animal models to investigate the role of spleen in the age-related accumulation of myeloid-biased $CD150^{hi}$ HSC. Our ageing model first confirmed increases in number of $CD150^{hi}$ LT-HSC in control old mice compared with young counterparts. Subsequently, comparison between old and old asplenic mice did not show any statistical difference in number of $CD150^{hi}$ LT-HSC. Our second model involved exbreeder mice which had undergone multiple rounds of EMH triggered by pregnancy which would have mobilized HSC into the spleen with each pregnancy. In this model, no decrease in the number of $CD150^{hi}$ LT-HSC was observed in exbreeder mice which had been splenectomised ahead of pregnancy compared with normal exbreeders. Overall, the data indicate that spleen does not play a significant role in the progressive myeloid-biased HSC shift over the lifetime of an animal. According to previous studies, young and old animals are considered

statistically different. Immunophenotyping may be a limitation in this instance, contributing to the variation that deterred the young and old controls from being statistically different. Therefore, we suggest no firm conclusion can be drawn due to a high risk of a type II error present within our results. For future studies, a prospective sample size calculation should consider the high degree of variability that is commonly seen within the old age group and adjust the expected power accordingly.

Analysis of aging based on differential CD150 expression introduces a gating bias and so results should be interpreted with caution. Furthermore, a recent study has suggested that CD150 may not accurately discriminate aged myeloid-biased HSC from the young counterpart (Kowalczyk et al., 2015). Using single cell RNA-seq technology has identified that cell cycle is a main source of transcriptional variation between HSCs populations as well as across young and old (Kowalczyk et al., 2015). Here we highlight the importance of future studies to consider using single cell RNA-seq applications alongside our proposed phenotypic analysis for a truly robust analysis. In future, a second marker for aging could be sought for use in conjunction with CD150 expression and CD41 is a possibility (Gekas & Graf, 2013). As with CD150, CD41 expression increases as HSC age. By using two positive markers for aging, analysis on the basis of MFI will remove any subjectivity during analysis. Further experiments are necessary for the pregnancy model, which will include an age-matched control to allow analysis of the role of spleen in specific age-related changes and a re-evaluation of necessary sample size and power to identify the impact that the spleen has on HSC over age.

CHAPTER 5

General Discussion

5.1 Introduction

The spleen is known to support hematopoiesis, particularly during stress- or disease-induced conditions. However, increasingly, research now indicates that the spleen plays a more significant role in hematopoietic regulation and aging than originally thought. Over a lifetime, long-term (LT)-HSC reportedly produce a shift in hematopoietic output, from balanced production of myeloid and lymphoid lineages typically associated with a 'young' phenotype, towards myeloid-biased production associated with aging (Beerman et al., 2010; Benz et al., 2012; Dykstra et al., 2007). Studies have proposed markers to distinguish balanced LT-HSC from myeloid-biased LT-HSC with the most promising marker defined as CD150, a member of the signaling lymphocyte activation molecule (SLAM) family (Morita et al., 2010; Oguro et al., 2013). Several previous studies report effective distinction of LT-HSC through differential expression of CD150, with LT-HSC showing balanced lineage potential identifiable as $CD150^{lo}$ cells and myeloid-biased LT-HSC identified as $CD150^{hi}$ cells (Beerman et al., 2010; Dykstra et al., 2011; Morita et al., 2010).

The spleen now identifies as a prominent site for extramedullary hematopoiesis (Inra et al., 2015; Robbins et al., 2012; Wilkins, Green, Wild, & Jones, 1994). However, spleen hematopoietic involvement during the steady-state condition has evaded rigorous study in the face of so many bone marrow studies. Stem cell migration is in constant flux and is evident by the presence of HSC in the peripheral blood at any given moment (Wright et al., 2001). HSC migration functions as an important component of systemic hematopoietic homeostasis. HSC migration mediates HSC redistribution which ensures bone marrow niches are not left unoccupied and functions as an immediate means of extramedullary recruitment in the event of stress (Wright et al., 2001).

The work in this thesis aimed firstly, to determine the steady-state lineage output of HSC which differentiate in the spleen, and secondly, to assess spleen contribution

to age-related myeloid-biased HSC differentiation. A novel diet-based transplantation preconditioning treatment is optimized for further use in characterizing spleen endogenous hematopoietic output under steady-state conditions. We have shown that valine availability at the time of transplantation determines donor-chimerism success. We found that reintroduction of valine two days prior to transplantation increased engraftment success. Furthermore, this thesis focused on identifying the contribution of spleen to myelopoietic dominance in old age. We designed an animal model to accelerate the effects of splenic influence during aging. This required only a third of the time to induce aged-associated hematopoietic change. This study showed that the spleen does not contribute to increases in myeloid-biased $CD150^{hi}$ HSC over a lifetime. Several limitations in analysis were noted in these experiments which hampered a firm conclusion. Reporting median fluorescence intensity of CD150 expression was found to be a more robust measurement of expression changes between aging groups than the subjective gating of $CD150^{hi}$ and $CD150^{lo}$ cell populations.

Valine-restriction preconditioning

Dietary-based preconditioning methods offer a fresh approach compared with traditional transplantation preconditioning methods that are the gold standard practice in patients suffering from myeloproliferative diseases such as leukemia. Recently, valine-depletion was shown to be a viable method for clearing the HSC niche in preparation for hematopoietic transplantation (Taya et al., 2016). The most notable feature of this dietary-based conditioning treatment was its complete reversibility, with recipients returning to full health once complete diet was reinstated. Here, we assess the viability of this, not only to condition the host HSC niche space, but to critically analyse valine-restriction as preconditioning treatment which maintained the steady-state condition.

Experiments were designed to optimize the valine-depletion method (Taya et al., 2016), but confirmed that valine depletion did not completely clear the niche of HSC like irradiation treatment. However, mixed reports have been published regarding the necessity of complete preconditioning for donor engraftment, with some studies reporting donor engraftment in unconditioned hosts (Bhattacharya et al., 2006; Ramshaw et al., 1995; Stewart et al., 1993; Westerhuis et al., 2011). In terms of a preconditioning method aimed at replacing ablative therapies in human allogeneic transplantation, incomplete niche clearance is one factor associated with increased risk of donor rejection (Mengarelli et al., 2002).

Chapter 3 investigates this novel valine depletion preconditioning approach, optimizes the method to enhance its capacity to clear HSC from the niche and to engraft donor cells for long- and short-term lineage reconstitution analysis. Experiments performed here confirm that valine restriction effectively depletes HSC from the host, and valine reintroduction reverses the ablative effects similar to the findings reported by Taya et al. (2016). In addition to demonstrating bone marrow clearance, our study confirms that the splenic niche is also cleared of HSC, which has not previously been shown.

Next, it was important to test the capacity for HSC to migrate into niche space cleared by valine restriction. Considering valine's demonstrated importance in HSC-niche interactions, we tested whether donor cell migration could be detected in the host within a few hours after refeeding was commenced. Valine depleted mice were considerably lethargic and weak. Upon return to a complete diet, mice did not begin to eat for a short while, adding a limitation to the use of the valine-restricted preconditioning approach for homing assays of less than 18 hours. A 48-hour homing analysis of transplanted splenocytes revealed donor chimerism in the peripheral blood and spleen but not in bone marrow. While it is difficult to draw conclusions from the findings of a single experiment, it is thought that this result is due to organ-selective homing, which not only implies that valine restriction allows

detection of unfractioned donor splenocytes, but also supports differential homing of tissue-specific cell populations (Szilvassy et al., 1999; Szilvassy, Meyerrose, Ragland, & Grimes, 2001).

The long-term engraftment assay was set up at the same time as the homing analysis with transplantation of lineage depleted bone marrow cells. Donor cell engraftment was not evident in both the bone marrow and spleen tissue of the host. Two days of valine refeeding prior to transplantation resulted in better engraftment, and showed that graft success relied largely on availability of valine at the time of transplantation. Lineage characterization at 4 weeks after transplantation from mice refed 2-days prior to transplant, identified similar B cell and myeloid cell reconstitution as unconditioned controls, with recovery to the levels reported by Taya et al. (2016). However, we were still unable to achieve donor chimerism levels comparable with that shown in the original report (Taya et al., 2016). This raises the question of whether remaining host-type cells have an advantage over donor-type cells in the race to occupy niche space as the biological concentration of valine increases.

In the normal mouse, ~0.1%-1% of HSC niches are available for engraftment at any time (Bhattacharya et al., 2006). In the mouse preconditioned through valine-restriction, ~10% donor chimerism is maintained by 12-weeks after transplantation (Taya et al., 2016). It is difficult to determine whether the cell dose given was insufficient to support hematopoietic reconstitution, or whether valine-restriction prevented donor cells from competing effectively with host type cells. Optimization of several parameters including cell dosage, donor cell capacity for LT- and ST-reconstitution and niche viability during the reintroduction phase, will be necessary in order to develop a complete understanding of the impact of valine-depletion on the HSC niche. Further understanding will ultimately dictate the validity of this conditioning method for studying steady-state spleen.

Aging

HSC in murine spleen are rare and phenotypically different to bone marrow HSC (Coppin et al., 2018). The spleen has been studied primarily for its contribution to hematopoiesis under stress situations, otherwise known as extramedullary hematopoiesis (Inra et al., 2015). Several studies report that the spleen contributes to myelopoiesis and erythropoiesis during extramedullary hematopoiesis (Inra et al., 2015; Mumau et al., 2018; Nakada et al., 2014; Tan & O'Neill, 2012; Yanai et al., 1991). The microenvironment of spleen and bone marrow differ, and evidence is emerging to suggest that the splenic niche impacts HSC both intrinsically and extrinsically (Coppin et al., 2018; Morita et al., 2011). An understanding of how the spleen contributes to hematopoiesis in the steady-state condition is important in terms of finding a mechanism for the age-associated decline of a balanced myeloid and lymphoid lineage output (Beerman et al., 2010). Ultimately this imbalance leads to increased prevalence of myeloproliferative diseases and deterioration of the adaptive immune system in the elderly (Lichtman & Rowe, 2004).

HSC primarily reside in bone marrow. However they migrate under normal conditions, evident by a constant flux of HSC in the peripheral blood (Wright et al., 2001). Researchers speculate that this constant reshuffling acts to maintain occupation of niche space during the constant turnover of HSC (Goodman & Hodgson, 1962; Wright et al., 2001). Comparison of the physiological migratory patterns of HSC over the duration of an animal's life in the absence and presence of the spleen has been a major aim of this study in order to identify whether the constant shuffling of HSC, i.e. exposing HSC to the spleen multiple times in a lifetime, has an impact on the progression of the myeloid-biased aging phenomenon.

In Chapter 4, two experimental models of aging were investigated based on the presence and absence of a spleen during a murine lifetime. The first model was adapted from Beerman et al. (2010), where the 'age' of LT-HSC was identified by

phenotype in normal young and old mice and in old asplenic mice. The second model involved exbreeders as a model to accelerate the effects of HSC aging by eliciting multiple bouts of pregnancy-induced extramedullary hematopoiesis. It is intended that this might exacerbate the migration of HSC towards the spleen, and so subject large quantities of HSC to the splenic niche and its possible myelopoietic effects. This study therefore directly compared the HSC phenotypic 'age' of exbreeders with and without a spleen.

Increasing expression of CD150 correlates with increasing HSC age (Beerman et al., 2010) and myeloid-biased differentiation capacity (Morita et al., 2010). This study has shown that cell surface expression of CD150 does not vary between aged normal and aged asplenic mice. The current field analyzes changes in CD150 expression on LT-HSC by comparing three cell fractions; $CD150^{hi}$, $CD150^{lo}$ and CD150. When $CD150^{-}$ cells were included within the LT-HSC subset analysis, accumulation of $CD150^{hi}$ cells with age was found not to be inversely related to a decline in the number of $CD150^{lo}$ cells. Therefore, we reasoned that $CD150^{hi}$ LT-HSC cells should be assessed for myeloid-bias based on the proportion of $CD150^{hi}$ cells amongst all $CD150^{+}$ cells. Through exclusion of the $CD150^{-}$ fraction, the inverse relationship of myeloid-biased and balanced phenotypes could be distinguished. Indeed, a more robust measurement of expression changes is achieved through comparison of median fluorescence intensity. However comparative studies by others have not reported such data.

Findings reported here suggest that there is no difference between LT-HSC in bone marrow of young, old and old asplenic mice, despite a growing consensus amongst researchers in the field that young bone marrow-derived LT-HSC are phenotypically more balanced ($CD150^{lo}$) than old LT-HSC, which are associated with increased myeloid-bias ($CD150^{hi}$). While we did demonstrate significant differences between young and old in terms of $\%CD150^{hi}$ LT-HSC (when $CD150^{-}$ was included), we did not see a significant difference for $\%CD150^{lo}$ LT-HSC between young and old, which

is expected to have an inverse relationship to $CD150^{hi}$ HSC. When data from a previously published study (Beerman et al., 2010) is recalculated to remove the $CD150^{-}$ expressing HSC fraction, our data for young and old asplenic mice both closely resembles 12-month old (midaged) mice and our old mice resemble 24-month old (old aged) mice from the Beerman et al. (2010) study. This comparison between studies supports that the absence of a spleen over a lifetime restricts myeloid-biased hematopoietic accumulation on the basis of $CD150^{+}$ expression. However, from CD150 MFI data, it cannot be statistically concluded that the absence of a spleen restricts myeloid-bias expansion over age.

Pregnancy-induced extramedullary hematopoiesis did not accelerate the effects of aging. Splenectomised mice were not statistically distinct from normal mice in terms of CD150 phenotype of LT-HSC. This finding suggests that an increased flux of migrating HSC towards spleen did not have an impact on aging phenotype in LT-HSC. Here we conclude that intrinsic forces of cell aging are more powerful than the extrinsic contribution of the spleen niche. One particular limitation to our study has been the absence of an age-matched 9-month-old control counterpart. This treatment group would have allowed the exbreeder data to be directly compared to a naturally aging group.

Future experiments will utilize $CD150^{+}$ expression to delineate age-associated changes in animals. Furthermore, the inclusion of CD41 and CD61 within future immunophenotyping analysis will help to delineate myeloid-bias within the LT-HSC subset (Mann et al., 2018; Gekas & Graf, 2013). Additionally, RNA-seq may be used more specifically to identify intrinsic changes at the single-cell level, providing a deeper insight into clonal distribution develops over age and the exact mechanisms responsible for these changes (Kowalczyk et al., 2015). The spleen has been shown to support myelopoiesis in several studies (Coppin et al., 2018; Morita et al., 2011; Slayton et al., 2002; Tan & O'Neill, 2010; Wu et al., 2018). It is difficult to understand how the small population of HSC that constantly resides in the spleen (Wolber et al.,

2002) in the steady-state condition, and is cycled into the migratory system and replaced (Wright et al., 2001), would contribute to myeloid-biased-associated aging on a long-term scale.

In conclusion, this study has optimized a dietary-mediated approach to preconditioning, which supports the steady-state condition. Spleen-specific hematopoiesis has not yet been studied in the steady-state condition, but can now be explored. The spleen did not contribute to the age-associated myeloid-biased progression over age in this study. However, it is not possible to draw firm conclusions due to the limitation's inherent in aging studies.

References

Abbuehl, J. P., Tatarova, Z., Held, W., & Huelsken, J. (2017). Long-Term Engraftment of Primary Bone Marrow Stromal Cells Repairs Niche Damage and Improves Hematopoietic Stem Cell Transplantation. *Cell Stem Cell, 21*(2), 241-255 e246. doi:10.1016/j.stem.2017.07.004

Adolfsson, J., Mansson, R., Buza-Vidas, N., Hultquist, A., Liuba, K., Jensen, C. T., . . . Jacobsen, S. E. (2005). Identification of Flt3+ lympho-myeloid stem cells lacking erythro-megakaryocytic potential: a revised road map for adult blood lineage commitment. *Cell, 121*(2), 295-306. doi:10.1016/j.cell.2005.02.013

Akashi, K., Traver, D., Miyamoto, T., & Weissman, I. L. (2000). A clonogenic common myeloid progenitor that gives rise to all myeloid lineages. *Nature, 404*(6774), 193-197. doi:10.1038/35004599

Axelrod, M., Gordon, V. L., Conaway, M., Tarcsafalvi, A., Neitzke, D. J., Gioeli, D., & Weber, M. J. (2013). Combinatorial drug screening identifies compensatory pathway interactions and adaptive resistance mechanisms. *Oncotarget, 4*(4), 622-635. doi:10.18632/oncotarget.938

Balazs, Fabian, Esmon, & Mulligan. (2006). Endothelial protein C receptor (CD201) explicitly identifies hematopoietic stem cells in murine bone marrow. *Blood, 107*(6), 2317-2321. doi:10.1182/blood-2005-06-2249

Beerman, I., Bhattacharya, D., Zandi, S., Sigvardsson, M., Weissman, I. L., Bryder, D., & Rossi, D. J. (2010). Functionally distinct hematopoietic stem cells modulate hematopoietic lineage potential during aging by a mechanism of clonal expansion. *Proc Natl Acad Sci U S A, 107*(12), 5465-5470. doi:10.1073/pnas.1000834107

Beerman, I., & Rossi, D. J. (2014). Epigenetic regulation of hematopoietic stem cell aging. *Exp Cell Res, 329*(2), 192-199. doi:10.1016/j.yexcr.2014.09.013

Benveniste, P., Cantin, C., Hyam, D., & Iscove, N. N. (2003). Hematopoietic stem cells engraft in mice with absolute efficiency. *Nat Immunol, 4*(7), 708-713. doi:10.1038/ni940

Benz, C., Copley, M. R., Kent, D. G., Wohrer, S., Cortes, A., Aghaeepour, N., . . . Eaves, C. J. (2012). Hematopoietic stem cell subtypes expand differentially

during development and display distinct lymphopoietic programs. *Cell Stem Cell, 10*(3), 273-283. doi:10.1016/j.stem.2012.02.007

Bergamaschi, G., Perfetti, V., Tonon, L., Novella, A., Lucotti, C., Danova, M., . . . Cazzola, M. (1996). Saporin, a ribosome-inactivating protein used to prepare immunotoxins, induces cell death via apoptosis. *Br J Haematol, 93*(4), 789-794. doi:10.1046/j.1365-2141.1996.d01-1730.x

Bhattacharya, D., Rossi, D. J., Bryder, D., & Weissman, I. L. (2006). Purified hematopoietic stem cell engraftment of rare niches corrects severe lymphoid deficiencies without host conditioning. *J Exp Med, 203*(1), 73-85. doi:10.1084/jem.20051714

Bowling, M. R., Cauthen, C. G., Perry, C. D., Patel, N. P., Bergman, S., Link, K. M., . . . Conforti, J. F. (2008). Pulmonary extramedullary hematopoiesis. *J Thorac Imaging, 23*(2), 138-141. doi:10.1097/RTI.0b013e31815b89aa

Brendolan, A., Rosado, M. M., Carsetti, R., Selleri, L., & Dear, T. N. (2007). Development and function of the mammalian spleen. *Bioessays, 29*(2), 166-177. doi:10.1002/bies.20528

Bronte, V., & Pittet, M. J. (2013). The spleen in local and systemic regulation of immunity. *Immunity, 39*(5), 806-818. doi:10.1016/j.immuni.2013.10.010

Bueno, C., Montes, R., de la Cueva, T., Gutierrez-Aranda, I., & Menendez, P. (2010). Intra-bone marrow transplantation of human CD34(+) cells into NOD/LtSz-scid IL-2rgamma(null) mice permits multilineage engraftment without previous irradiation. *Cytotherapy, 12*(1), 45-49. doi:10.3109/14653240903377052

Calvi, L. M., Adams, G. B., Weibrecht, K. W., Weber, J. M., Olson, D. P., Knight, M. C., . . . Scadden, D. T. (2003). Osteoblastic cells regulate the haematopoietic stem cell niche. *Nature, 425*(6960), 841-846. doi:10.1038/nature02040

Camargo, F. D., Chambers, S. M., Drew, E., McNagny, K. M., & Goodell, M. A. (2006). Hematopoietic stem cells do not engraft with absolute efficiencies. *Blood, 107*(2), 501-507. doi:10.1182/blood-2005-02-0655

Cao, Y.-A., Wagers, A. J., Beilhack, A., Dusich, J., Bachmann, M. H., Negrin, R. S., . . . Contag, C. H. (2004). Shifting foci of hematopoiesis during reconstitution from single stem cells. *Proceedings of the National Academy of Sciences, 101*(1), 221-226. doi:10.1073/pnas.2637010100

Carlson, A. L., Fujisaki, J., Wu, J., Runnels, J. M., Turcotte, R., Celso, C. L., . . . Lin, C. P. (2013). Tracking Single Cells in Live Animals Using a Photoconvertible Near-Infrared Cell Membrane Label. *PLOS ONE, 8*(8), e69257. doi:10.1371/journal.pone.0069257

Cavazzana-Calvo, M., Fischer, A., Bushman, F. D., Payen, E., Hacein-Bey-Abina, S., & Leboulch, P. (2011). Is normal hematopoiesis maintained solely by long-term multipotent stem cells? *Blood, 117*(17), 4420-4424. doi:10.1182/blood-2010-09-255679

Challen, G. A., Boles, N., Lin, K. K., & Goodell, M. A. (2009). Mouse hematopoietic stem cell identification and analysis. *Cytometry A, 75*(1), 14-24. doi:10.1002/cyto.a.20674

Challen, G. A., Boles, N. C., Chambers, S. M., & Goodell, M. A. (2010). Distinct hematopoietic stem cell subtypes are differentially regulated by TGF-beta1. *Cell Stem Cell, 6*(3), 265-278. doi:10.1016/j.stem.2010.02.002

Chambers, S. M., Shaw, C. A., Gatza, C., Fisk, C. J., Donehower, L. A., & Goodell, M. A. (2007). Aging hematopoietic stem cells decline in function and exhibit epigenetic dysregulation. *PLoS Biol, 5*(8), e201. doi:10.1371/journal.pbio.0050201

Chatterjee, R., Mills, W., Katz, M., McGarrigle, H. H., & Goldstone, A. H. (1994). Germ cell failure and Leydig cell insufficiency in post-pubertal males after autologous bone marrow transplantation with BEAM for lymphoma. *Bone Marrow Transplant, 13*(5), 519-522.

Chen, Deng, Cui, Fang, Zuo, Deng, . . . Zhao. (2018). Inflammatory responses and inflammation-associated diseases in organs. *Oncotarget, 9*(6), 7204-7218. doi:10.18632/oncotarget.23208

Chen, Ellison, Keyvanfar, Omokaro, Desierto, Eckhaus, & Young. (2008). Enrichment of hematopoietic stem cells with SLAM and LSK markers for the detection of hematopoietic stem cell function in normal and Trp53 null mice. *Experimental Hematology, 36*(10), 1236-1243. doi:10.1016/j.exphem.2008.04.012

Chhabra, A., Ring, A. M., Weiskopf, K., Schnorr, P. J., Gordon, S., Le, A. C., . . . Shizuru, J. A. (2016). Hematopoietic stem cell transplantation in immunocompetent hosts without radiation or chemotherapy. *Sci Transl Med, 8*(351), 351ra105. doi:10.1126/scitranslmed.aae0501

Christensen, J. L., & Weissman, I. L. (2001). Flk-2 is a marker in hematopoietic stem cell differentiation: a simple method to isolate long-term stem cells. *Proc Natl Acad Sci U S A, 98*(25), 14541-14546. doi:10.1073/pnas.261562798

Copley, M. R., & Eaves, C. J. (2013). Developmental changes in hematopoietic stem cell properties. *Exp Mol Med, 45*, e55. doi:10.1038/emm.2013.98

Coppin, E., Florentin, J., Vasamsetti, S. B., Arunkumar, A., Sembrat, J., Rojas, M., & Dutta, P. (2018). Splenic hematopoietic stem cells display a pre-activated phenotype. *Immunol Cell Biol*. doi:10.1111/imcb.12035

Cui, J., Wahl, R. L., Shen, T., Fisher, S. J., Recker, E., Ginsburg, D., & Long, M. W. (1999). Bone marrow cell trafficking following intravenous administration. *Br J Haematol, 107*(4), 895-902. doi:10.1046/j.1365-2141.1999.01779.x

Cusick, P. K., Koehler, K. M., Ferrier, B., & Haskell, B. E. (1978). The neurotoxicity of valine deficiency in rats. *J Nutr, 108*(7), 1200-1206. doi:10.1093/jn/108.7.1200

Czechowicz, A., Kraft, D., Weissman, I. L., & Bhattacharya, D. (2007). Efficient transplantation via antibody-based clearance of hematopoietic stem cell niches. *Science, 318*(5854), 1296-1299. doi:10.1126/science.1149726

Dor, F. J., Ramirez, M. L., Parmar, K., Altman, E., Huang, C., Down, J., & Cooper, D. (2006). Primitive hematopoietic cell populations reside in the spleen: studies in the pig, baboon, and human. *Exp Hematol, 34*(11), 1573-1582. doi:10.1016/j.exphem.2006.06.016

Draper, J. E., Sroczynska, P., Fadlullah, M. Z. H., Patel, R., Newton, G., Breitwieser, W., . . . Lacaud, G. (2018). A novel prospective isolation of murine fetal liver progenitors to study in utero hematopoietic defects. *PLoS Genet, 14*(1), e1007127. doi:10.1371/journal.pgen.1007127

Dykstra, B., Kent, D., Bowie, M., McCaffrey, L., Hamilton, M., Lyons, K., . . . Eaves, C. (2007). Long-term propagation of distinct hematopoietic differentiation programs in vivo. *Cell Stem Cell, 1*(2), 218-229. doi:10.1016/j.stem.2007.05.015

Dykstra, B., Olthof, S., Schreuder, J., Ritsema, M., & de Haan, G. (2011). Clonal analysis reveals multiple functional defects of aged murine hematopoietic stem cells. *J Exp Med, 208*(13), 2691-2703. doi:10.1084/jem.20111490

Dzierzak, E., & Philipsen, S. (2013). Erythropoiesis: development and differentiation. *Cold Spring Harb Perspect Med, 3*(4), a011601. doi:10.1101/cshperspect.a011601

Eilken, H. M., Nishikawa, S., & Schroeder, T. (2009). Continuous single-cell imaging of blood generation from haemogenic endothelium. *Nature, 457*(7231), 896-900. doi:10.1038/nature07760

Ema, H., Morita, Y., & Suda, T. (2014). Heterogeneity and hierarchy of hematopoietic stem cells. *Exp Hematol, 42*(2), 74-82 e72. doi:10.1016/j.exphem.2013.11.004

Ergen, A. V., & Goodell, M. A. (2010). Mechanisms of hematopoietic stem cell aging. *Exp Gerontol, 45*(4), 286-290. doi:10.1016/j.exger.2009.12.010

Florian, M. C., Dörr, K., Niebel, A., Daria, D., Schrezenmeier, H., Rojewski, M., . . . Geiger, H. (2012). Cdc42 activity regulates hematopoietic stem cell aging and rejuvenation. *Cell Stem Cell, 10*(5), 520-530. doi:10.1016/j.stem.2012.04.007

Gekas, C., & Graf, T. (2013). CD41 expression marks myeloid-biased adult hematopoietic stem cells and increases with age. *Blood, 121*(22), 4463-4472. doi:10.1182/blood-2012-09-457929

Gerrits, A., Dykstra, B., Kalmykowa, O. J., Klauke, K., Verovskaya, E., Broekhuis, M. J., . . . Bystrykh, L. V. (2010). Cellular barcoding tool for clonal analysis in

the hematopoietic system. *Blood, 115*(13), 2610-2618. doi:10.1182/blood-2009-06-229757

Goodman, J. W., & Hodgson, G. S. (1962). Evidence for stem cells in the peripheral blood of mice. *Blood, 19*, 702-714.

Grover, A., Sanjuan-Pla, A., Thongjuea, S., Carrelha, J., Giustacchini, A., Gambardella, A., . . . Nerlov, C. (2016). Single-cell RNA sequencing reveals molecular and functional platelet bias of aged haematopoietic stem cells. *Nat Commun, 7*, 11075. doi:10.1038/ncomms11075

Guidi, N., Sacma, M., Standker, L., Soller, K., Marka, G., Eiwen, K., . . . Geiger, H. (2017). Osteopontin attenuates aging-associated phenotypes of hematopoietic stem cells. *EMBO J, 36*(7), 840-853. doi:10.15252/embj.201694969

Gur-Cohen, S., Itkin, T., Chakrabarty, S., Graf, C., Kollet, O., Ludin, A., . . . Lapidot, T. (2015). PAR1 signaling regulates the retention and recruitment of EPCR-expressing bone marrow hematopoietic stem cells. *Nat Med, 21*(11), 1307-1317. doi:10.1038/nm.3960

Harrison, D. E. (1979). Mouse erythropoietic stem cell lines function normally 100 months: loss related to number of transplantations. *Mech Ageing Dev, 9*(5-6), 427-433.

Hirota, J., & Shimizu, S. (2012). *Routes of administration. The laboratory mouse* (H. Hedrich Ed. 2nd ed.): Academic Press.

Hoppe, P. S., Schwarzfischer, M., Loeffler, D., Kokkaliaris, K. D., Hilsenbeck, O., Moritz, N., . . . Schroeder, T. (2016). Early myeloid lineage choice is not initiated by random PU.1 to GATA1 protein ratios. *Nature, 535*(7611), 299-302. doi:10.1038/nature18320

Inra, C. N., Zhou, B. O., Acar, M., Murphy, M. M., Richardson, J., Zhao, Z., & Morrison, S. J. (2015). A perisinusoidal niche for extramedullary haematopoiesis in the spleen. *Nature, 527*(7579), 466-471. doi:10.1038/nature15530

Ito, & Frenette. (2016). HSC Contribution in Making Steady-State Blood. *Immunity, 45*(3), 464-466. doi:10.1016/j.immuni.2016.09.002

Ito, Hirao, Arai, Takubo, Matsuoka, Miyamoto, . . . Suda. (2006). Reactive oxygen species act through p38 MAPK to limit the lifespan of hematopoietic stem cells. *Nat Med, 12*(4), 446-451. doi:10.1038/nm1388

Jeyarajah, D. R., & Thistlethwaite, J. R., Jr. (1993). General aspects of cytokine-release syndrome: timing and incidence of symptoms. *Transplant Proc, 25*(2 Suppl 1), 16-20.

Johns, J. L., & Christopher, M. M. (2012). Extramedullary hematopoiesis: a new look at the underlying stem cell niche, theories of development, and occurrence in animals. *Vet Pathol, 49*(3), 508-523. doi:10.1177/0300985811432344

Kamminga, L. M., van Os, R., Ausema, A., Noach, E. J., Weersing, E., Dontje, B., . . . de Haan, G. (2005). Impaired hematopoietic stem cell functioning after serial transplantation and during normal aging. *Stem Cells, 23*(1), 82-92. doi:10.1634/stemcells.2004-0066

Kent, D. G., Copley, M. R., Benz, C., Wöhrer, S., Dykstra, B. J., Ma, E., . . . Eaves, C. J. (2009). Prospective isolation and molecular characterization of hematopoietic stem cells with durable self-renewal potential. *Blood, 113*(25), 6342.

Kiel, M. J., Yilmaz, Ö. H., Iwashita, T., Yilmaz, O. H., Terhorst, C., & Morrison, S. J. (2005). SLAM family receptors distinguish hematopoietic stem and progenitor cells and reveal endothelial niches for stem cells. *Cell, 121*(7), 1109-1121. doi:10.1016/j.cell.2005.05.026

Kim, E. J., Kim, S., Kang, D. O., & Seo, H. S. (2014). Metabolic activity of the spleen and bone marrow in patients with acute myocardial infarction evaluated by 18f-fluorodeoxyglucose positron emission tomograpic imaging. *Circ Cardiovasc Imaging, 7*(3), 454-460. doi:10.1161/CIRCIMAGING.113.001093

King, M. A., Covassin, L., Brehm, M. A., Racki, W., Pearson, T., Leif, J., . . . Greiner, D. L. (2009). Human peripheral blood leucocyte non-obese diabetic-severe combined immunodeficiency interleukin-2 receptor gamma chain gene

mouse model of xenogeneic graft-versus-host-like disease and the role of host major histocompatibility complex. *Clin Exp Immunol, 157*(1), 104-118. doi:10.1111/j.1365-2249.2009.03933.x

Kiss, T. L., Sabry, W., Lazarus, H. M., & Lipton, J. H. (2007). Blood and marrow transplantation in elderly acute myeloid leukaemia patients - older certainly is not better. *Bone Marrow Transplant, 40*(5), 405-416. doi:10.1038/sj.bmt.1705747

Kondo, M., Weissman, I. L., & Akashi, K. (1997). Identification of clonogenic common lymphoid progenitors in mouse bone marrow. *Cell, 91*(5), 661-672.

Kovtonyuk, L. V., Fritsch, K., Feng, X., Manz, M. G., & Takizawa, H. (2016). Inflamm-Aging of Hematopoiesis, Hematopoietic Stem Cells, and the Bone Marrow Microenvironment. *Front Immunol, 7*, 502. doi:10.3389/fimmu.2016.00502

Kowalczyk, M. S., Tirosh, I., Heckl, D., Rao, T. N., Dixit, A., Haas, B. J., … Regev, A. (2015). Single-cell RNA-seq reveals changes in cell cycle and differentiation programs upon aging of hematopoietic stem cells. *Genome Res, 25*(12), 1860-72. doi: 10.1101/gr.192237.115

Krause, D. S., Theise, N. D., Collector, M. I., Henegariu, O., Hwang, S., Gardner, R., . . . Sharkis, S. J. (2001). Multi-organ, multi-lineage engraftment by a single bone marrow-derived stem cell. *Cell, 105*(3), 369-377. doi:10.1016/s0092-8674(01)00328-2

Laing, S. T., Griffey, S. M., Moreno, M. E., & Stoddart, C. A. (2015). CD8-positive lymphocytes in graft-versus-host disease of humanized NOD.Cg-Prkdc(scid)Il2rg(tm1Wjl)/SzJ mice. *J Comp Pathol, 152*(2-3), 238-242. doi:10.1016/j.jcpa.2014.12.010

Lanzkron, S. M., Collector, M. I., & Sharkis, S. J. (1999). Hematopoietic stem cell tracking in vivo: a comparison of short-term and long-term repopulating cells. *Blood, 93*(6), 1916-1921.

Lapidot, T., Dar, A., & Kollet, O. (2005). How do stem cells find their way home? *Blood, 106*(6), 1901-1910. doi:10.1182/blood-2005-04-1417

Lavender, K. J., Pang, W. W., Messer, R. J., Duley, A. K., Race, B., Phillips, K., . . . Hasenkrug, K. J. (2013). BLT-humanized C57BL/6 Rag2-/-gammac-/-CD47-/- mice are resistant to GVHD and develop B- and T-cell immunity to HIV infection. *Blood, 122*(25), 4013-4020. doi:10.1182/blood-2013-06-506949

Lichtman, M. A., & Rowe, J. M. (2004). The relationship of patient age to the pathobiology of the clonal myeloid diseases. *Semin Oncol, 31*(2), 185-197.

Linton, P. J., & Dorshkind, K. (2004). Age-related changes in lymphocyte development and function. *Nat Immunol, 5*(2), 133-139. doi:10.1038/ni1033

Lu, R., Czechowicz, A., Seita, J., Jiang, D., & Weissman, I. L. (2019). Clonal-level lineage commitment pathways of hematopoietic stem cells in vivo. *Proc Natl Acad Sci U S A, 116*(4), 1447-1456. doi:10.1073/pnas.1801480116

Lux, M., Brinkman, R. R., Chauve, C., Laing, A., Lorenc, A., Abeler-Dorner, L., & Hammer, B. (2018). flowLearn: fast and precise identification and quality checking of cell populations in flow cytometry. *Bioinformatics, 34*(13), 2245-2253. doi:10.1093/bioinformatics/bty082

Mann, M., Mehta, A., de Boer, C. G., Kowalczyk, M. S., Lee, K., Haldeman, P., … Baltimore, D. (2018). Heterogeneous Responses of Hematopoietic Stem Cells to Inflammatory Stimuli are Altered with Age. *Cell Reports, 25*, 2992-3005. doi:10.1016/j.celrep.2018.11.056

Massberg, S., Schaerli, P., Knezevic-Maramica, I., Kollnberger, M., Tubo, N., Moseman, E. A., . . . von Andrian, U. H. (2007). Immunosurveillance by hematopoietic progenitor cells trafficking through blood, lymph, and peripheral tissues. *Cell, 131*(5), 994-1008. doi:10.1016/j.cell.2007.09.047

Maymon, R., Strauss, S., Vaknin, Z., Weinraub, Z., Herman, A., & Gayer, G. (2006). Normal sonographic values of maternal spleen size throughout pregnancy. *Ultrasound Med Biol, 32*(12), 1827-1831. doi:10.1016/j.ultrasmedbio.2006.06.017

McKim, D. B., Yin, W., Wang, Y., Cole, S. W., Godbout, J. P., & Sheridan, J. F. (2018). Social Stress Mobilizes Hematopoietic Stem Cells to Establish

Persistent Splenic Myelopoiesis. *Cell Rep, 25*(9), 2552-2562 e2553. doi:10.1016/j.celrep.2018.10.102

Mebius, R. E., & Kraal, G. (2005). Structure and function of the spleen. *Nat Rev Immunol, 5*(8), 606-616. doi:10.1038/nri1669

Mengarelli, A., Iori, A., Guglielmi, C., Romano, A., Cerretti, R., Torromeo, C., . . . Arcese, W. (2002). Standard versus alternative myeloablative conditioning regimens in allogeneic hematopoietic stem cell transplantation for high-risk acute leukemia. *Haematologica, 87*(1), 52-58.

Miki, T., Takano, C., Garcia, I. M., & Grubbs, B. H. (2019). Construction and Evaluation of a Subcutaneous Splenic Injection Port for Serial Intraportal Vein Cell Delivery in Murine Disease Models. *Stem Cells Int, 2019*, 5419501. doi:10.1155/2019/5419501

Mohty, M., & Apperley, J. F. (2010). Long-term physiological side effects after allogeneic bone marrow transplantation. *Hematology Am Soc Hematol Educ Program, 2010*, 229-236. doi:10.1182/asheducation-2010.1.229

Morita, Y., Ema, H., & Nakauchi, H. (2010). Heterogeneity and hierarchy within the most primitive hematopoietic stem cell compartment. *J Exp Med, 207*(6), 1173-1182. doi:10.1084/jem.20091318

Morita, Y., Iseki, A., Okamura, S., Suzuki, S., Nakauchi, H., & Ema, H. (2011). Functional characterization of hematopoietic stem cells in the spleen. *Experimental Hematology, 39*(3), 351-359.e353. doi:http://dx.doi.org/10.1016/j.exphem.2010.12.008

Muller-Sieburg, Cho, Karlsson, Huang, & Sieburg. (2004). Myeloid-biased hematopoietic stem cells have extensive self-renewal capacity but generate diminished lymphoid progeny with impaired IL-7 responsiveness. *Blood, 103*(11), 4111-4118. doi:10.1182/blood-2003-10-3448

Muller-Sieburg, Sieburg, Bernitz, & Cattarossi. (2012). Stem cell heterogeneity: implications for aging and regenerative medicine. *Blood, 119*(17), 3900-3907. doi:10.1182/blood-2011-12-376749

Muller-Sieburg, C., & Sieburg, H. B. (2008). Stem cell aging: survival of the laziest? *Cell Cycle, 7*(24), 3798-3804. doi:10.4161/cc.7.24.7214

Mumau, M. D., Vanderbeck, A. N., Lynch, E. D., Golec, S. B., Emerson, S. G., & Punt, J. A. (2018). Identification of a Multipotent Progenitor Population in the Spleen That Is Regulated by NR4A1. *J Immunol, 200*(3), 1078-1087. doi:10.4049/jimmunol.1701250

Nakada, Oguro, Levi, Ryan, Kitano, Saitoh, . . . Morrison. (2014). Oestrogen increases haematopoietic stem-cell self-renewal in females and during pregnancy. *Nature, 505*(7484), 555-558. doi:10.1038/nature12932

Ng, A. P., & Alexander, W. S. (2017). Haematopoietic stem cells: past, present and future. *Cell Death Discovery, 3*, 17002. doi:10.1038/cddiscovery.2017.2

Nimmo, R. A., May, G. E., & Enver, T. (2015). Primed and ready: understanding lineage commitment through single cell analysis. *Trends Cell Biol, 25*(8), 459-467. doi:10.1016/j.tcb.2015.04.004

Nombela-Arrieta, C., Pivarnik, G., Winkel, B., Canty, K. J., Harley, B., Mahoney, J. E., . . . Silberstein, L. E. (2013). Quantitative imaging of hematopoietic stem and progenitor cell localization and hypoxic status in the bone marrow microenvironment. *Nature cell biol, 15*(5), 533-543. doi:10.1038/ncb2730

O'Neill, H. C., Wilson, H. L., Quah, B., Abbey, J. L., Despars, G., & Ni, K. (2004). Dendritic Cell Development in Long-Term Spleen Stromal Cultures. *Stem Cells, 22*(4), 475-486. doi:10.1634/stemcells.22-4-475

O'Neill, H. (2012). Niches for extramedullary hematopoiesis in the spleen. *Niche, 1*(1), 12-16. doi:10.5152/niche.2012.03

Oda, A., Tezuka, T., Ueno, Y., Hosoda, S., Amemiya, Y., Notsu, C., … Goitsuka, R. (2018). Niche-induced extramedullary hematopoiesis in the spleen in regulated by the transcription factor Tlx1. *Scientific Reports, 8*, 8308. doi: 10.1038/s41598-018-26693-x

Ogawa, M., Porter, P. N., & Nakahata, T. (1983). Renewal and commitment to differentiation of hemopoietic stem cells (an interpretive review). *Blood, 61*(5), 823-829.

Oguro, Ding, & Morrison. (2013). SLAM family markers resolve functionally distinct subpopulations of hematopoietic stem cells and multipotent progenitors. *Cell Stem Cell, 13*(1), 102-116. doi:10.1016/j.stem.2013.05.014

Oguro, McDonald, Zhao, Umetani, Shaul, & Morrison. (2017). 27-Hydroxycholesterol induces hematopoietic stem cell mobilization and extramedullary hematopoiesis during pregnancy. *J Clin Invest, 127*(9), 3392-3401. doi:10.1172/JCI94027

Osawa, M., Hanada, K.-i., Hamada, H., & Nakauchi, H. (1996). Long-term lymphohematopoietic reconstitution by a single CD34-low/negative hematopoietic stem cell. *Science, 273*(5272), 242.

Palchaudhuri, R., Saez, B., Hoggatt, J., Schajnovitz, A., Sykes, D. B., Tate, T. A., . . . Scadden, D. T. (2016). Non-genotoxic conditioning for hematopoietic stem cell transplantation using a hematopoietic-cell-specific internalizing immunotoxin. *Nat Biotechnol, 34*(7), 738-745. doi:10.1038/nbt.3584

Pang, W. W., Price, E. A., Sahoo, D., Beerman, I., Maloney, W. J., Rossi, D. J., . . . Weissman, I. L. (2011). Human bone marrow hematopoietic stem cells are increased in frequency and myeloid-biased with age. *Proc Natl Acad Sci U S A, 108*(50), 20012-20017. doi:10.1073/pnas.1116110108

Plett, P. A., Frankovitz, S. M., & Orschell, C. M. (2003). Distribution of marrow repopulating cells between bone marrow and spleen early after transplantation. *Blood, 102*(6), 2285-2291. doi:10.1182/blood-2002-12-3742

Prakash, S., Hoffman, R., Barouk, S., Wang, Y. L., Knowles, D. M., & Orazi, A. (2012). Splenic extramedullary hematopoietic proliferation in Philadelphia chromosome-negative myeloproliferative neoplasms: heterogeneous morphology and cytological composition. *Mod Pathol, 25*(6), 815-827. doi:10.1038/modpathol.2012.33

Ramshaw, H. S., Rao, S. S., Crittenden, R. B., Peters, S. O., Weier, H. U., & Quesenberry, P. J. (1995). Engraftment of bone marrow cells into normal unprepared hosts: effects of 5-fluorouracil and cell cycle status. *Blood, 86*(3), 924-929.

Rao, S. S., Peters, S. O., Crittenden, R. B., Stewart, F. M., Ramshaw, H. S., & Quesenberry, P. J. (1997). Stem cell transplantation in the normal nonmyeloablated host: relationship between cell dose, schedule, and engraftment. *Exp Hematol, 25*(2), 114-121.

Reya, T., Morrison, S. J., Clarke, M. F., & Weissman, I. L. (2001). Stem cells, cancer, and cancer stem cells. *Nature, 414*(6859), 105-111. doi:10.1038/35102167

Robbins, C. S., Chudnovskiy, A., Rauch, P. J., Figueiredo, J. L., Iwamoto, Y., Gorbatov, R., . . . Swirski, F. K. (2012). Extramedullary hematopoiesis generates Ly-6C(high) monocytes that infiltrate atherosclerotic lesions. *Circulation, 125*(2), 364-374. doi:10.1161/CIRCULATIONAHA.111.061986

Rodriguez, R., Lim, H. Y., Bartkowski, L. M., & Simons, J. W. (1998). Identification of diphtheria toxin via screening as a potent cell cycle and p53-independent cytotoxin for human prostate cancer therapeutics. *Prostate, 34*(4), 259-269.

Rossi, D. J., Bryder, D., Seita, J., Nussenzweig, A., Hoeijmakers, J., & Weissman, I. L. (2007). Deficiencies in DNA damage repair limit the function of haematopoietic stem cells with age. *Nature, 447*(7145), 725-729. doi:10.1038/nature05862

Rossi, D. J., Bryder, D., Zahn, J. M., Ahlenius, H., Sonu, R., Wagers, A. J., & Weissman, I. L. (2005). Cell intrinsic alterations underlie hematopoietic stem cell aging. *Proc Natl Acad Sci U S A, 102*(26), 9194-9199. doi:10.1073/pnas.0503280102

Sanjuan-Pla, A., Macaulay, I. C., Jensen, C. T., Woll, P. S., Luis, T. C., Mead, A., . . . Jacobsen, S. E. (2013). Platelet-biased stem cells reside at the apex of the haematopoietic stem-cell hierarchy. *Nature, 502*(7470), 232-236. doi:10.1038/nature12495

Sawai, C. M., Babovic, S., Upadhaya, S., Knapp, D. J., Lavin, Y., Lau, C. M., . . . Reizis, B. (2016). Hematopoietic stem cells are the major source of multilineage hematopoiesis in adult animals. *Immunity, 45*(3), 597-609. doi:10.1016/j.immuni.2016.08.007

Saxe, D. F., Boggs, S. S., & Boggs, D. R. (1984). Transplantation of chromosomally marked syngeneic marrow cells into mice not subjected to hematopoietic stem cell depletion. *Exp Hematol, 12*(4), 277-283.

Schofield, R. (1978). The relationship between the spleen colony-forming cell and the haemopoietic stem cell. *Blood Cells, 4*(1-2), 7-25.

Seita, J., & Weissman, I. L. (2010). Hematopoietic stem Cell: self-renewal versus differentiation. *Wiley Interdiscip Rev Syst Biol Med, 2*(6), 640-653. doi:10.1002/wsbm.86

Shao, L., Wang, Y., Chang, J., Luo, Y., Meng, A., & Zhou, D. (2013). Hematopoietic stem cell senescence and cancer therapy-induced long-term bone marrow injury. *Transl Cancer Res, 2*(5), 397-411. doi:10.3978/j.issn.2218-676X.2013.07.03

Shultz, L. D., Brehm, M. A., Garcia-Martinez, J. V., & Greiner, D. L. (2012). Humanized mice for immune system investigation: progress, promise and challenges. *Nat Rev Immunol, 12*(11), 786-798. doi:10.1038/nri3311

Sidney, L. E., Branch, M. J., Dunphy, S. E., Dua, H. S., & Hopkinson, A. (2014). Concise review: evidence for CD34 as a common marker for diverse progenitors. *Stem Cells, 32*(6), 1380-1389. doi:10.1002/stem.1661

Sieburg, H. B., Cho, R. H., Dykstra, B., Uchida, N., Eaves, C. J., & Muller-Sieburg, C. E. (2006). The hematopoietic stem compartment consists of a limited number of discrete stem cell subsets. *Blood, 107*(6), 2311-2316. doi:10.1182/blood-2005-07-2970

Singh, H. (1996). Gene targeting reveals a hierarchy of transcription factors regulating specification of lymphoid cell fates. *Curr Opin Immunol, 8*(2), 160-165.

Slayton, W. B., Georgelas, A., Pierce, L. J., Elenitoba-Johnson, K. S., Perry, S. S., Marx, M., & Spangrude, G. J. (2002). The spleen is a major site of megakaryopoiesis following transplantation of murine hematopoietic stem cells. *Blood, 100*(12), 3975-3982. doi:10.1182/blood-2002-02-0490

Socie, G., Salooja, N., Cohen, A., Rovelli, A., Carreras, E., Locasciulli, A., . . . Marrow, T. (2003). Nonmalignant late effects after allogeneic stem cell transplantation. *Blood, 101*(9), 3373-3385. doi:10.1182/blood-2002-07-2231

Song, M. K., Park, B. B., & Uhm, J. E. (2018). Understanding Splenomegaly in Myelofibrosis: Association with Molecular Pathogenesis. *Int J Mol Sci, 19*(3). doi:10.3390/ijms19030898

Spangrude, G. J., Heimfeld, S., & Weissman, I. L. (1988). Purification and characterization of mouse hematopoietic stem cells. *Science, 241*(4861), 58-62.

Steiniger, B. S. (2015). Human spleen microanatomy: why mice do not suffice. *Immunology, 145*(3), 334-346. doi:10.1111/imm.12469

Stewart, F. M., Crittenden, R. B., Lowry, P. A., Pearson-White, S., & Quesenberry, P. J. (1993). Long-term engraftment of normal and post-5-fluorouracil murine marrow into normal nonmyeloablated mice. *Blood, 81*(10), 2566-2571.

Sudo, K., Ema, H., Morita, Y., & Nakauchi, H. (2000). Age-associated characteristics of murine hematopoietic stem cells. *J Exp Med, 192*(9), 1273-1280.

Swirski, F. K., & Robbins, C. S. (2013). Neutrophils usher monocytes into sites of inflammation. *Circ Res, 112*(5), 744-745. doi:10.1161/CIRCRESAHA.113.300867

Szilvassy, S. J., Bass, M. J., Van Zant, G., & Grimes, B. (1999). Organ-selective homing defines engraftment kinetics of murine hematopoietic stem cells and is compromised by Ex vivo expansion. *Blood, 93*(5), 1557-1566.

Szilvassy, S. J., Meyerrose, T. E., Ragland, P. L., & Grimes, B. (2001). Differential homing and engraftment properties of hematopoietic progenitor cells from murine bone marrow, mobilized peripheral blood, and fetal liver. *Blood, 98*(7), 2108-2115. doi:10.1182/blood.v98.7.2108

Tall, A. R., & Yvan-Charvet, L. (2015). Cholesterol, inflammation and innate immunity. *Nat Rev Immunol, 15*(2), 104-116. doi:10.1038/nri3793

Tan, J. K., & O'Neill, H. C. (2010). Haematopoietic stem cells in spleen have distinct differentiative potential for antigen presenting cells. *J Cell Mol Med, 14*(8), 2144-2150. doi:10.1111/j.1582-4934.2009.00923.x

Tan, J. K., & O'Neill, H. C. (2012). Myelopoiesis in spleen-producing distinct dendritic-like cells. *J Cell Mol Med, 16*(8), 1924-1933. doi:10.1111/j.1582-4934.2011.01490.x

Taya, Y., Ota, Y., Wilkinson, A. C., Kanazawa, A., Watarai, H., Kasai, M., . . . Yamazaki, S. (2016). Depleting dietary valine permits nonmyeloablative mouse hematopoietic stem cell transplantation. *Science, 354*(6316), 1152-1155. doi:10.1126/science.aag3145

Thackeray, J. T., Derlin, T., Haghikia, A., Napp, L. C., Wang, Y., Ross, T. L., . . . Bengel, F. M. (2015). Molecular Imaging of the Chemokine Receptor CXCR4 After Acute Myocardial Infarction. *JACC Cardiovasc Imaging, 8*(12), 1417-1426. doi:10.1016/j.jcmg.2015.09.008

Tian, Y., Pan, D., Chordia, M. D., French, B. A., Kron, I. L., & Yang, Z. (2016). The spleen contributes importantly to myocardial infarct exacerbation during post-ischemic reperfusion in mice via signaling between cardiac HMGB1 and splenic RAGE. *Basic Res Cardiol, 111*(6), 62. doi:10.1007/s00395-016-0583-0

Tichelli, A., Rovo, A., Passweg, J., Schwarze, C. P., Van Lint, M. T., Arat, M., . . . Marrow, T. (2009). Late complications after hematopoietic stem cell transplantation. *Expert Rev Hematol, 2*(5), 583-601. doi:10.1586/ehm.09.48

Van Zant, G., de Haan, G., & Rich, I. N. (1997). Alternatives to stem cell renewal from a developmental viewpoint. *Exp Hematol, 25*(3), 187-192.

Vas, V., Senger, K., Dorr, K., Niebel, A., & Geiger, H. (2012). Aging of the microenvironment influences clonality in hematopoiesis. *PLOS ONE, 7*(8), e42080. doi:10.1371/journal.pone.0042080

Veillette, A. (2010). SLAM-family receptors: immune regulators with or without SAP-family adaptors. *Cold Spring Harb Perspect Biol, 2*(3), a002469. doi:10.1101/cshperspect.a002469

Visnjic, D., Kalajzic, Z., Rowe, D. W., Katavic, V., Lorenzo, J., & Aguila, H. L. (2004). Hematopoiesis is severely altered in mice with an induced osteoblast deficiency. *Blood, 103*(9), 3258-3264. doi:10.1182/blood-2003-11-4011

Wang, J., Sun, Q., Morita, Y., Jiang, H., Gross, A., Lechel, A., . . . Rudolph, K. L. (2012). A differentiation checkpoint limits hematopoietic stem cell self-renewal in response to DNA damage. *Cell, 148*(5), 1001-1014. doi:10.1016/j.cell.2012.01.040

Weidle, U. H., Tiefenthaler, G., Schiller, C., Weiss, E. H., Georges, G., & Brinkmann, U. (2014). Prospects of bacterial and plant protein-based immunotoxins for treatment of cancer. *Cancer Genomics Proteomics, 11*(1), 25-38.

Westerhuis, G., van Pel, M., Toes, R. E., Staal, F. J., & Fibbe, W. E. (2011). Chimerism levels after stem cell transplantation are primarily determined by the ratio of donor to host stem cells. *Blood, 117*(16), 4400-4401. doi:10.1182/blood-2011-01-328518

Wilkins, B. S., Green, A., Wild, A. E., & Jones, D. B. (1994). Extramedullary haemopoiesis in fetal and adult human spleen: a quantitative immunohistological study. *Histopathology, 24*(3), 241-247.

Wilkinson, A. C., Morita, M., Nakauchi, H., & Yamazaki, S. (2018). Branched-chain amino acid depletion conditions bone marrow for hematopoietic stem cell transplantation avoiding amino acid imbalance-associated toxicity. *Exp Hematol, 63*, 12-16 e11. doi:10.1016/j.exphem.2018.04.004

Wilson, N., Kent, David G., Buettner, F., Shehata, M., Macaulay, Iain C., Calero-Nieto, Fernando J., . . . Göttgens, B. (2015). Combined single-cell functional and gene expression analysis resolves heterogeneity within stem cell populations. *Cell Stem Cell, 16*(6), 712-724. doi:10.1016/j.stem.2015.04.004

Wolber, F. M., Leonard, E., Michael, S., Orschell-Traycoff, C. M., Yoder, M. C., & Srour, E. F. (2002). Roles of spleen and liver in development of the murine hematopoietic system. *Exp Hemato, 30*(9), 1010-1019. doi:10.1016/S0301-472X(02)00881-0

Wols, H. A., Johnson, K. M., Ippolito, J. A., Birjandi, S. Z., Su, Y., Le, P. T., & Witte, P. L. (2010). Migration of immature and mature B cells in the aged microenvironment. *Immunology, 129*(2), 278-290. doi:10.1111/j.1365-2567.2009.03182.x

Woolthuis, C. M., & Park, C. Y. (2016). Hematopoietic stem/progenitor cell commitment to the megakaryocyte lineage. *Blood, 127*(10), 1242-1248. doi:10.1182/blood-2015-07-607945

Wright, D. E., Wagers, A. J., Gulati, A. P., Johnson, F. L., & Weissman, I. L. (2001). Physiological Migration of Hematopoietic Stem and Progenitor Cells. *Science, 294*(5548), 1933.

Wu, C., Ning, H., Liu, M., Lin, J., Luo, S., Zhu, W., . . . Zheng, L. (2018). Spleen mediates a distinct hematopoietic progenitor response supporting tumor-promoting myelopoiesis. *J Clin Invest, 128*(8), 3425-3438. doi:10.1172/JCI97973

Xue, X., Pech, N. K., Shelley, W. C., Srour, E. F., Yoder, M. C., & Dinauer, M. C. (2010). Antibody targeting KIT as pretransplantation conditioning in immunocompetent mice. *Blood, 116*(24), 5419-5422. doi:10.1182/blood-2010-07-295949

Yamamoto, R., Morita, Y., Ooehara, J., Hamanaka, S., Onodera, M., Rudolph, K. L., . . . Nakauchi, H. (2013). Clonal analysis unveils self-renewing lineage-restricted progenitors generated directly from hematopoietic stem cells. *Cell, 154*(5), 1112-1126. doi:10.1016/j.cell.2013.08.007

Yamamoto, R., Wilkinson, A. C., Ooehara, J., Lan, X., Lai, C. Y., Nakauchi, Y., . . . Nakauchi, H. (2018). Large-Scale Clonal Analysis Resolves Aging of the Mouse Hematopoietic Stem Cell Compartment. *Cell Stem Cell, 22*(4), 600-607 e604. doi:10.1016/j.stem.2018.03.013

Yanai, N., Satoh, T., & Obinata, M. (1991). Endothelial cells create a hematopoietic inductive microenvironment preferential to erythropoiesis in the mouse spleen. *Cell Struct Funct, 16*(1), 87-93.

Appendices

Appendix A.1 HSC gating used in valine restricted pre-conditioning optimization

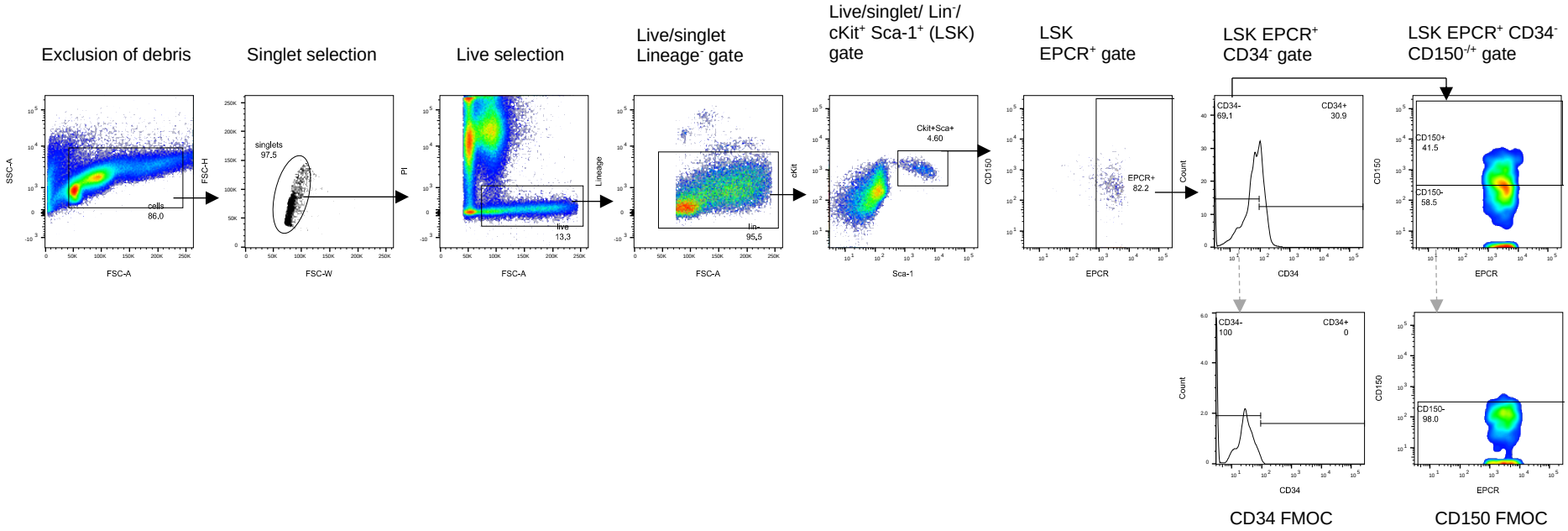

A.1 Lineage depleted bone marrow or spleen was stained with fluorochrome conjugated antibodies as outlined in Figure 4.2.1. Cells were analysed by flow cytometry for the LSKCD34^{-}CD150^{+} EPCR^{+} phenotype using antibodies specific for cKit (2B8; FITC), Sca-1 (D7; BV421), CD150 (mSHAD150; PE-Cy7), CD34 (RAM34; eFluor 660) and CD201 (eBio1560; PE). Streptavidin (SA)-APC-eFluor 780 was used as a secondary reagent to detect any remaining undepleted lineage^{+} cells. Prior to flow cytometry, cells were stained with propidium iodine (PI^{-}) to include only PI^{-} viable cells in further analyses. Gating strategy identifies the gating criteria for LT-HSC and defines CD150$^{+/-}$ boundaries. Percent positive cells is indicated in each plot. Specific gates for CD34^{-} and CD150^{-} were set based on forward minus one controls (FMOC). Final plot displays events using a 'smoothing' feature with outlier's present. All HSC analyses of valine-depleted animals follows this gating strategy and reports the final gated percentage of the LSK EPCR^{+} CD34^{-} CD150^{+} gate.

Appendix A.2 Spleen destruction

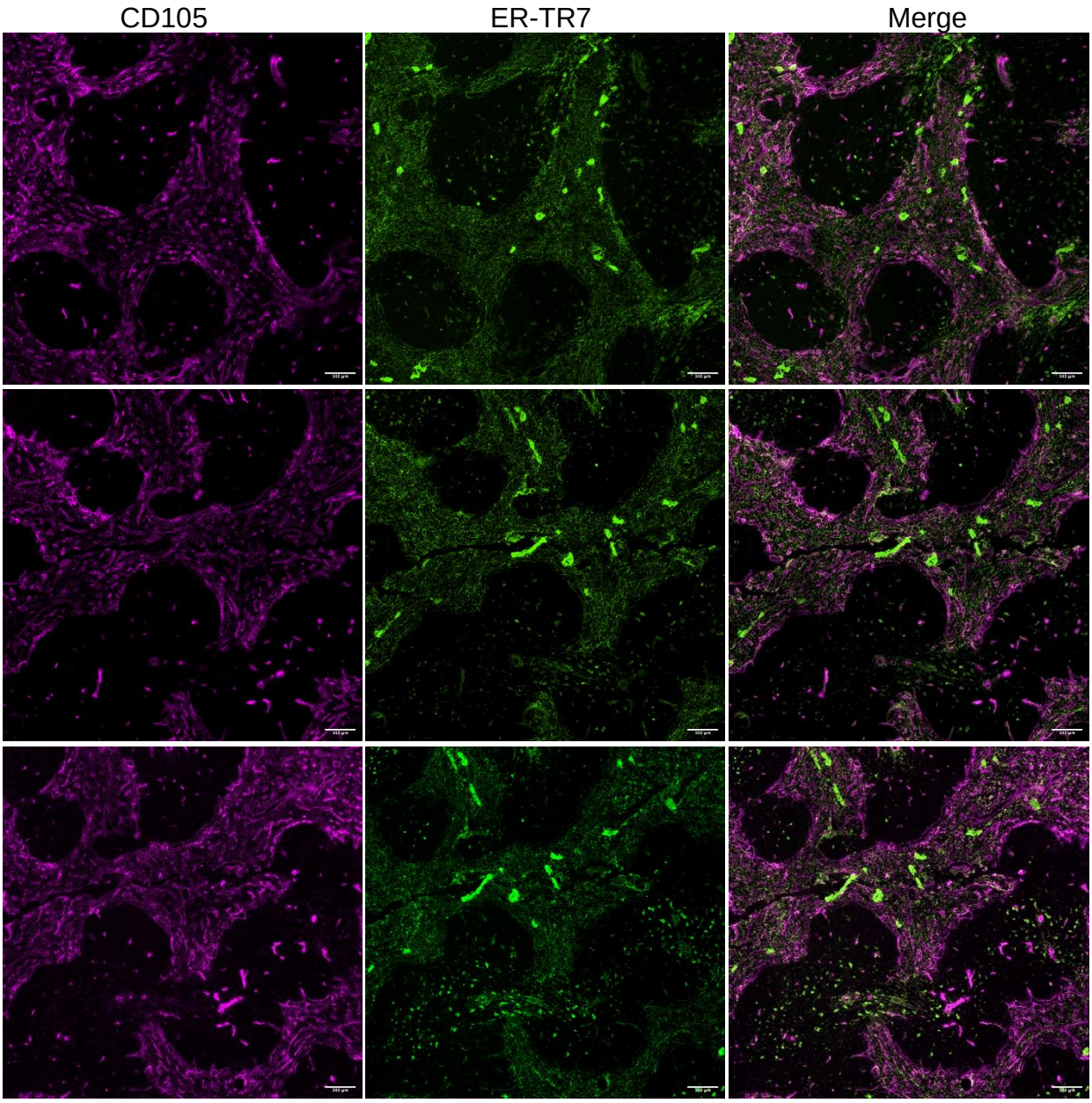

A.2 A spleen injected with an ultrafine 0.2mL needle and an untreated spleen were frozen and cryo-sectioned into 7±1µm thick sections for analysis. Spleen sections were fixed with acetone for 5 minutes at room temperature and then washed three times in PBS. Each tissue section was first blocked with FcBlock (CD16/32; clone 93) before primary antibodies for CD105 (MJ7/18; PE) and ER-TR7 (SC-73355; af488) were used. Images were captured using Nikon Live Cell Ti2 Microscope and processed using ImageJ FIJI software. First image row is the untreated spleen and the following two rows show tissue damage from serial sections. Scale bar on the bottom right corner of each image is 100µm.

Appendix A.3 Control gating for homing analysis

A

B6.SJL Control (CD45.2$^-$)

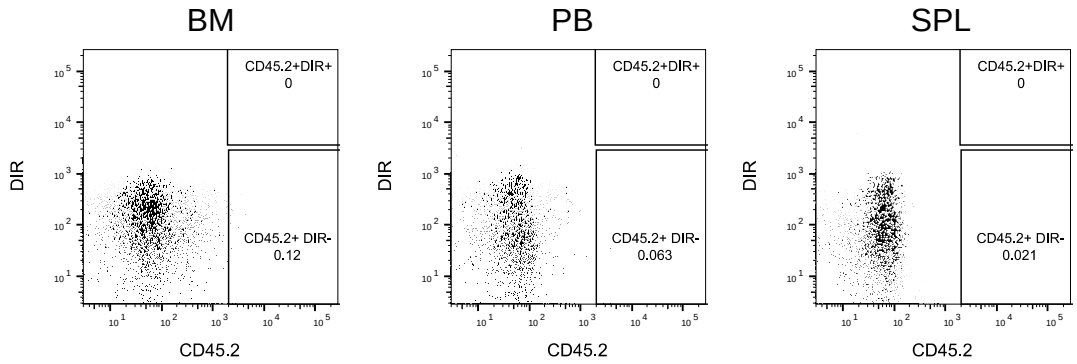

B

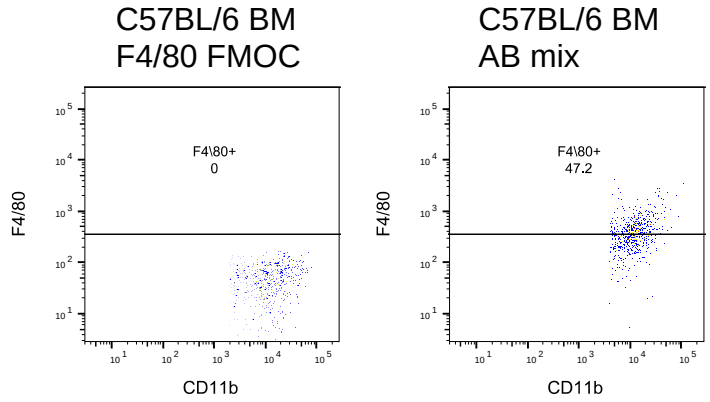

A.3 Donor CD45.2$^+$DIR$^+$ gates were set using B6.SJL as a control. A) Bone marrow (BM), peripheral blood (PB) and spleen (SPL) were analysed. Dot plots display a standardized number of events (5578). B) The F4/80$^+$ gate was set using an F4/80 forward minus one control (FMOC) and a complete antibody mix on C57BL/6J mice (donor type).

Appendix A.4 Percentage of B cells amongst whole spleen leukocytes

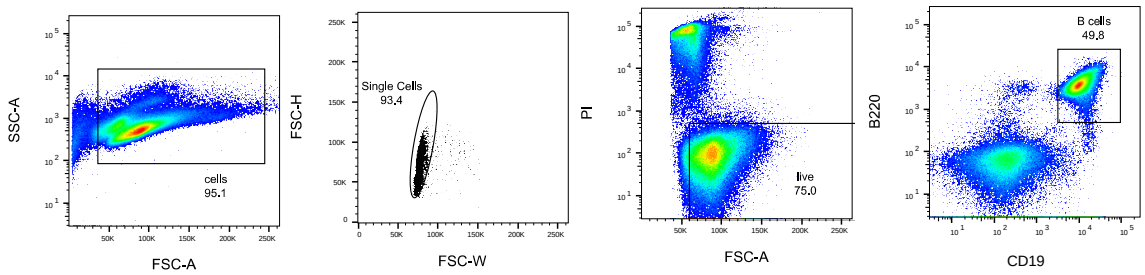

A.4 The percentage of B cells amongst whole spleen leukocytes were identified as the final gated percentage of single live $B220^{+}CD19^{+}$ expressing cells from a 2-month-old C57BL/6J mice (donor type).

Appendix A.5 Control gating for donor reconstitution

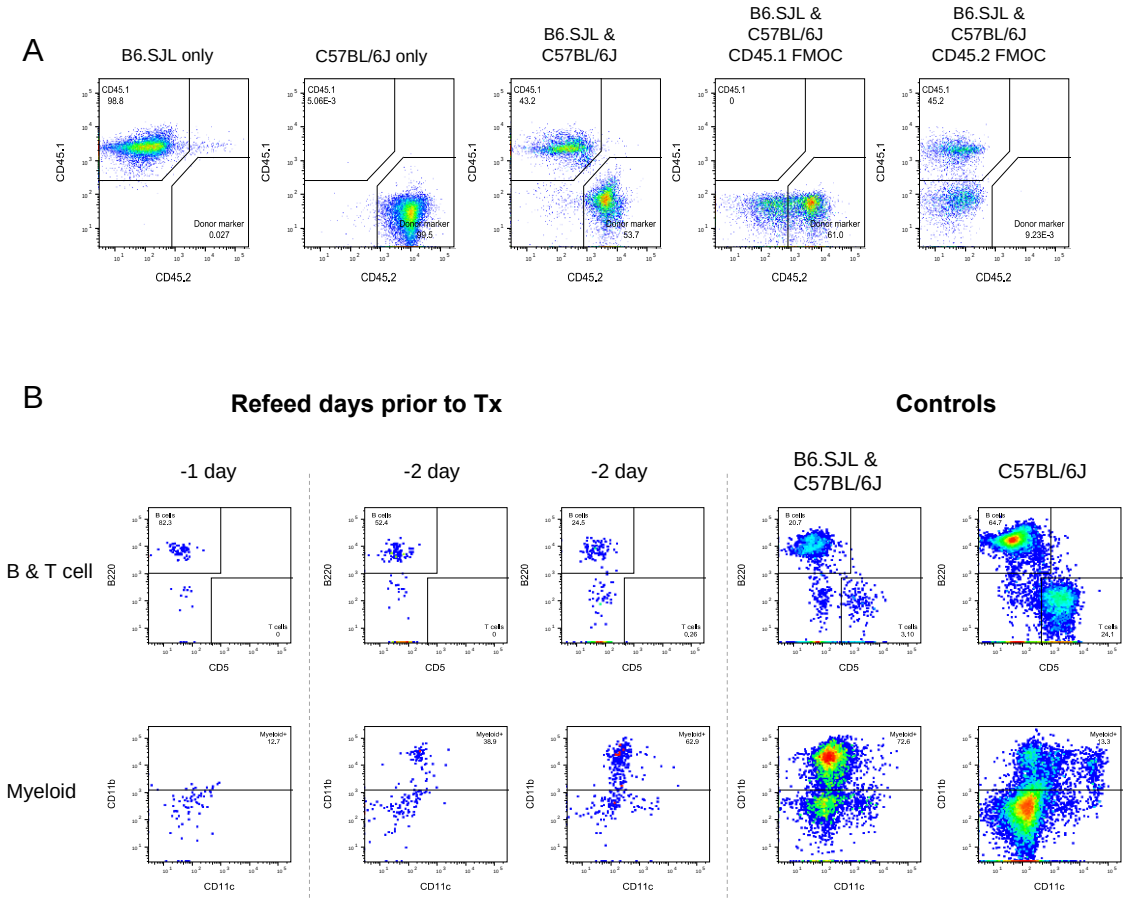

A.5 Donor gating for long-term and short-term reconstitution. A) Bone marrow of untreated B6.SJL and C57BL/6J mice were stained for CD45.1 and CD45.2 (donor marker). A mix of bone marrow from both C57BL/6J mice and B6.SJL mice was analysed as a positive control, alongside the C57BL/6J (donor type) only sample. B6.SJL mice were used as the host type and used as a negative control for $CD45.2^+$ gating. Background $CD45.2^+$ (donor expression) never exceeded 0.03%, therefore treatment samples were positive for donor chimerism when the percentage of donor marker was >0.1%. B) Lineage reconstitution analysis for -1 and -2 day refeed before transplant groups and control groups are examined for B ($B220^+$), T ($CD5^+$) and myeloid ($CD11b^+$ & $CD11c^+$) cell expression. C57BL/6J control lineage percentages are used to compare treatment group percentages.

Appendix A.6 Influence of valine on lineage⁻ cell count and calculating LSK frequency within the lineage⁻ fraction

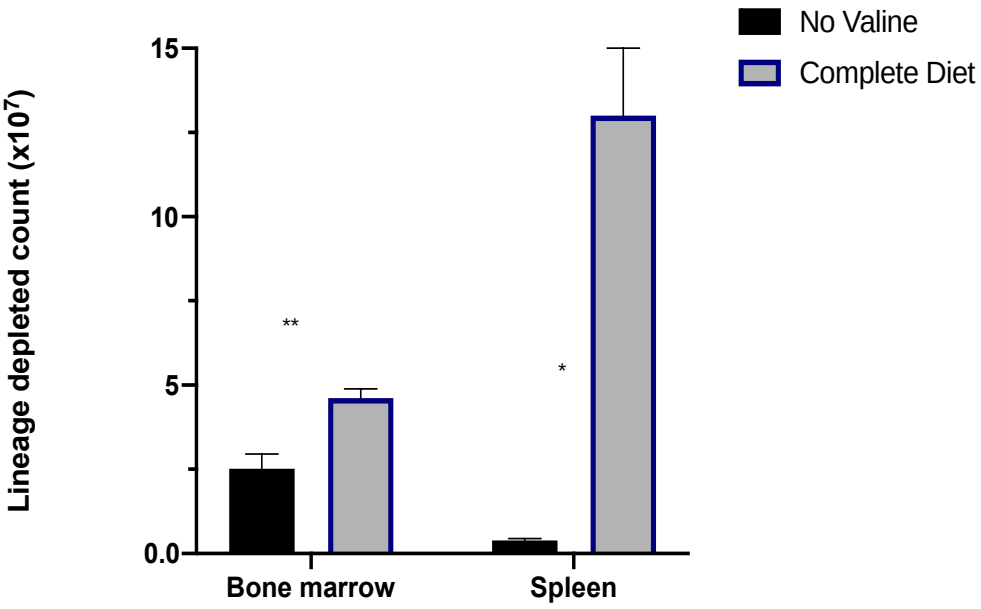

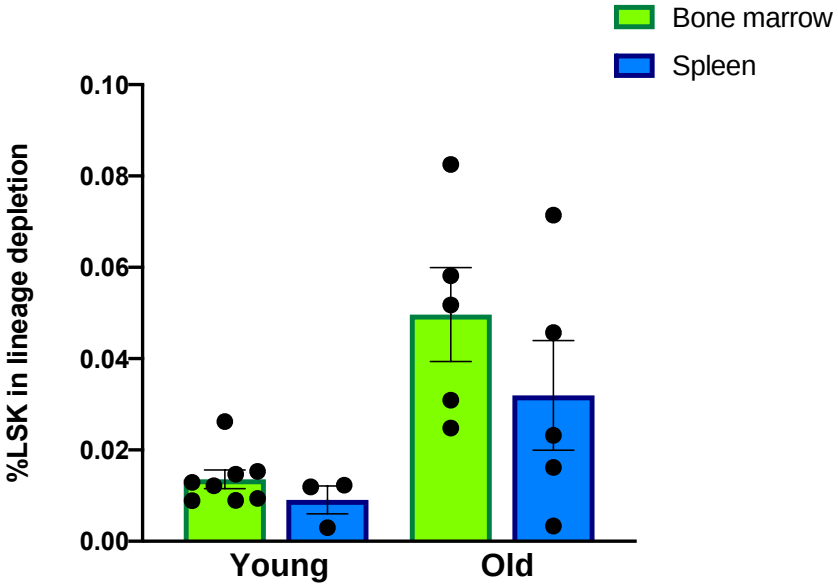

A.6A Bone marrow and spleen were homogenized, RBC lysed and single cell strained before magnetic depletion of lineage$^+$ cells. Lineage depleted bone marrow or spleen of valine restricted mice or control mice that were maintained on complete diet were stained with trypan blue (1:4 dilution) and counted using a hemocytometer. The graph shows number of lineage depleted cells in bone marrow and spleen of mice fed valine-restricted diet or complete diet after a 3-week valine depletion phase. Statistical significance was tested using an unpaired Student's t-test. Statistical significance is indicated when (**) $P<0.005$ and (*) $P<0.05$.

A.6B Calculating the frequency of LSK within a lineage depleted fraction of either bone marrow or spleen cells to identify the number of LSK within a transplant of lineage depleted bone marrow or spleen leukocytes. The absolute percentage of LSK cells were determined by multiplying the gated percentage of lineage$^-$ cells by the gated percentage of cKit$^+$Sca-1$^+$ cells (represented in graph). The absolute percentage can then be multiplied by the number of lineage depleted cells to identify the number of LSK cells within the lineage depleted fraction.

Appendix A.7 Spleen atrophy from valine depletion

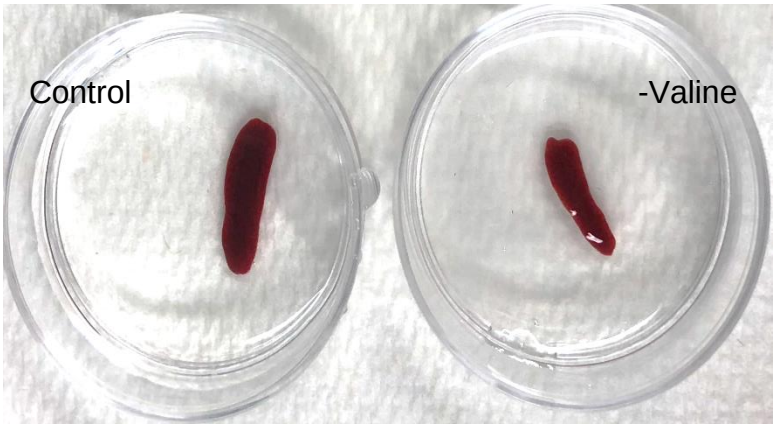

A.7 An untreated control spleen (left) and a valine-restricted spleen (right) from 11-week old mice depicts the degree of atrophy in the spleen after 3-weeks of valine restriction. The spleen from valine-restricted mice is noticeably smaller than mice that were fed a complete diet. These observations were consistent between all mice fed valine-restricted diets.

Appendix A.8 CD48 Co-expression analysis

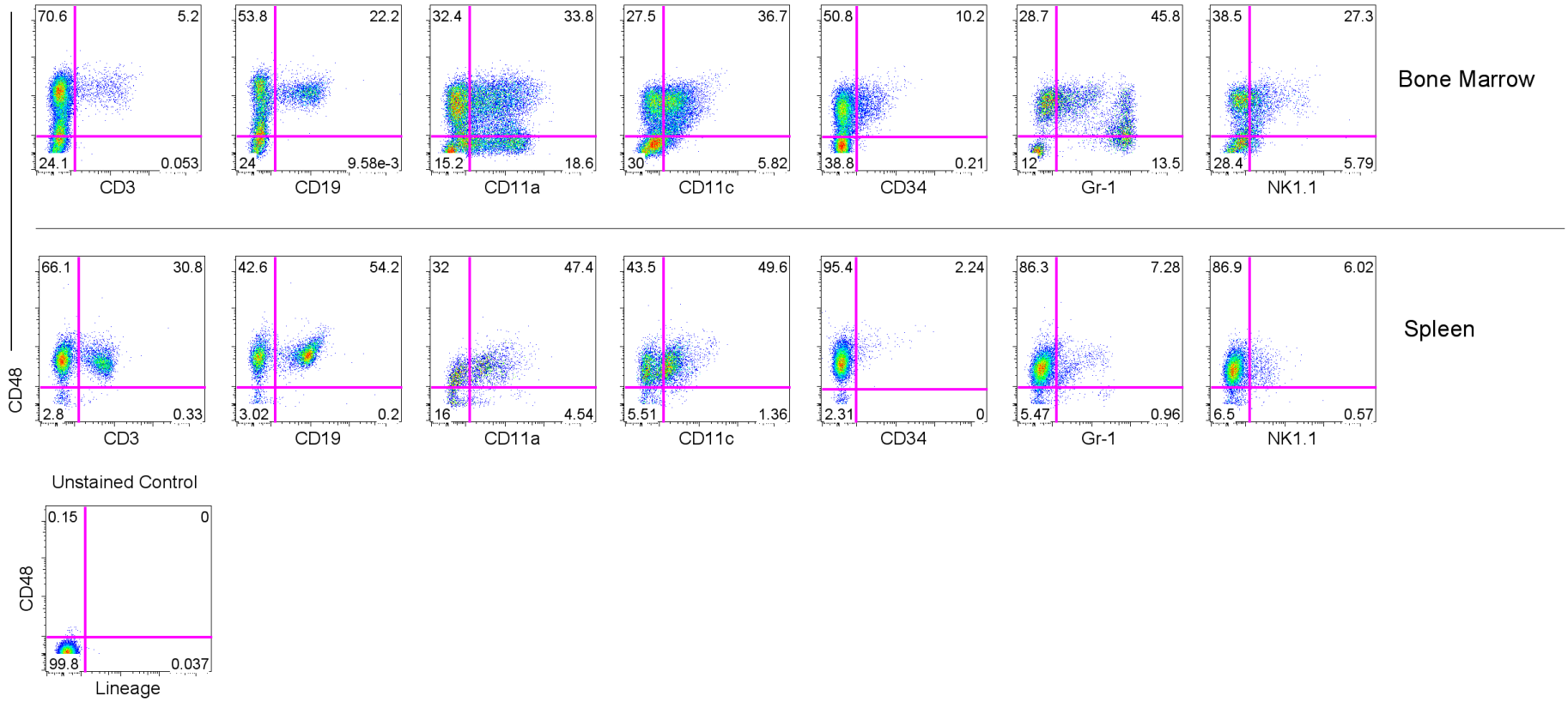

A.8 To isolate HSC, a cell suspension must first be enriched for rare progenitor populations. This step facilitates the sorting for HSC as $Lin^{-}Sca\text{-}1^{+}cKit^{+}CD150^{+}CD48^{-}CD34^{-}EPCR^{+}$ cells, which can then be used for *in vivo* transplantation assays and LT-HSC analysis. Lineage depletion requires multiple antibodies in order to deplete mature cell lineages from the desired LT-HSC population. Cells from both bone marrow (top row) and spleen (middle row) were analysed for co-expression of CD48 with mature lineage markers. Co-expression is denoted by events in the top right quadrant of a plot. An unstained control is displayed on the bottom row. CD48 co-expression is exhibited for all antibodies except CD11a, CD11c, Gr-1 and NK1.1. Therefore, the lineage depletion cocktail used for all LT-HSC enrichment was CD48, CD11c, Gr-1, NK1.1 as well as Fc Block (CD16/32). CD11a was not included due to cost associated with the antibody.

Appendix A.9 Percent of CD150^{hi} LT-HSC calculated from Beerman et al. (2010)

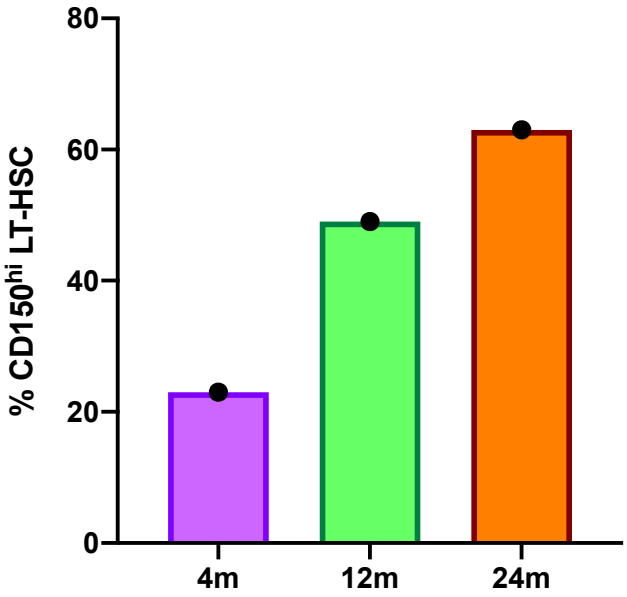

A.9 CD150^{hi} LT-HSC calculated from Figure 3D of the Beerman et al. (2010) study; *'Functionally distinct hematopoietic stem cells modulate hematopoietic lineage potential during aging by a mechanism of clonal expansion'.* To compare CD150^{+} expression frequencies from the published study to our own data, we transformed ($_T$) the reported CD150^{-}, CD150^{lo} and CD150^{hi} values to exclude CD150^{-}, identifying CD150$^{hi}{}_T$ and CD150$^{lo}{}_T$ as fractions of 100%.

$$\%\ \mathrm{CD150^{hi}}_T = \frac{\mathrm{CD150^{hi}}}{(\mathrm{CD150^{hi}} + \mathrm{CD150^{lo}})} \times 100$$

Since CD150^{hi} and CD150^{lo} are inversely related, we represent only CD150^{hi} percentages from 4-month-old (4m), 12-month-old (12m) and 24-month-old (24m) mice. The CD150 populations were originally gated within the LSKCD34^{-} flt3^{-} compartment. The data adapted from Beerman et al. (2010) were averaged values (*n=3* for each age).

Appendix A.10 Supplier addresses

Source	Location
ARC	Perth, WA, Australia
Darvall Vet	Gladesville ,NSW, Australia
Biolegend	San Diego, CA, USA
Bio-rad	Hercules, CA, USA
Beckton Dickinson	San Jose, CA, USA
Corning Inc.	Corning, NY, USA
Cosmo Bio	Tokyo, Japan
eBioscience	San Diego, CA, USA
Ethicon Inc.	Somerville, NJ, USA
Fisher Scientific	Hampton, NH, USA
FlowJo	Ashland, OR, USA
GraphPad Software	San Diego, CA, USA
Greiner Bio-One	Kremsmunster, Austria
InstrumeC	Victoria, Australia
Kimberly-Clark	Irving, TX, USA
LOCI	Maddison, WI, USA
Leica Microsystems	Wetzlar, Germany
Livingstone International	Toronto, Canada
Miltenyi Biotec	Gladbach, Germany
Research Diets Inc.	New Brunswick, NJ, USA
Sakura Finetek	Tokyo, Japan
Santa Cruz Biotechnology	Dallas, TX, USA
Sigma-Aldrich	St. Louis, MO, USA
StemCell Technologies	Vancouver, Canada
Terumo	Tokyo, Japan
ThermoFischer	Victoria, Australia
Thomas Scientific	Swedesboro, NJ, USA